



National Library  
of Canada

Acquisitions and  
Bibliographic Services Branch

395 Wellington Street  
Ottawa, Ontario  
K1A 0N4

Bibliothèque nationale  
du Canada

Direction des acquisitions et  
des services bibliographiques

395, rue Wellington  
Ottawa (Ontario)  
K1A 0N4

*Your file - Votre référence*

*Our file - Notre référence*

## NOTICE

The quality of this microform is heavily dependent upon the quality of the original thesis submitted for microfilming. Every effort has been made to ensure the highest quality of reproduction possible.

If pages are missing, contact the university which granted the degree.

Some pages may have indistinct print especially if the original pages were typed with a poor typewriter ribbon or if the university sent us an inferior photocopy.

Reproduction in full or in part of this microform is governed by the Canadian Copyright Act, R.S.C. 1970, c. C-30, and subsequent amendments.

## AVIS

La qualité de cette microforme dépend grandement de la qualité de la thèse soumise au microfilmage. Nous avons tout fait pour assurer une qualité supérieure de reproduction.

S'il manque des pages, veuillez communiquer avec l'université qui a conféré le grade.

La qualité d'impression de certaines pages peut laisser à désirer, surtout si les pages originales ont été dactylographiées à l'aide d'un ruban usé ou si l'université nous a fait parvenir une photocopie de qualité inférieure.

La reproduction, même partielle, de cette microforme est soumise à la Loi canadienne sur le droit d'auteur, SRC 1970, c. C-30, et ses amendements subséquents.

THE UNIVERSITY OF ALBERTA

Geology and geochemistry of the Prairie Creek Zn, Pb, Ag deposits, southern MacKenzie  
Mountains, N.W.T.

by

Stuart Campbell Fraser



A THESIS

SUBMITTED TO THE FACULTY OF GRADUATE STUDIES AND RESEARCH

IN PARTIAL FULFILMENT FOR THE DEGREE

OF Master of Science

Geology

EDMONTON, ALBERTA

Spring, 1996



National Library  
of Canada

Acquisitions and  
Bibliographic Services Branch

395 Wellington Street  
Ottawa, Ontario  
K1A 0N4

Bibliothèque nationale  
du Canada

Direction des acquisitions et  
des services bibliographiques

395, rue Wellington  
Ottawa (Ontario)  
K1A 0N4

*Your file - Votre référence*

*Our file - Notre référence*

The author has granted an irrevocable non-exclusive licence allowing the National Library of Canada to reproduce, loan, distribute or sell copies of his/her thesis by any means and in any form or format, making this thesis available to interested persons.

L'auteur a accordé une licence irrévocable et non exclusive permettant à la Bibliothèque nationale du Canada de reproduire, prêter, distribuer ou vendre des copies de sa thèse de quelque manière et sous quelque forme que ce soit pour mettre des exemplaires de cette thèse à la disposition des personnes intéressées.

The author retains ownership of the copyright in his/her thesis. Neither the thesis nor substantial extracts from it may be printed or otherwise reproduced without his/her permission.

L'auteur conserve la propriété du droit d'auteur qui protège sa thèse. Ni la thèse ni des extraits substantiels de celle-ci ne doivent être imprimés ou autrement reproduits sans son autorisation.

ISBN 0-612-10710-8

Canada

UNIVERSITY OF ALBERTA

RELEASE FORM

**Name of Author:** Stuart Campbell Fraser


**Title of Thesis:** Geology and geochemistry of the Prairie  
Creek Zn, Pb, Ag deposits, southern  
MacKenzie Mountains, N.W.T.

**Degree:** Master of Science

**Year this Degree Granted:** Spring, 1996

Permission is hereby granted to the University of Alberta Library to reproduce single copies of this thesis and to lend or sell such copies for private, scholarly or scientific research purposes only.

The author reserves all other publication and other rights in association with the copyright in this thesis, and except as hereinbefore provided, neither the thesis nor any substantial portion thereof may be printed or otherwise reproduced in any material form whatever without the author's prior written permission.

  
\_\_\_\_\_

10705-139 Street  
Edmonton  
Alberta  
T5M 1P6

Data: January 29 1996

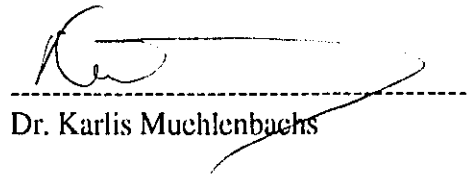
UNIVERSITY OF ALBERTA

FACULTY OF GRADUATE STUDIES AND RESEARCH

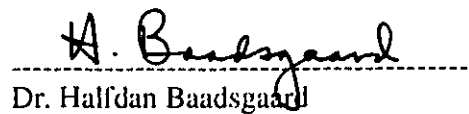
The Undersigned certify that they have read, and recommend to the Faculty of Graduate Studies and Research for acceptance, a thesis entitled: **Geology and Geochemistry of the Prairie Creek Zn, Pb, Ag Deposits, southern MacKenzie Mountains, N.W.T.** submitted by Stuart C. Fraser in partial fulfillment of the requirements for the Degree of **MASTER OF SCIENCE**.



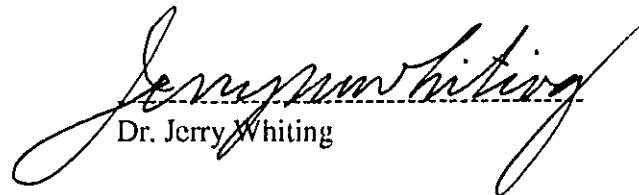
Dr. Bruce Nesbitt, Supervisor



Dr. Karlis Muchlenbachs



Dr. Halfdan Baadsgaard



Dr. Jerry Whiting

Dated January 28 1996

## Abstract

The Prairie Creek dolomite-hosted Zn, Pb, Ag deposits located in the southern MacKenzie Mountains, N.W.T., consist of three distinct types of mineralization. These include; 1) Type I stratiform mineralization which is characterized by banded, fine grained pyrite and sphalerite in a mottled, chert-rich, dolostone unit of late Ordovician, early Silurian Whittaker Formation; 2) Type II, MVT-style mineralization, within middle Silurian, Root River Formation; and 3) a final phase of mineralization consists of cross-cutting, quartz-sulfide veins characterized by a more complex mineralogy consisting of pyrite, sphalerite, galena  $\pm$  tetrahedrite. Saddle dolomite gangue associated with both types I and II mineralization, have distinctly different geochemistry.

Gangue dolomite associated with Type I mineralization possess highly radiogenic  $^{87}\text{Sr}/^{86}\text{Sr}$  isotopic ratios (up to 0.723), as well as enriched manganese (up to two weight percent), indicative of a Proterozoic source. Fluid inclusion results from inclusions in sphalerite (average homogenization temperature of 130 °C) and heavy  $\delta^{18}\text{O}$  values (+23‰ SMOW) support relatively low temperatures of formation. Type I mineralization is interpreted as syndiagenetic with Zn-Pb mineralization forming within the Prairie Creek Embayment, interpreted by Morrow and Cook, (1987) as an extensional tectonic structure associated with rifting.

Dolomitic cement associated with Type II mineralization show geochemical signatures characteristic of MVT mineralization. These include  $^{87}\text{Sr}/^{86}\text{Sr}$  isotopic values of 0.710,  $\delta^{18}\text{O}$  values to +14‰ SMOW, and  $\delta^{13}\text{C}$  values suggesting oxidation of organic matter. Fluid inclusion results from inclusions in gangue dolomite and sphalerite indicate salinities greater than 20 eq. wt. % NaCl and  $T_h$  of 150-200 °C.

Type III mineralization is characterized by a broad spread in salinity,  $T_h$ , and  $\delta^{18}\text{O}$  values suggesting that meteoric fluids were subjected to extensive water-rock interaction through MacKenzie shelf carbonate rocks. Measured  $\delta\text{D}$  values versus calculated  $\delta^{18}\text{O}$  values suggests that Type III mineralization is indicative of syn- to post-orogenic Laramide fluids, consistent with the findings of Nesbitt and Muehlenbachs, (1994). While Pb/Pb isotopic values statistically, all fall along a single isochron suggesting that all mineralization types have similar source and age, geological and geochemical variation for mineralization types suggest an alternative interpretation. This study suggests that mineralization types I and II are of Devonian-Mississippian age, while Type III (silver-rich) mineralization fall along a lead line supporting a Laramide age for mineralization.

## ACKNOWLEDGEMENTS

I would like to thank my supervisor, Bruce Nesbitt, who first suggested the idea of an M.Sc. thesis project and who supported me financially through NSERC grants, during what seemed to be a never-ending project. I am particularly thankful to his patience and swiftness in reviewing and ably editing my early attempts at penmanship. I also wish to thank Dr. Hans Machel and Harold Huebner for their input in thin section observations and use of cathodoluminescent microscopy, which first identified high manganese concentrations within saddle dolomite gangue.

To the personnel within the stable isotope lab, I particularly owe a debt of thanks. Susan Fitzpatrick guided me through the endless glass menagerie, and remarked, matter of factly, after I pumped away my first sample, that most of us have done this in the past. I want to thank Rob King who analyzed most of the quartz samples on the silicate line and James Steer, who performed his wiswardry on the hydrogen line. Thank you to Karlis Muehlenbachs who always supplied not only equipment freely, but also encouragement and a willing ear. At the University of Calgary, I wish to thank Dr. Ron Krouse for running sulfur isotope samples.

I wish to thank Rob Hardy for his patience and skill in assisting me in fluid inclusion analyses, as well as preparing fluid inclusion chips. Here also, I must thank Don Russeltay in the thin section lab who would often correct my bevelled surfaces for fluid inclusion samples, and also for his cheerfulness, which rubbed off on everyone around him.

I further wish to thank Dragon Krstic for his work on common lead isotopic analyses and for his excellent plots, which are essentially duplicated here in this thesis. Dragon offered helpful discussion and a writeup of the Pb-Pb results, which made a difficult subject more clear. On the subject of radiogenic isotopes, I also wish to thank, Prof. H. Baadsgaard in offering valuable criticism in Chapter 6.

I also wish to thank San Andreas Resources for giving me the opportunity to visit and work on this project and to Sandy Gibson, in particular, who assisted with transport and equipment at the minesite and offered valuable insight on the project. I further wish to thank San Andreas Resources for free access to company data.

Finally I wish to thank my wife and my daughters, for their patience and understanding, who put up with a part time husband and father for much of the last few years and assisting me with encouragement when I needed it.

## TABLE OF CONTENTS

Chapter:	page
<b>I: Introduction</b>	
1 Location.....	1
Access.....	1
Exploration and mining history.....	2
2 Previous Work.....	2
3 Research Objectives.....	2
<b>II: Geology and Tectonic setting of the Prairie Creek deposits</b>	
1 Regional geology of the Virginia Falls map area.....	6
Stratigraphy.....	6
Structure.....	10
Devono-Mississippian Tectonics and Heat Flow Events.....	11
Regional Mineralization in the MacKenzie Platform.....	14
2 Local Geology of the Prairie Creek Deposits.....	15
Stratigraphy.....	15
Structure.....	17
3 Geology of Mineralization at Prairie Creek	
Ore Types.....	20
Stratiform Mineralization - Type I.....	20
Zebra Showing Mineralization - Type II.....	23
Quartz Veining - Type III mineralization.....	26
Unmineralized Veins and Brecciation.....	27
<b>III: Mineralogy and Paragenesis of the Prairie Creek Deposits</b>	
1 Introduction.....	28



## TABLE OF CONTENTS

### III: Mineralogy and Paragenesis of the Prairie Creek Deposits Continued

#### 2 Petrographic Observations

Regional Dolomitization.....	29
Type I Mineralization.....	31
Type II Mineralization.....	33
Type III Mineralization.....	34
Other Veining and Brecciation.....	37

3 Sphalerite Chemistry.....	38
-----------------------------	----

### IV: Fluid Inclusion Study

1 Introduction.....	40
---------------------	----

Analytical Techniques.....	42
----------------------------	----

#### 2 Results of Fluid Inclusion Studies

Petrographic Observations.....	44
--------------------------------	----

##### Inclusions in Quartz

Two phase aqueous inclusions.....	44
-----------------------------------	----

CO <sub>2</sub> inclusions in quartz.....	47
---	----

Inclusions in Sphalerite.....	47
-------------------------------	----

Inclusions in Calcite.....	49
----------------------------	----

Inclusions in Dolomite.....	52
-----------------------------	----

3 Geothermometry and Geobarometry.....	55
--	----

4 Fluid Inclusion Data Summary.....	55
-------------------------------------	----

### V: Light Stable Isotope Study

Introduction.....	59
-------------------	----

Technique.....	60
----------------	----

Sulfur Isotope Data.....	61
--------------------------	----

## TABLE OF CONTENTS

### Chapter V: Light Stable Isotope study continued

C, O, and H Isotope Results.....	63
Type I ores.....	63
Type II ores.....	63
Type III ores.....	64
Calcite veining.....	64
Discussion.....	71

### VI: Radiogenic Isotopes

1 Lead Isotope Systematics.....	81
Techniques.....	86
Results.....	89
Interpretations.....	93
2 Rubidium-Strontium Systematics.....	96
Analytical Techniques.....	98
Results.....	98
Interpretations.....	102
Conclusions on Radiogenic Isotope Results.....	103

### VII: Discussion

1 Variation in Types I, II and III.....	104
Geological variation.....	105
Geochemical variations.....	107
Age constraints.....	110

## TABLE OF CONTENTS

### **VII: Discussion continued**

Structural variation.....	111
2 A Heat Source and Conodont Alteration Index (CAI) Values.....	112
3 Comparison with other Cordilleran Pb-Zn deposits	
MacMillan Pass shale-hosted deposits and Type I mineralization.....	112
Robb Lake and Type II mineralization.....	113
Midway and Type III mineralization.....	114
4 Conclusions and Implications for Exploration.....	114
<b>References.....</b>	<b>117</b>
<b>Appendix I Table IV-1 Fluid Inclusion Data.....</b>	<b>127</b>
<b>Appendix II- Microprobe data on Prairie Creek Dolomites.....</b>	<b>132</b>
<b>Appendix III - Sphalerite Geochemistry.....</b>	<b>140</b>
<b>Appendix IV - Linear regression program for common lead analyses.....</b>	<b>146</b>

## LIST OF TABLES

Table II-1	Stratigraphy of Whittaker Formation.....	19
Table III-1	Paragenetic Relationships.....	28
Table III-2	Microprobe Analyse (averages in wt %) for Trace Elements from Dolomites.....	29
Table III-3	Sphalerite Geochemistry from Microprobe Analyses.....	39
Table IV-1	Fluid Inclusion Data (Appendix I).....	126
Table V-1	Prairie Creek $\delta^{34}\text{S}$ data (‰).....	62
Table V-2	Prairie Creek stable isotope data (wall rock dolomites).....	65
Table V-3	Prairie Creek stable isotope data (mineral separates).....	66
Table V-4	Calculated $\delta^{18}\text{O}_{\text{fluid}}$ values.....	76
Table VI-1	Lead Isotope Data.....	87
Table VI-2	Strontium Isotopic Results.....	100
Table VII-1	Comparison of Mineralization Types.....	105

## LIST OF FIGURES

Figure	page
1	Location Map, (modified from Morrow and Cook, 1987).....4
2	Prairie Creek property showing quartz-sulfide mineralized zones from Thorpe, (1972).....5
3	Stratigraphic column for Prairie Creek area (modified from Morrow and Cook, 1987).....9
4	Local geology of the Prairie Creek area (modified from the map of Morrow and Cook, 1987).....13
5	Lead-zinc mineralization in the northern Cordillera (adapted from Brock, 1976).....16
6	Regional cross-section across Southern MacKenzie Mountains illustrating high angle reverse faults in the Prairie Creek area.....18
7	Thickness contours of Type I stratiform mineralization in the #3 Zone area, Prairie Creek.....21
8	Fluid inclusion results- Th versus salinity for minerals investigated....38
9	Homogenization temperature in inclusions in sphalerites.....50
10	Salinity results from inclusions in sphalerite.....51
11	Salinity results from inclusions in gangue dolomite.....53
12	Homogenization temperature in inclusions in dolomite.....54
13	Trapping temperature and pressures from intersecting CO <sub>2</sub> and NaCl isochores.....58
14	$\delta^{18}\text{O}$ versus $\delta^{13}\text{C}$ plot of selected Prairie Creek carbonate rocks.....68
15	Section 6288N $\delta^{18}\text{O}$ and $\delta^{13}\text{C}$ values from wholerock dolomite.....69
16	Section 6045N $\delta^{18}\text{O}$ and $\delta^{13}\text{C}$ values from wholerock dolomite.....70
17	$\delta\text{D}_{\text{Fl}}$ versus $\delta^{18}\text{O}_{\text{fluid}}$ plot.....73
18	$\delta\text{D}$ versus salinity plot.....78
19	$\delta^{18}\text{O}_{\text{fluid}}$ versus homogenization temperature (after Land, 1985).....80

## LIST OF FIGURES

Continued

20	Pb/Pb plot based on shale growth curve of Godwin et al, (1982).....	84
21	Pb/Pb plot of Prairie Creek data.....	90
22	$^{208}\text{Pb}/^{204}\text{Pb}$ versus $^{206}\text{Pb}/^{204}\text{Pb}$ plot.....	92
23	Pb-Pb plot showing slope derived from linear regression program (Yorkfit).....	94
24	Section 6288N showing $^{87}\text{Sr}/^{86}\text{Sr}$ values in relation to stratiform mineralization.....	99
25	Burke et al.(1982) plot of $^{87}\text{Sr}/^{86}\text{Sr}$ values for Phanerozoic carbonate rocks and values from gangue dolomites associated with Types I and II mineralization at Prairie Creek.....	101

## LIST OF PLATES

Plate 1	Type I mineralization with fine to very grained pyrite and sphalerite, within siliceous matrix.....	22
Plate 2	Distinct mottled texture associated with Type I mineralization...	24
Plate 3	Coarse-grained saddle dolomite cement associated with Type II sphalerite and pyrite mineralization.....	25
Plate 4	Coarse-grained euhedral dolomite trapped within microcrystalline quartz suggesting that dolomitization and silicification are contemporaneous.....	30
Plate 5	Photomicrograph of zoned sphalerite (Type I mineralization)....	32
Plate 6	Thin section of saddle dolomite cement illustrating curved cleavage planes and distinctive undulose extinction under cross polars.....	35
Plate 6	Deformation features developed in sphalerite from Type III mineralization.....	36
Plate 7	Evaporite pseudomorphs seen within siliceous sections of early (regional) dolomite.....	74

## Chapter I Introduction

### Introductory Remarks

The purpose of the thesis is to address different styles of mineralization present at Prairie Creek, N.W.T. Early exploration in the Prairie Creek area was focused on quartz-sulfide veins which host silver. Stepout drilling in 1992 intersected a different style of mineralization which had not previously been observed within the MacKenzie Platform carbonate succession. This thesis provides evidence, based on geology and geochemistry, for three distinct styles of mineralization. By illustrating that stratiform Zn-Pb mineralization forms in extensional basins, within the MacKenzie Platform carbonate package, by implication, the thesis provides a framework for further Zn-Pb mineralization in addition to MVT-style, Pb-Zn mineralization previously described in the platformal carbonate rocks.

### 1.0 Location

The Prairie Creek Zn-Pb-Ag deposit is located within the Virginia Falls map area NTS 95F in the southwestern NWT, at latitude  $61^{\circ} 33'N$  and longitude  $124^{\circ} 46'W$  (Figure 1). The deposit is adjacent to Prairie Creek, a tributary draining south into the South Nahanni River (Figure 2).

### Access

A small airstrip is located just east of the Prairie Creek tributary. A winter road from Fort Simpson, NWT was earlier used to ferry mining equipment into the minesite. No roads lead south through Nahanni National Park, located approximately six km south of the minesite.



## Exploration and Mining History

The Prairie Creek deposit, formerly known as the Cadillac mine, is presently operated by San Andreas Resources of Vancouver. Exploration history goes back to 1928, when the mineralization was first staked (DIAND, 1984). Early prospecting began in the mid-1960's when Fort Reliance Minerals, and later Cadillac Resources, acquired the ground, developed several adits, and did limited diamond drilling.

Twelve separate zones, aligned roughly north-south, are outlined by surface work and drilling (Figure 2). The zones are characterized by steeply-dipping quartz veins with variable amounts of tetrahedrite, sphalerite, galena and pyrite (Thorpe, 1972). Cadmium and tungsten mineralization is also present (Financial Post, 1980). Zone #3 has received most of the exploration attention. Adits are developed on zones 3, 7 and 8. In 1992, drilling by San Andreas Resources intersected stratiform Pb-Zn mineralization at depth.

### 1.2 Previous Work

Douglas and Norris, (1961) initially mapped the regional geology in the Virginia Falls and Sibbeston Lake map areas. They mention lead-zinc mineralization occurring near the Laird River. Thorpe (1972) and (DIAND, 1984) describe lead-zinc mineralization in quartz veins at Prairie Creek. Sangster and Lancaster (1976) report two other lead-zinc occurrences in lower Paleozoic carbonate rocks near Prairie Creek, but offer no details. McLarin and Godwin (1981) describe minor elements in sphalerite from carbonate-hosted zinc-lead deposits, including Prairie Creek, in the Yukon and District of MacKenzie, NWT. Morrow and Cook (1987) and Morrow et al. (1991) describe the Lower Paleozoic stratigraphy in the Prairie Creek area.

### 1.3 Research Objectives

The objectives of this study are to characterize the fluids that formed the Prairie Creek mineralization, and to document the temporal and spatial relationships of various styles of mineralization. To achieve these objectives, the writer uses several geological and

geochemical techniques. Following the documentation of mineralogical and paragenetic relations, supported by electron microprobe analyses (Chapter III), a fluid inclusion microthermometry study (Chapter IV) documents the chemistry (temperature of homogenization, composition and pressures) of mineralizing and non-mineralizing fluids. Fluid inclusion analyses result from quartz, calcite, dolomite and sphalerite samples. The chemistry of the mineralizing fluids is evaluated further through light, stable isotopic analyses (Chapter V). Radiogenic isotope (Pb-Pb and Rb/Sr) data in Chapter VI augment earlier data (Morrow et al. 1991) from Prairie Creek to constrain the source of metals and the timing of mineralization.

Drawing on the geological, mineralogical and geochemical observations, in Chapter VII, comparisons are made with other Pb-Zn deposits in the Canadian Cordillera, including Midway, a high temperature mantle deposit, and Robb Lake, an MVT deposit and the Tom deposit, a shale-hosted, sedimentary-exhalative (sedex) deposit in the Selwyn Basin.

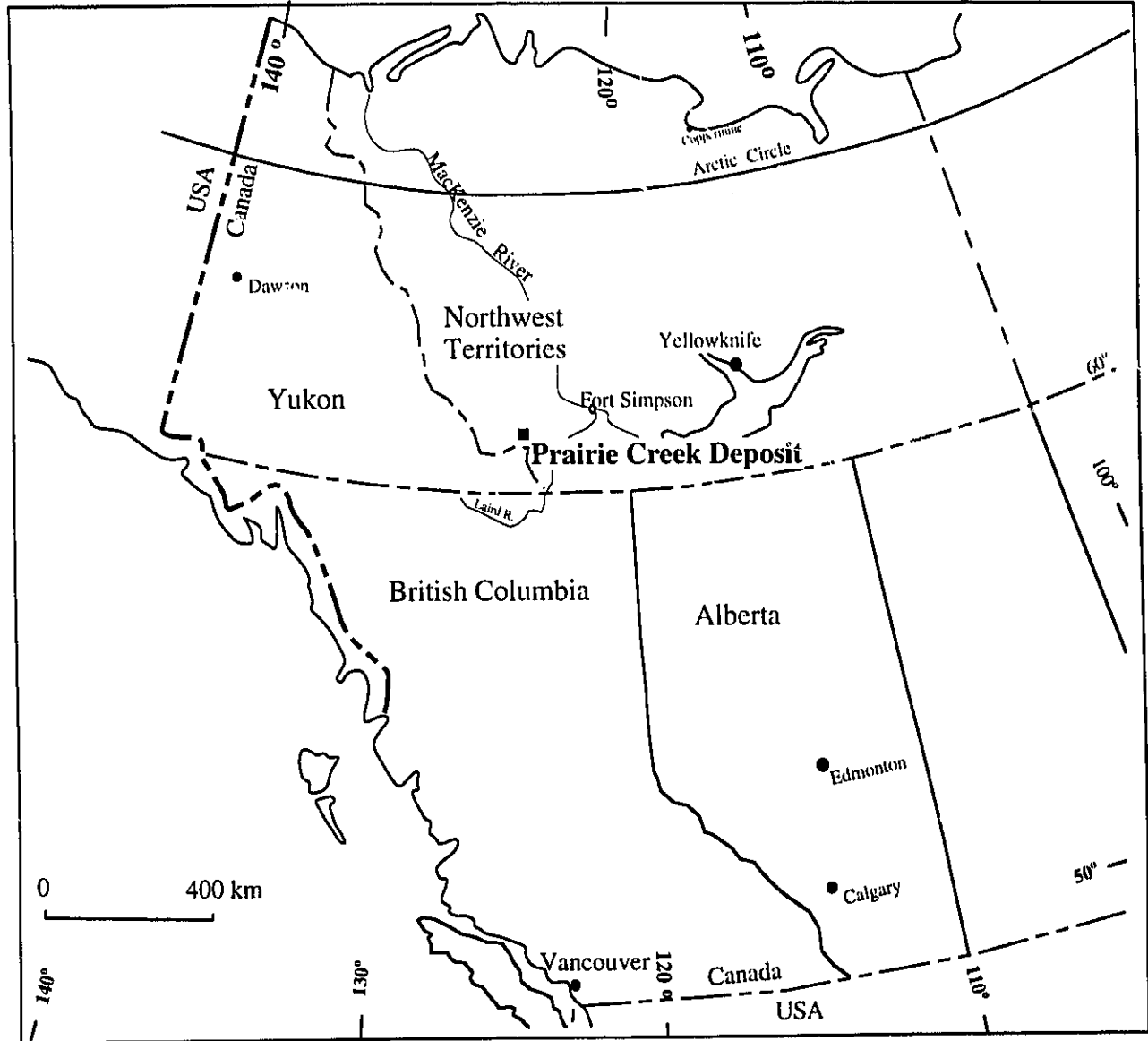


**Figure 1** Location map of the Prairie Creek Zn,Pb, Ag deposit, southern MacKenzie Mountains, N.W.T.

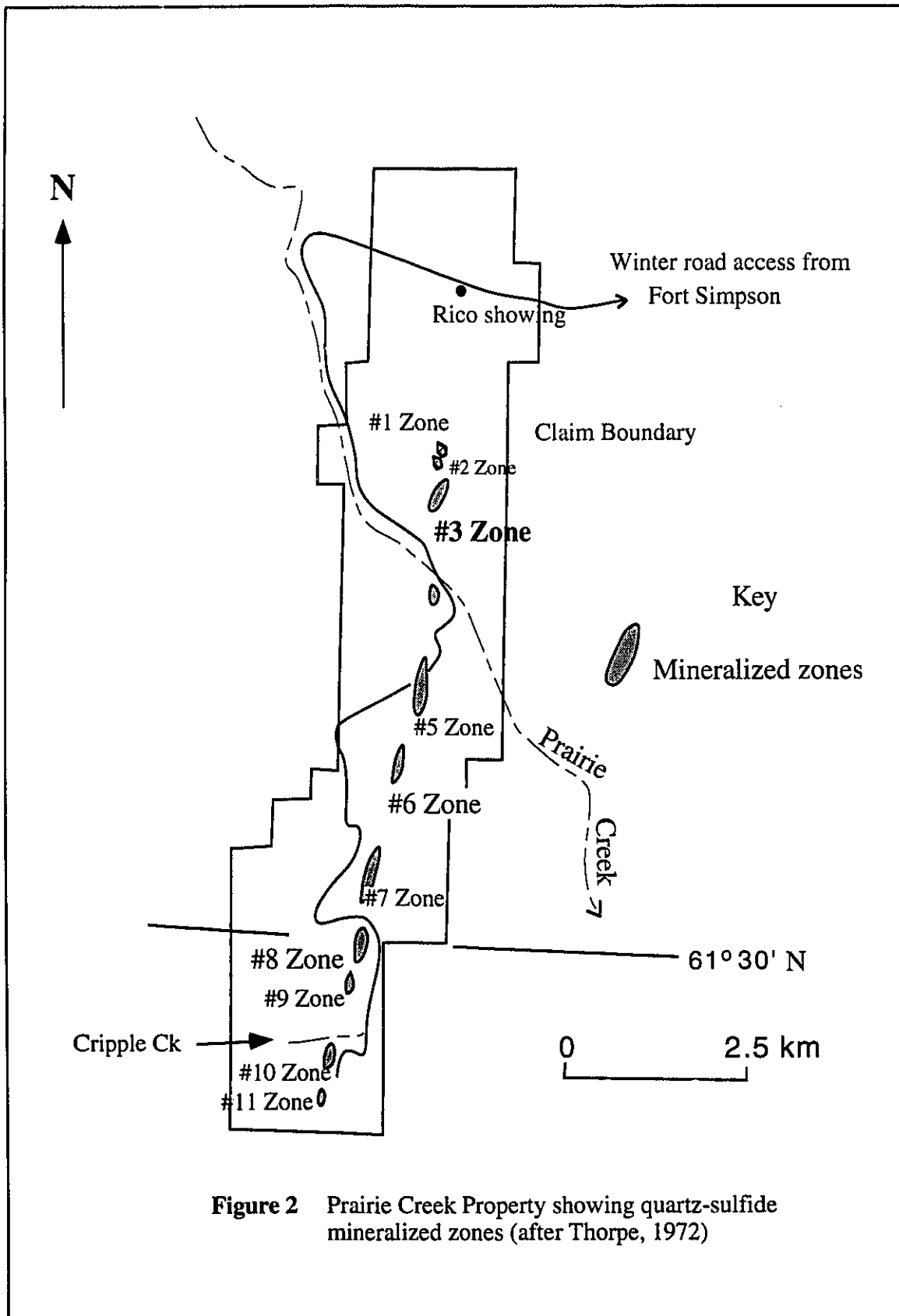


**Figure 2** Prairie Creek Property showing quartz-sulfide mineralized zones (after Thorpe, 1972)

## **Chapter II Geology and tectonic setting of the Prairie Creek deposits**

### **2.1 Regional geology of the Virginia Falls map area**

The Virginia Falls map area (Douglas and Norris, 1960) hosts the Prairie Creek deposits. This area lies within the MacKenzie Shelf, which is part of the Foreland Belt or Fold and Thrust Belt of the northern Canadian Cordillera. The belt is characterized by imbricated and folded miogeoclinal and clastic wedge assemblages overlapping ancestral North America. Paleozoic shelf carbonates and clastics form prominent outcrops in the southern MacKenzie Mountains. To the west, the MacKenzie Shelf is flanked by deep-water shales of the Selwyn Basin, while to the east lie undeformed, platformal sedimentary rocks of the Interior Plains (Law, 1970).

The area of the study lies within a paleo-depression, the Prairie Creek Embayment, which is characterized by subtidal slope deposits (Morrow, 1984) and bounded on the east, north, and west by shelf carbonates. To the south and southwest, sedimentary rocks become increasingly more shaly and grade into Siluro-Devonian Road River Formation shales.

#### **2.1.1 Stratigraphy**

The upper Proterozoic and lower Paleozoic stratigraphy of the southern MacKenzie Mountains has been described by Douglas and Norris (1960), Gabrielse et al., (1973) Norford and MacQueen (1975), Meijer-Drees, (1975), Ludvigsen, (1975), Morrow (1984), and Morrow and Cook (1987). The summation below is based on their observations.

Within the MacKenzie Mountains, approximately 1500 to 5500 metres of Helikian strata are unconformably overlain by more than 3000 metres of Hadrynian sedimentary rocks (Meijer-Drees, 1975). Cambrian stratigraphy west of Fort Simpson NWT, based on drill hole data compiled by Meijer-Drees (1975), is characterized by fine-grained clastics in

the Lower to Middle Cambrian and anhydrite in the Upper Cambrian Saline River Formation (Figure 3). Bore hole data (Meijer-Drees, 1975) suggest that the Saline River Formation may finger out before reaching the Prairie Creek area. Gabrielse et al. (1973), mapping west of Virginia Falls map area, interpreted a variably sandy to silty dolomitic unit (Broken Skull Formation) as Upper Cambrian conformably grading into Lower Ordovician argillaceous limestone (Sunblood Formation).

In the Prairie Creek area, Morrow and Cook (1987) divided lower Paleozoic strata into four main subdivisions: 1) the Sunblood platform; 2) the Mount Kindle-Root River assemblage; 3) the Prairie Creek assemblage and 4) the the Middle Devonian Funeral-Headless assemblage. The Sunblood platform (Middle Ordovician) consists wholly of the Sunblood Formation argillaceous limestones. The Mount Kindle-Root River assemblage consists of the Whittaker, Road River and Root River Formations. Morrow and Cook (1987) divided the Whittaker Formation of the Mount Kindle-Root River assemblage into three parts with the lower two units as middle to upper Ordovician and an upper Ordovician-Silurian unit. These include a lower crystalline limestone ( $\mu\text{Ow}1$ ), a middle part consisting of a fine-grained quartzite ( $\mu\text{Ow}2$ ), and an upper part consisting of laminated dark grey to black, finely crystalline dolostone with nodular and discontinuous lenses of chert ( $\text{OSw}3$ ). The Siluro-Devonian Road River Formation is composed of a graptolite-bearing shale sequence conformably overlying Whittaker Formation dolostones. The Silurian, Root River Formation comprises light grey dolostone. While the contact between Road River shales and Root River dolostones is not exposed, Morrow and Cook (1987) infer a conformable contact with a tongue of the underlying Road River shales (Figure 3). Meijer-Drees (1975) reports the presence of anhydrite in the Mount Kindle Formation (correlative with Whittaker Formation rocks). Meijer-Drees (1975) has further described a major unconformity at the base of the Mount Kindle/Whittaker Formation . The Prairie Creek assemblage consists of two phases, the lower and upper Cadillac (Morrow, 1982), which formed as a result of late Silurian sea level drop. Gordey, (1991)

suggests that Silurian sealevel drop resulted in erosional debris filling the Root Basin, a major bathymetric feature (Gabrielse, 1973), allowing the formation of the Prairie Creek Embayment (Morrow, 1984). The lower Cadillac phase is composed of orange weathering siltstone and megabreccia of the Cadillac Formation, the Vera Formation a variably colored argillaceous limestone, and the Camsell Formation a fine-grained, in part brecciated, limestone. The upper Cadillac phase comprises the Sombre, Arnica (a dark grey to black dolostone) and pink shale members of the Cadillac Formation. The Cadillac Formation, and parts of the Sombre and Arnica are confined to the Prairie Creek Embayment, while additional members of the Arnica and Sombre Formations extend beyond the embayment. The Middle Devonian Funeral-Headless assemblage including the Landry, Funeral, Headless, and Nahanni Formations, records the disappearance of the Prairie Creek Embayment. This assemblage consists of two phases, the Funeral-Landry comprised of shales and grey weathering massive limestones, and the Headless and Nahanni Formations. The Headless Formation consists of recessive shale and argillaceous limestone. The Nahanni Formation forms resistant limestone at the top of the Lower Paleozoic sequence (Figure 3). The late Middle Devonian and Upper Devonian stratigraphy consists of the Besa River shales (de Wit et al. 1971).

Morrow et al. (1990) have described the Manetoe Facies ( Figure 3) as a continuation of the Presqu'ile Facies, with both consisting of coarse-grained, epigenetic or hydrothermal dolomite. Following the observations of Douglas and Norris (1960) who initially mapped the facies as a formation, Morrow et al. (1990) outline the facies as occurring at the top of the Arnica Formation and extending to the top of the Landry Formation. Locally, where the fluids which formed the sparry dolomite of the Manetoe Facies migrated upwards through Nahanni Formation rocks, gas fields such as Pointed Mountain and Beaver River have formed below shale horizons (Morrow et al. 1986). In the Pine Point area, Pb-Zn mineralization is intimately associated with sparry dolomite

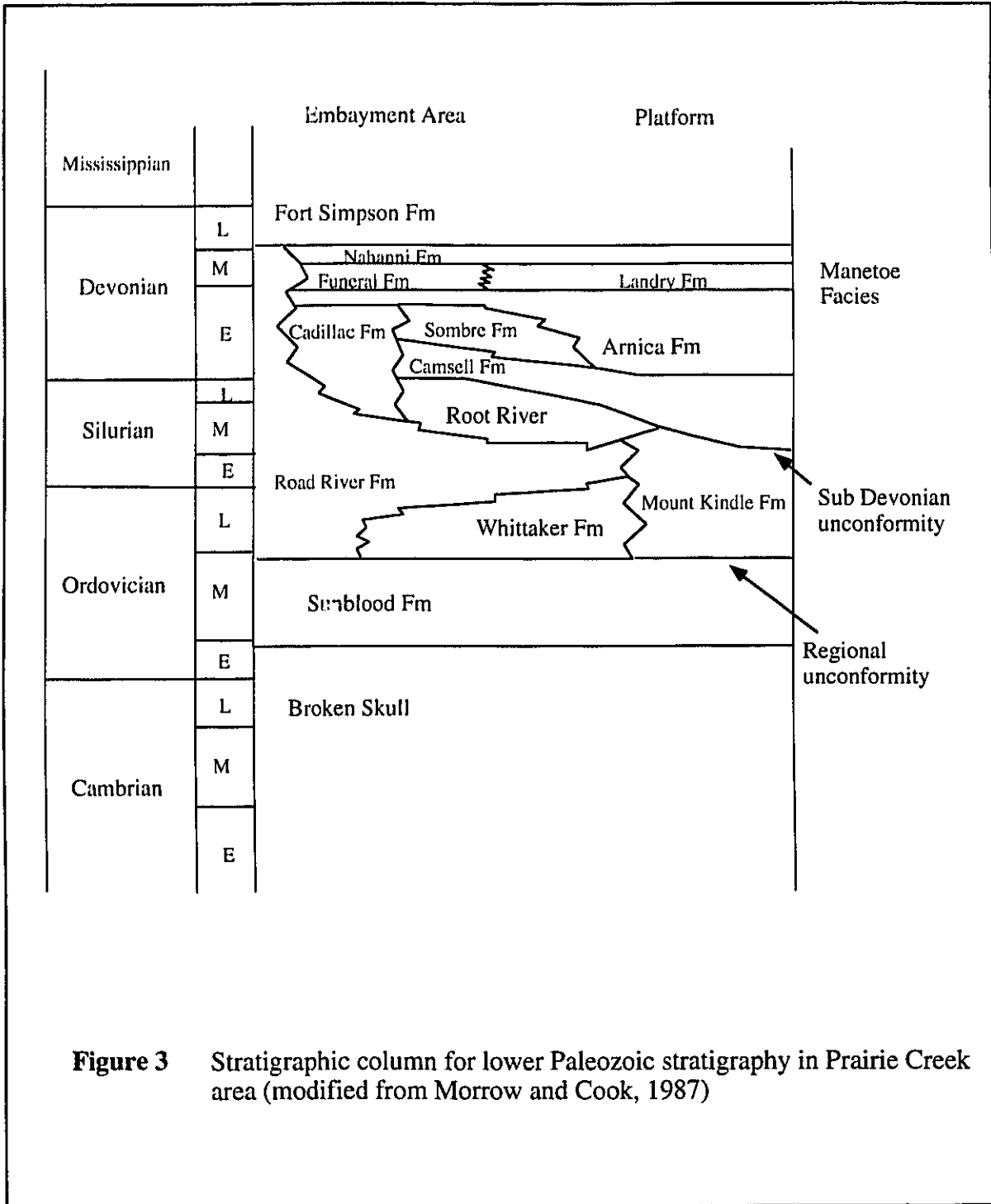


**Figure 3** Stratigraphic column for lower Paleozoic stratigraphy in Prairie Creek area (modified from Morrow and Cook, 1987)



within Presqu'île Facies (Skall, 1979; Krebs and MacQueen, 1984; Qing and Mountjoy, 1992). Pb-Zn mineralization has also been observed in Manetoe Facies at Mount Camsell, 116 km west of Fort Simpson, where thicknesses up to four metres of galena and sphalerite are reported in sparry dolomite at the Wrigley-Lou Pb-Zn occurrence (DIAND, 1976; Heal, 1976).

### 2.1.2. Structure

The southern MacKenzie Mountains are characterized by north to north-northeast trending structures within the Foreland Belt. In the Virginia Falls map area, lower Paleozoic strata are often concentrically folded (flexural folds) into doubly plunging, faulted anticlines and broad, flat bottomed synclines, which presently expose Upper Devonian shale (Gabrielse, 1991). The anticlines are commonly asymmetrical and axial planes within these folds are shown to change dip. de Wit et al. (1970) suggest that this phenomenon can be explained by transcurrent movements. Another characteristic of the MacKenzie Mountains is the sinuous arrangement of folds and thrust faults, with generally north-trending fold axes. Locally, fold axes are deflected to the north-northeast along several shear zones (de Wit et al., 1970). In contrast to the southern Rocky Mountain foothills, with their low angle thrust faults, the faults within the Mackenzie Platform have steeper dips, and therefore movement in this area has been vertical rather than horizontal (Law, 1971). Consequently, tectonic shortening has been considerably less in this region, in comparison to the southern Canadian Cordillera (Law, 1971).

Cook (1977) describes three phases of deformation within the Prairie Creek area, all within the Prairie Creek Embayment. These include early folding as seen in the Nahanni Formation. This folding is later cut by steeply dipping wrench faults, which were rejuvenated as high angle reverse faults, such as the Gate Fault (Figure 4). Morrow and Cook (1987) suggest that evidence for right-lateral wrench movement on the reverse faults is seen in folds just north of the South Nahanni River. Furthermore Morrow and Cook

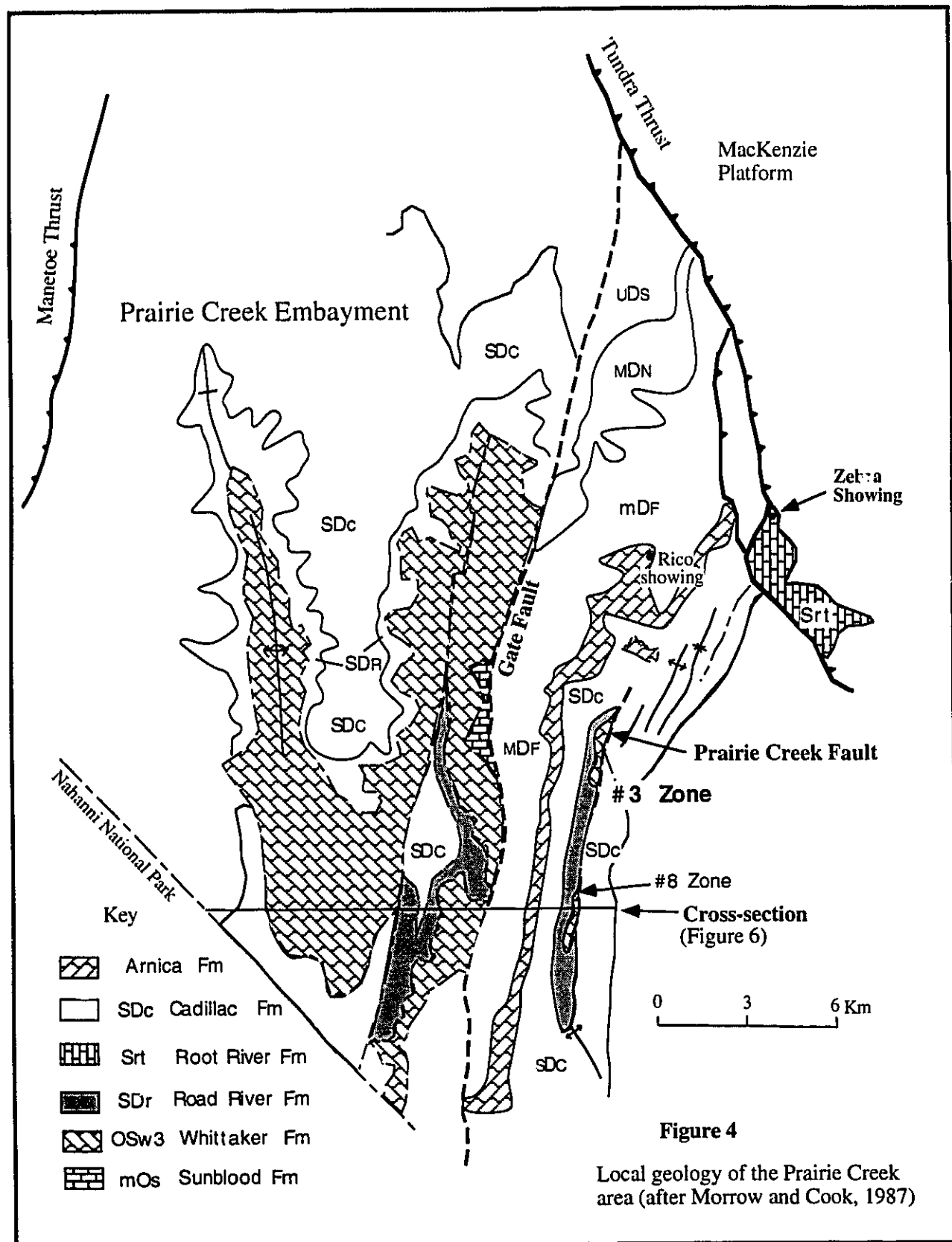
(1987) suggest that additional evidence for extensional structures include rapid changes in stratigraphy suggesting rapid subsidence within the Prairie Creek Embayment. While present flexural folds and reverse faults support compressional tectonics (Laramide deformation), the role of detachment faults is unclear. Kuszniir et al. (1987) have described similar basins in northwest Europe, where extension was replaced by compression. The authors mention that many of the faults that facilitated extension now inverted and became either high angle reverse or thrust faults, with attachments controlling not only the extensional tectonics, but also their inversion. The reverse faults are postdated by major, bedding-parallel thrust faults, such as the Tundra and Manetoe thrusts (Figure 4), which are found along the east and west flanks of the embayment. Cook (pers. comm., 1995) interprets all structures as being younger than Late Devonian.

### 2.1.3. Devono-Mississippian Tectonics and Heat Flow Events

There are no intrusions known to outcrop within the MacKenzie Platform and no volcanics have been documented in the southern MacKenzie Mountains. Morrow et al. (1990) suggested a regional thermal event occurred in the late Devonian to Mississippian from observation of the thermal maturation in conodonts from Lower Paleozoic sedimentary rocks in the Prairie Creek area. Ten conodonts from Middle Devonian carbonates possess color alteration index (CAI) values equal to 5, while Mississippian to Pennsylvanian rocks showed CAI values from 1 - 1.5. These indexes suggest temperatures ranging from 300 to 480°C for the former, with values from 50 to 90°C for the latter. While CAI is insensitive to pressure, it is affected by time (Harris, 1979; Utting et al., 1989) as well as temperature. To corroborate these findings and those of Aulstead and Spencer, (1985) and Feinstein et al. (1991), Morrow et al. (1993) determined vitrinite reflectance values from drill hole samples in the Laird Basin and Interior Plains. They found vitrinite reflectance values (Ro%) increase from a low value of 0.30% at the top of

the Carboniferous Mattson Formation to about 4.50% at the top of the Devonian Nahanni Formation in Laird Basin. In the Interior Plains, they observed less variation in vitrinite reflectance. The results indicate that Cretaceous burial in the Interior Plains was probably greater than in the Laird Basin north of 60 °N latitude. Morrow et al. (1993) suggest that the data indicate geothermal gradients approaching 65 °C/km during the Late Paleozoic in the Laird Basin and 45 °C/km in the Interior Plains, compared to present day gradients of 30-40 °C/km. These results therefore suggest a thermal event occurred within the southern MacKenzie Mountains region, during the late Devonian to early Mississippian.

Suggestions of a middle Devonian to early Mississippian tectonic event, known as Antler Orogeny in southeastern Yukon (Gordey et al. 1987; Smith et al. 1993), further support the concept of a thermal event in the MacKenzie Platform. Eisbacher (1983) has suggested sinistral movement of Proterozoic assemblages along the Richardson-Hess fault zone may have occurred during the late Paleozoic. This is consistent with possible major fault activity along the eastern edge of the Cordillera connecting the Devonian-Mississippian Ellesmerian orogen of the Arctic with the Antler orogen of the western U.S. (Boucot et al. 1974). The Misty Creek Embayment, in northern MacKenzie Mountains (Cecile, 1982), has been interpreted as a rift basin in which Middle Ordovician and Late Silurian to Middle Devonian volcanism was centred (Fritz et al. 1991). Within the Selwyn Basin, volcanic rocks are associated with Devonian-Mississippian sedimentary-exhalative (sedex) mineralization along syndepositional graben faults at MacMillan Pass (Abbott, 1986).



#### 2.1.4 Regional Mineralization in the Mackenzie Platform

Sangster and Lancaster (1976) refer to carbonate-hosted, Pb-Zn occurrences in the northern Cordillera as the MacKenzie Valley Lead-Zinc District, due to numerous occurrences of Pb-Zn mineralization in the region (Figure 5). Most of these occurrences are located in the northern MacKenzie Mountains and are hosted by rocks older than late Devonian, mostly Lower Cambrian Sekwi Formation (Dawson, 1975). Brock (1976) has described the early history of exploration for Pb-Zn mineralization in the Selwyn Basin and the northern MacKenzie fold belt including Goz Creek within the Bonnet-Plume Camp, Gayna River deposits within Proterozoic units (Hewton, 1982) and the Bear-Twit claims at Godlin Lakes. Brock (1976) states the latter deposit is hosted within intra-formational breccias of lower Ordovician shale-carbonate transition facies, possibly related to an overlying unconformity. At Godlin Lakes, Norford and MacQueen (1975) also reported that stratiform zinc-lead mineralization is found in Lower Cambrian Sekwi Formation dolostones and tetrahedrite, sphalerite and galena mineralization occurs in cross-cutting quartz veins. Heal (1976) describes Pb-Zn mineralization within Devonian carbonate rocks at the Wrigley-Lou occurrence.

Cecile and Morrow (1978) described coarsely crystalline sphalerite and galena occurring sporadically in vugs in Ordovician to Devonian dolomites of the Mount Kindle, Delorme (Morrow and Cook, 1987) and Arnica Formations, and massive sphalerite and minor galena in dolomitic veins cutting Delorme Formation near Palmer Lake, NWT. They suggested that the en echelon, west-northwest trending veins (perpendicular to the slope of the Misty Creek Embayment) may be related to dilational fracturing caused by compaction of thick basinal shaly strata or possibly to post-thrusting stress relaxation, because the veins are subparallel to thrust faults.

In the southern Logan Mountains, Dawson (1979) described stratiform occurrences of massive sphalerite-galena-pyrite, hosted by a cherty and carbonaceous black shale

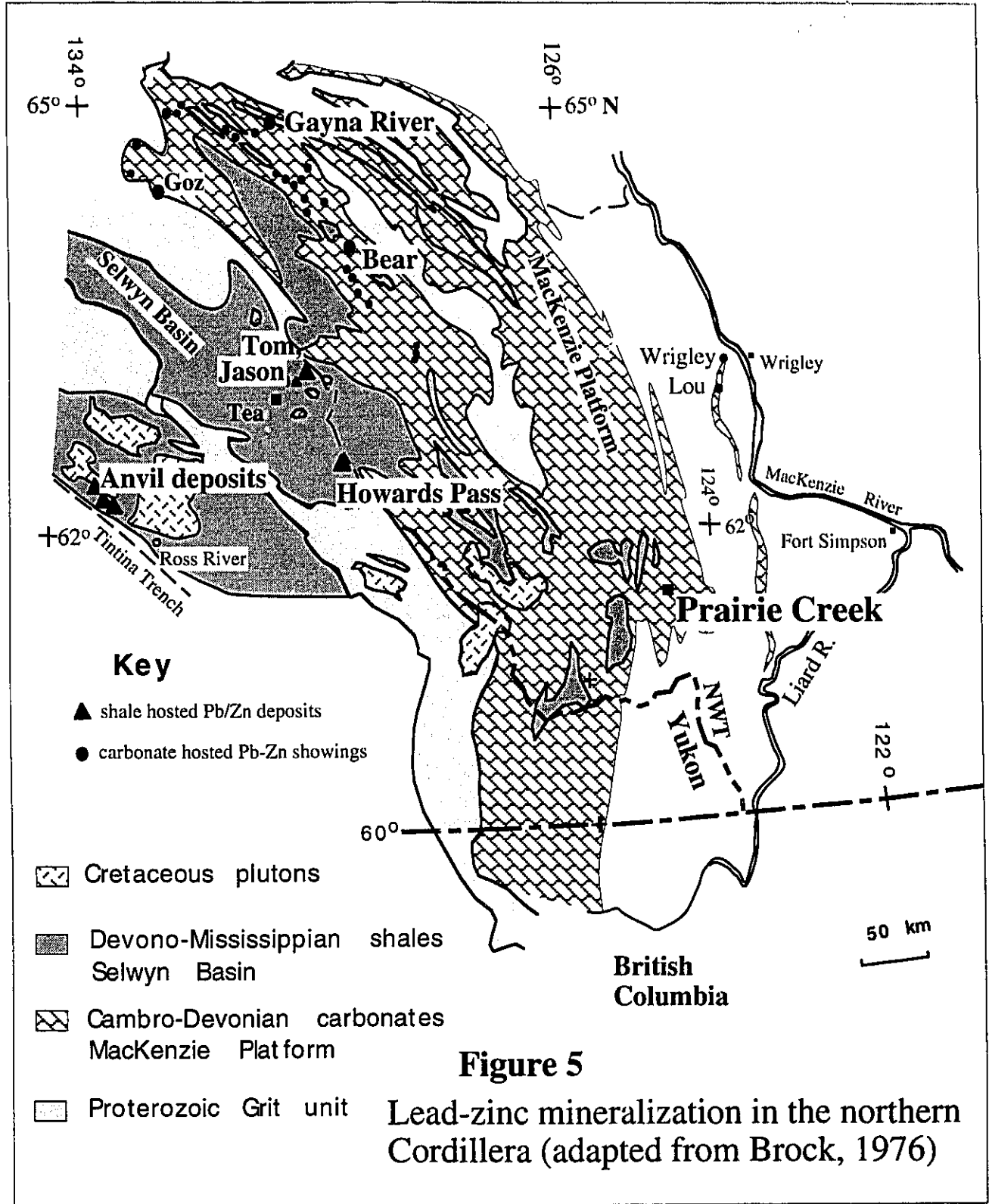
horizon of approximately 100 metre thickness. This shale horizon overlies a pyritic amygdaloidal basalt of similar thickness. Dawson (1979) suggests that the graptolitic shales are equivalent to Road River Formation host rocks at Howard's Pass. He also alludes to a massive sulfide occurrence in Ordovician volcanics and shales in the same area.

McLaren and Godwin (1979) determined minor element concentrations in sphalerite from carbonate-hosted zinc-lead deposits, along the edge of the Selwyn Basin and MacKenzie Platform. Concentrations of Ag, Cd, Co, Cu, Fe, Mn, Ni, Pb and Hg, were determined from 166 sphalerite specimens from 48 deposits. McLaren and Godwin (1979) determined that minor element variations within individual samples were insignificant compared to between deposit variations and concluded that each deposit could be characterized by minor elements in sphalerite. Their results indicate a bi-modal distribution, with enrichments in copper, lead and mercury and depletions in iron, relative to sphalerite from other zinc-lead districts in North America. They suggest that low concentrations of minor elements in sphalerite occur mainly in mineralization in Ordovician to Devonian units, while Proterozoic and lower Cambrian rocks host mineralization with higher concentrations of minor elements in sphalerite. They further suggest that the results reflect two ages of regional metallogeny, with two different mineralizing processes; 1) dewatering of a shale basin (Selwyn Basin) to produce metal-rich brines in younger (Ordovician to Devonian) hosts and 2) karst mineralization related to major unconformities during the middle to late Cambrian.

## **2.2.0 Local geology of the Prairie Creek Deposits**

### **2.2.1 Stratigraphy**

Nomenclature adopted for the stratigraphy of the Prairie Creek area is based on Morrow and Cook (1987). Middle Ordovician through upper Devonian sedimentary rocks



outcrop in the immediate Prairie Creek area (Figure 4). East of the Gate Fault, anticlinal ridges expose Whittaker Formation dolostones in apparent conformable relationship with overlying Road River Formation shales. At Cripple Creek (Figure 2), a drainage separating the #9 and #10 zones, Cadillac, Road River and Whittaker Formations appear conformable in outcrop. Middle Ordovician Sunblood argillaceous limestones are seen west of the Gate Fault and while an unconformity between Whittaker and Sunblood Formations has been reported by Morrow and Cook (1987), this was not observed by the author. From limited outcrop examination and drill core data, only one main unit of Whittaker Formation (unit OSw3) was seen in the study area (Figure 3). A detailed description of this unit is presented in Table II-1 below. The data are based on drill hole observations from San Andreas geologists. The relationship between sub-unit OSw3/1, a quartz arenite seen in drill holes PC-12, PC-29 and PC-41 and unit muOw2 quartzite mapped by Morrow and Cook (1987) were not investigated by the writer. Drill core cross-sections (6288N and 6045N), shown in Figures 15 and 16, illustrate stratigraphic relationships.

### 2.2.2 Structure

The Prairie Creek Fault is the main structural feature in the Prairie Creek area. This reverse dipping structure is up to 40 metres in thickness and is strongly graphitic. A 1500 metre displacement on this fault is interpreted from cross section (Morrow and Cook, 1987 Figure 6). On Section 6045N, Cadillac Formation is seen faulted below the Whittaker Formation at the bottom of the hole. Fractures are pervasive throughout Whittaker Formation carbonate rocks and calcite  $\pm$  quartz veining is generally seen filling millimetre to centimetre sized fractures.



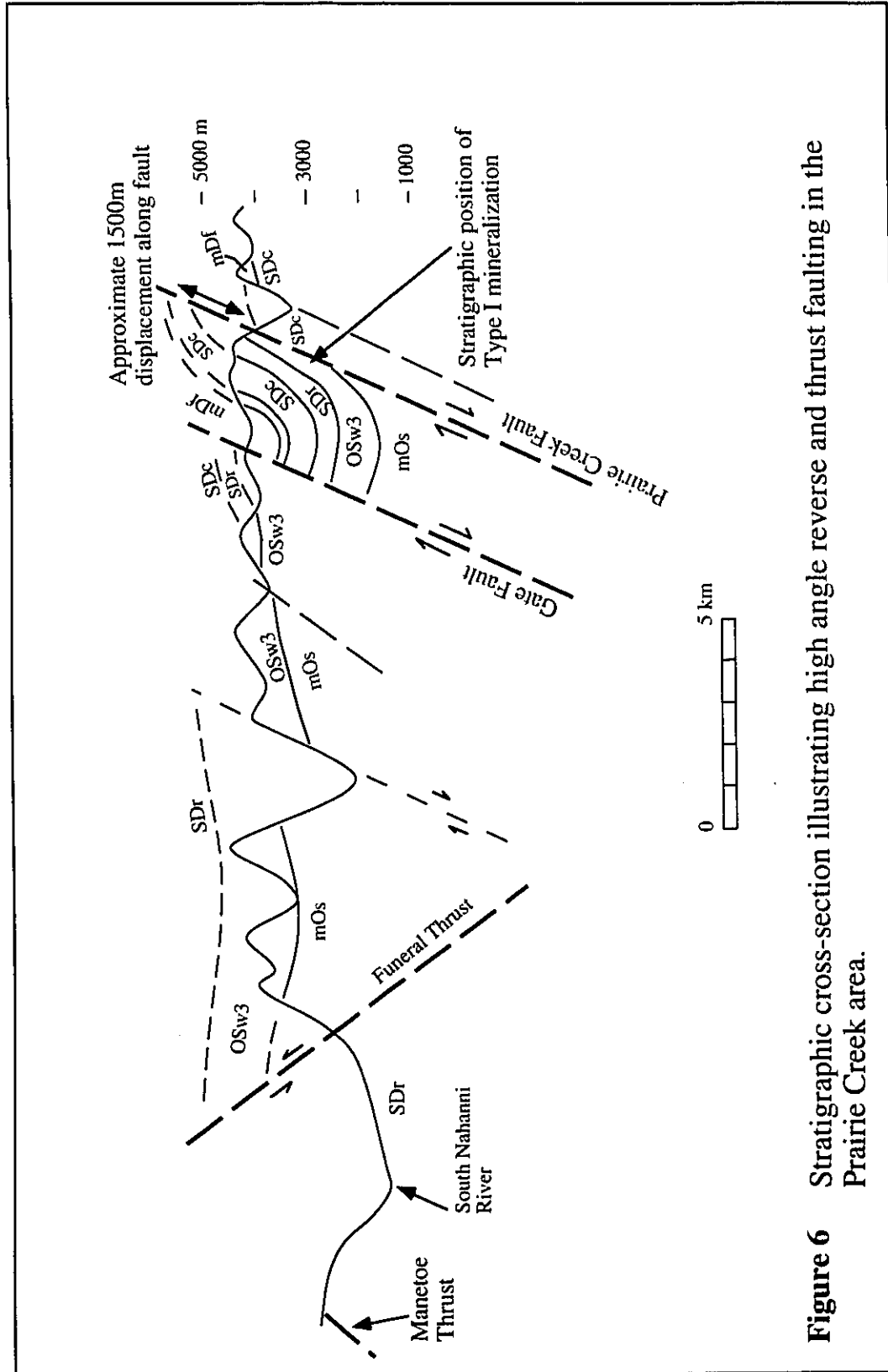


**Figure 6** Stratigraphic cross-section illustrating high angle reverse and thrust faulting in the Prairie Creek area.

**Table II-I** Stratigraphy of Whittaker Formation, (sub-unit OSw3/1 to 7) to Cadillac Formation from drill hole observations

Unit	Description	
SDc	Cadillac Formation	argillaceous limestone
SDr	Road River Formation	graptolitic shale to argillaceous limestone
<b>OSw3</b>	<b>Whittaker Formation</b>	
/7	Ribbon chert/ dolomite unit	Thin interbedded black chert bands (ribbon chert) and medium grained, brownish grey dolomite beds. Sharp contact with /6 below.
/6	Transition unit	Massive to weakly bedded dark grey, fine grained dolomite with rare chert bands overlying a 1 metre section of interbedded chert and dolomite.
/5	Upper spar unit	Massive to crudely bedded medium grey dolomite with abundant 1-6cm oval shaped pods of white sparry dolomite $\pm$ calcite $\pm$ quartz with long axes oriented parallel to bedding. Sulfides occasionally within or around the oval spar. Common thin walled brachiopod and crinoid fragments.
/4	Upper chert nodule/ dolomite unit grey	Medium to coarse grained, generally poorly bedded dolomite with occasional rounded nodules 1-5cm of to black chert
/3	Lower spar unit	Defined by first occurrence of significant sparry dolomite
	<b>Stratiform Massive Sulfide</b>	Banded pyrite, iron rich sphalerite and galena with sparry dolomite/calcite/quartz and jasperoid/chert
/2	Lower chert nodule/ dolomite unit	Similar to unit 4 but with more chert nodules and more extensively silicified
/1	Quartzite	Massive beds of granular, dirty quartzite interbedded with fine olive green to grey variably fossiliferous siltstone and dolomite

## **2.3.0 Geology of Mineralization at Prairie Creek**

### **2.3.1 Ore Types**

Three types of mineralization are present at Prairie Creek; 1) stratiform mineralization and 2) open-space fill epigenetic, possibly Mississippi-Valley Type (MVT) mineralization, and 3) quartz-sulfide veining. In addition, unmineralized calcite and quartz veining and brecciation structures are present.

#### **Stratiform Mineralization -Type I**

This style of mineralization, only observed in drill core, was discovered in 1992, from drilling in the #3 Zone. The term stratiform is used for the mineralization as it appears conformable with bedding. Section 6288N (Figure 15) illustrates the stratigraphic position of this mineralization within the Whittaker Formation. Figure 7 shows an isopach map illustrating thicknesses of stratiform mineralization intersected within the #3 Zone. This map, compiled by San Andreas geologists, compares the trend of stratiform mineralization (approximately 330 °N), to the trend of the quartz vein mineralization projected to surface (approximately 025 °N), in Zone #3. Figure 15 illustrates a cross section through the thickest portion of the stratiform mineralization (drill holes PC-11, 08, 13, 14 and PC-40) and the spatial relationship of the stratiform mineralization to quartz veining. Figure 16 (6045N), shows a cross-section through more pyritic-rich mineralization and its relationship to the Prairie Creek Fault. Figures 15 and 8 illustrate the tabular nature of the stratiform mineralization.

Stratiform mineralization consists of very fine to medium grained, locally banded pyrite and sphalerite (Plate 1), and rare galena. Mineralization from sphalerite and galena with minor pyrite grades outward into more pyritic zones, with disseminated sphalerite, along its upper and lower contacts with dolostone. Sphalerite also occurs disseminated within massive pyrite (sample PC-11 261.3m). Gangue dolomite, as blebs and as veinlets

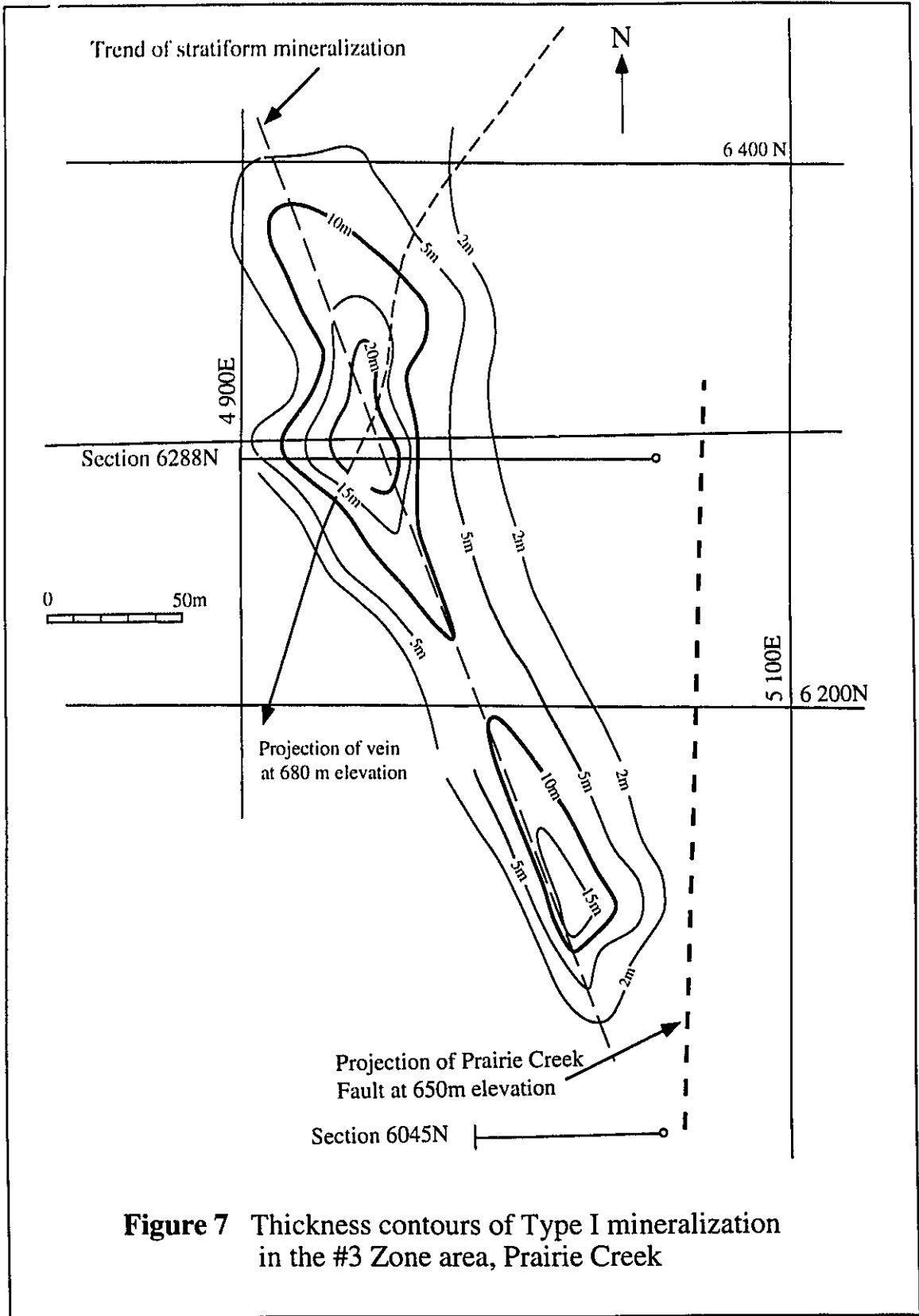


**Figure 7** Thickness contours of Type I mineralization in the #3 Zone area, Prairie Creek

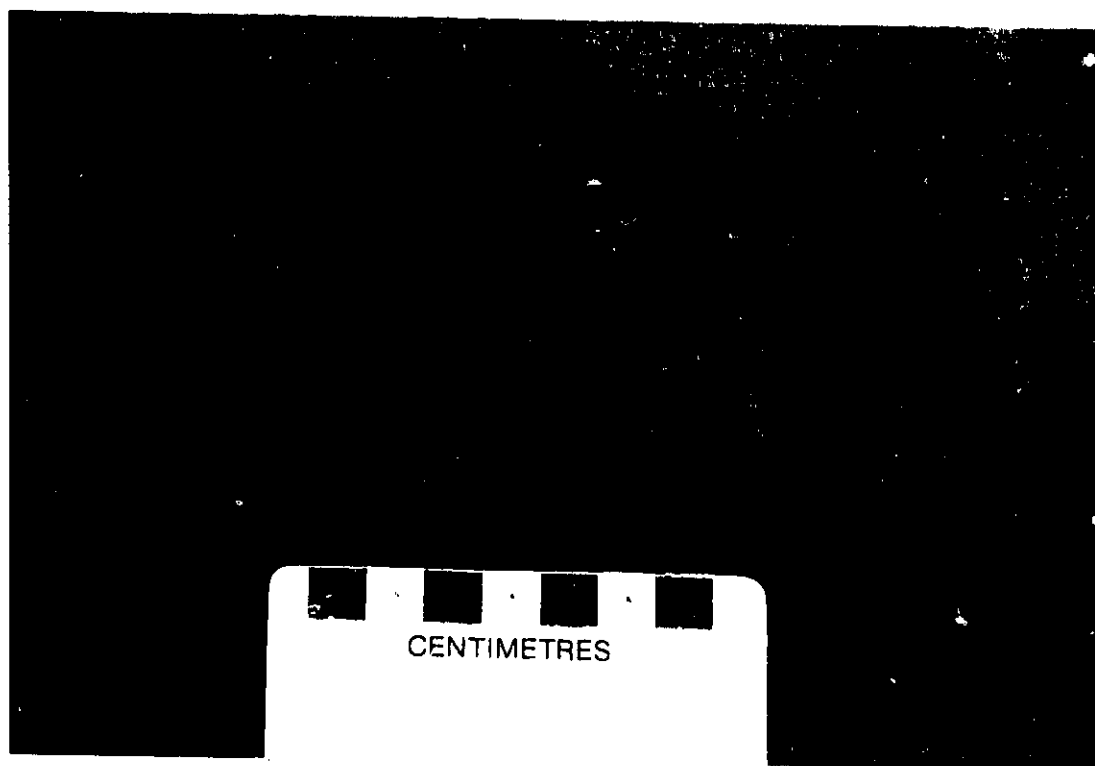


Plate 1 Type I mineralization with fine to very fine grained pyrite and sphalerite within (mottled) siliceous matrix with top of mineralization to the left of photo. Sphalerite appears pink to buff colored in centre of photo, adjacent pyrite. Sample # PC-08 295.7m.

up to two centimetres in width, are present in stratiform mineralization. Drilling to the end of 1994 indicated stratiform mineralization extends south to the #8 zone. Drilling to 1994 indicated zones #3 and #6 have significant Zn-Pb intersections in stratiform mineralization, while drilling on zones #7 and #8 intersected mainly pyritic rich mineralization. Stratiform mineralization in places is strongly associated with a mottled texture seen in dolomitic host rock (Plate 2). This mottling texture comprises microcrystalline quartz, quartz overgrowths, coarse-grained euhedral dolomite and locally pyrite grains. Sparry calcite pods with pyritic rims are found stratigraphically above stratiform mineralization. Drilling during 1995 suggests that these calcite pods with pyrite are stacked massive sulfide lenses and may be distal (?) to stratiform, Pb-Zn mineralization (personal communication, B. Nesbitt).

### **Zebra style mineralization - Type II**

A second style of Pb-Zn mineralization is seen at the Zebra showing, which is located approximately 5 km to the northeast of the #3 Zone (Figure 4). Prior to 1994, limited diamond drilling had been done on this showing. The showing is hosted in middle Silurian Root River dolostones (personal communication, D. Morrow). This style of Zn-Pb mineralization differs from the previous ore types in its association with saddle dolomite cement (Radke and Mathis, 1980) observed here as coarse-grained and yellowish to white. (Plate 3). Sphalerite occurs as a reddish-orange variety in blebs, often with anhedral pyrite, as rims to dolomitic cement. A second variety of sphalerite, a dull, grayish-brown colloform sphalerite, also occurs at the Zebra showing and is associated with coarse-grained, yellowish dolomitic cement. Minor galena is present. A similar style of mineralization is also present at the Zulu showing, located north of the Zebra showing.

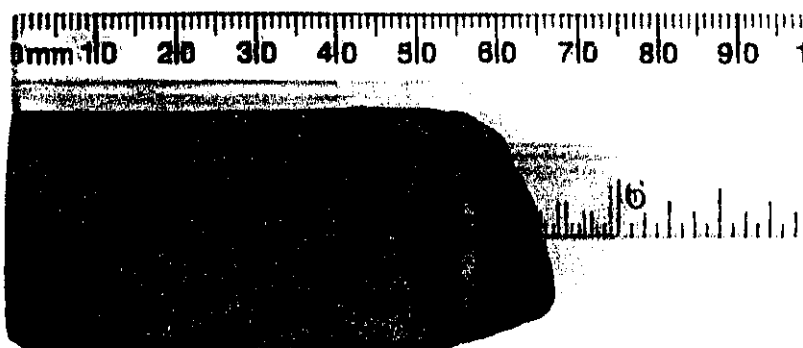


Plate 2      Distinct mottled texture associated with Type I mineralization

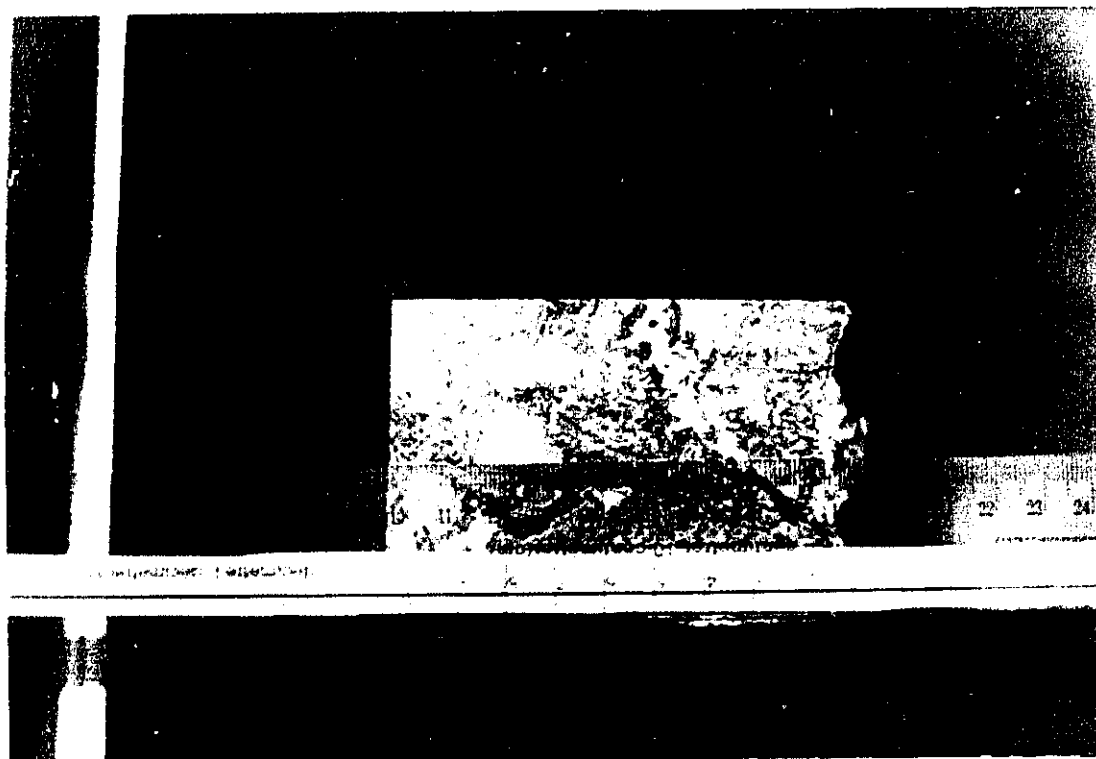


Plate 3

Coarse-grained saddle dolomite cement (white in photo) associated with Type II sphalerite and pyrite mineralization



### Quartz Veining - Type III ores

Quartz-sulfide veining at Prairie Creek, described by Thorpe (1972), constitutes approximately 1.4 million tons of mineralization grading 10.9% Pb, 13.5% Zn, 192 oz/ton Ag, 0.52% Cu and 0.09% Cd (DIAND, 1984). Thorpe (1972) examined quartz veins in 11 different zones over an eleven kilometre length along the system (Figure 2) and found that the quartz veins were formed along shear zones and were not continuous along strike.

Observations in this study in the 3050 Level portal indicate that the quartz veins form along graphitic faults. In zones 1 and 2 east of the Prairie Creek tributary, the veins strike N45°W and dip east, while in zones 3 to 11, quartz veining follows a shear zone that strikes N10°E and dips between 54 and 60° east (Thorpe, 1972). While relationship of the Prairie Creek Fault to shearing along quartz veins is unclear, common graphitic slips suggest that the shearing may be related to splays from the Prairie Creek Fault. The width of the quartz veins vary from 0.6 to 6.1m and average 4.5m (DIAND, 1984). Vein quartz is characteristically massive, white quartz with locally drusy quartz overgrowths. Yellowish-white dolomite is often seen in vein quartz, probably as wallrock fragments. Drill hole and surface observations at Prairie Creek indicate that quartz veining cuts the Upper Ordovician-Lower Silurian Whittaker Formation (unit OSw3/1) and the Lower Devonian, Arnica Formation dolostones. Smithsonite, from quartz veining and massive boulders (a metre in size), is seen in the #8 Zone. In the #9 Zone, tetrahedrite mineralization is found with malachite and azurite.

Thorpe (1972) documented a zonation in metal concentrations in the quartz veins. In zones 1 and 2, he observed high Pb-Ag values in comparison to zones to the south (Figure 2). From zones 3 to 11, Thorpe (1972) found increasing zinc and copper concentrations with lesser silver values.

### **Unmineralized Veins and Brecciation**

Unmineralized calcite veining is common throughout the drill core, generally ranging from one to two millimetres in width and is occasionally present as blebs, up to a centimetre in diameter. Thicker calcite veining up to 25 centimetres is observed in the Zone #8 adit. This vein is approximately five metres east of the Prairie Creek Fault, in Cadillac argillaceous limestone and runs parallel to the structure. Graphitic contacts along this vein and its close position to the Prairie Creek Fault, suggest a temporal relationship to shearing along the Prairie Creek Fault.

While calcite veining is generally not mineralized, crackle breccia (Morrow, 1982) is seen with non-ferroan calcite and pyrite as cement, over less than a metre thickness (sample PC-13 282.3m). Rounded and fragmented galena and sphalerite grains in the breccia suggest brecciation is post-mineralization. The extent of this mineralization appears limited and its relationship to faulting is unclear.

Brecciated quartz veining appears to be generally unmineralized in Whittaker Formation rocks. In sample PC-28 108m, brecciated quartz is unmineralized over several metres thickness and in section appears podiform. DIAND (1984) geologists have interpreted such brecciated quartz as tectonic quartz produced by Laramide tectonics. Post-mineralization brecciation of quartz, pyrite, galena and sphalerite is seen in drill hole PC-14 at 247.9m. At the Rico showing, in Arica Formation dolostone, sphalerite, galena and tetrahedrite mineralization are seen in brecciated quartz (0.5m thickness) and brecciation appears to be post-mineralization.

## Chapter III Mineralogy and Paragenesis of the Prairie Creek Deposits

### 3.0 Introduction

Microscopic examinations of thin and polished ore sections as well as cathodoluminescence observations of sparry dolomite, were used in documenting mineralogy, alteration and paragenetic relationships. Microprobe analyses of sphalerites and dolomites were used in determining trace element concentrations. Table III-1 lists the paragenetic sequence in the Prairie Creek deposit.

**Table III-1 Paragenetic Relationships**

Sequences	Early	Late
Limestone deposition and silicicastics formation	-----	
Early formation of stylolites	---	
Early dolomitization of limestone	----	
Formation of authigenic quartz and euhedral dolomite	---	
Stratiform Type I mineralization, gangue dolomite	-----	
Saddle dolomite formation and Type II mineralization	----	
Hydrocarbons	--?--	
Quartz veining with pyrite, sphalerite, galena, tennantite/tetrahedrite mineralization (Type III)		-----
Quartz overgrowths		-----Quartz
brecciation		---
Calcite veining		---
Stylolite formation		---
Brecciation (calcite fluids)		---
Smithsonite, malachite formation through weathering		---

### 3.1 Petrographic Observations

#### *Regional Dolomitization*

Three phases of dolomitization are present in the Prairie Creek area, based on petrographic and cathodoluminescence observations. Early pervasive dolomitization of coral and crinoid bearing shelf carbonates occurred during the middle Devonian (Morrow and Cook, 1987). Dolomitized fossil fragments in Whittaker Formation generally show little disturbance. Coarse grained euhedral dolomite forms as trapped rhombohedral crystals within microcrystalline quartz (Plate 4). Cathodoluminescence studies indicate that the coarse euhedral dolomite has a similar luminescence to matrix dolomite and therefore suggest that pervasive dolomitization is coincident in part, with silicification. Sample PC-08 at 239m illustrates stylolites, within early dolomitization, that are partially truncated by infilling chert masses and therefore indicates early stylolitization occurred roughly contemporaneously with chert formation.

Descriptions of gangue dolomites associated with mineralization Types I, II and III appear below with respective ore type. Listed below in Table III-2 are microprobe analyses for trace elements Fe, Zn, Sr, and Mn from dolomites.

**Table III-2** Microprobe Analyses (averages in wt %) for Trace Elements from Dolomites

Dolomite type	# of analyses	Fe	Zn	Sr	Mn
Type I gangue dolomite (4 samples)	37	0.24 ± 0.15	0.22 ± 0.12	0.033 ± 0.01	1.40 ± 0.11
Type II dolomitic cement (Zebra and Zulu cements)	15	undetected	0.008 ± 0.001	0.013 ± 0.006	0.026 ± 0.014
Type II host dolomite (Zebra showing)	14	0.013 ± 0.08	0.013 ± 0.01	0.009 ± .004	0.018 ± .006

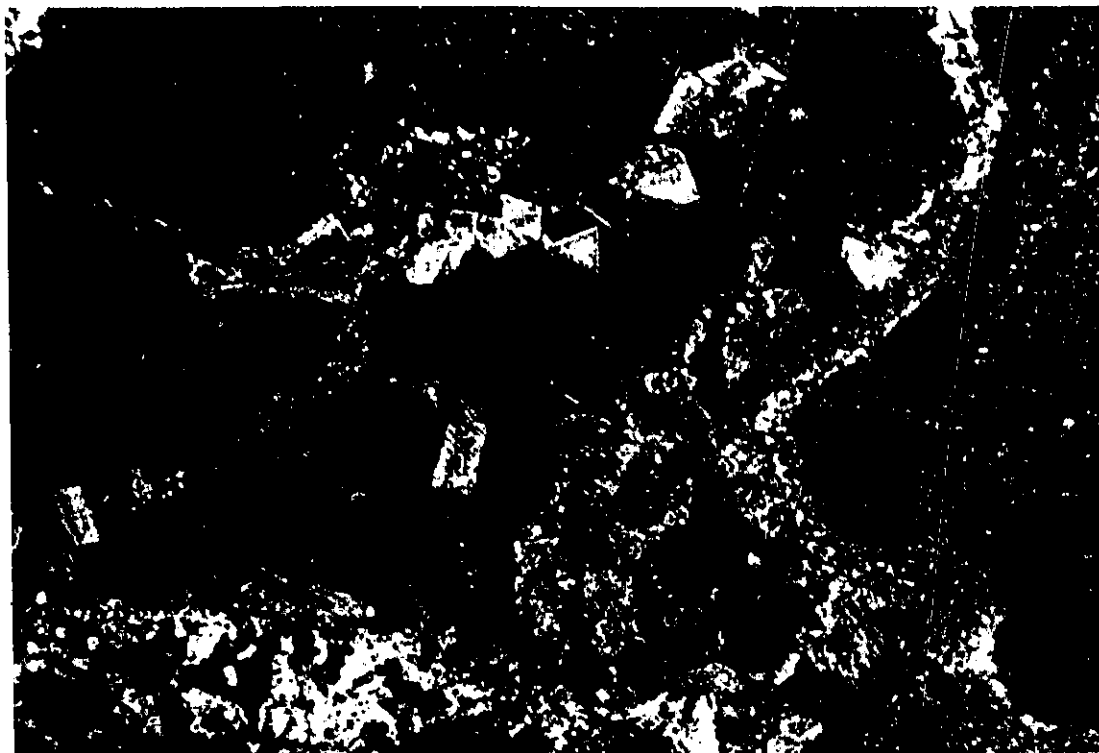


Plate 4

Coarse-grained euhedral dolomite trapped within microcrystalline quartz suggesting that dolomitization and silicification are contemporaneous.

### *Type I mineralization*

The mineralogy of the stratiform, Type I ores is composed of sphalerite, galena and pyrite and/or marcasite. Galena wraps around pyrite and sphalerite suggesting a late timing for its deposition. Gangue mineralogy consists of sparry dolomite, vein calcite, euhedral quartz and trace fluorite.

Two types of sphalerite have been observed in the stratiform mineralization. These include, 1) a fine-grained, zoned sphalerite ranging in color from orange to amber to clear (Plate 5). This sphalerite is often enclosed within poikilitic crystals of variably sized pyrite and/or marcasite. The sphalerite appears to have grown across dolomite rhombs suggesting formation by replacement of dolomite. 2) The second type of sphalerite appears to have filled open spaces in gangue dolomite. Locally sphalerite veinlets, cut coarse-grained gangue dolomite. This cross-cutting relationship is well illustrated by cathodoluminescence. The second type of sphalerite is characterized by opaque inclusions in sphalerite. Pyrite is present as variably sized anhedral grains and often forms a border to both gangue dolomite and/or sphalerite and sparry calcite. Pyrite abundances increase toward the upper and lower dolomitic contacts of the stratiform mineralization. Galena, which is minor in abundance, occurs as relatively coarse-grained blebs up to two mm, often near more sphalerite-rich sections.

A second phase of dolomitization is associated with stratiform (Type I) mineralization and consists of a white gangue dolomite in Whittaker Formation. In thin section, these dolomites are up to two mm in diameter, and have clear rims and cloudy centres. The cloudiness results from a core rich in inclusions. Under cathodoluminescence, these gangue, white dolomites are characterized by a bright red luminescence. Microprobe analyses of these dolomites indicate low iron, zinc, and strontium but high manganese values, up to two weight percent. Averages from these gangue dolomites for iron, zinc, strontium, and manganese include  $0.24 \pm 0.15$ ,  $0.22 \pm 0.12$ ,  $0.13 \pm 0.00$ , and  $1.40 \pm 0.11$  weight percents respectively (Table III-2 and appendix). The high manganese

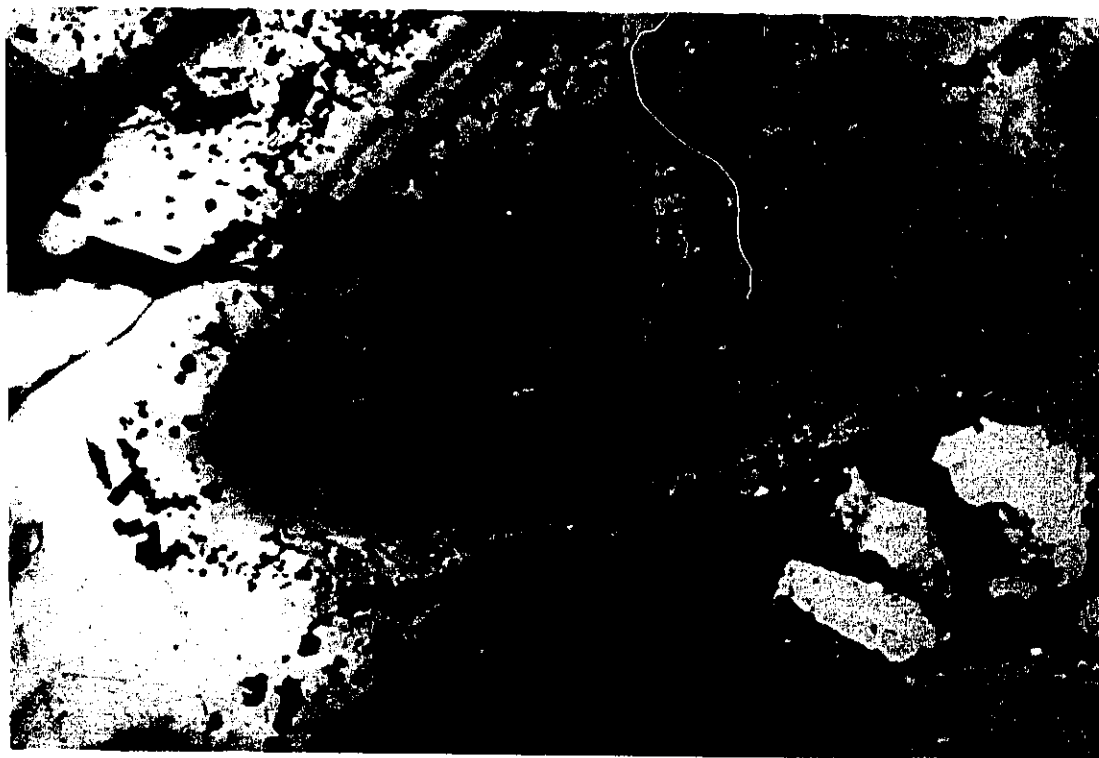


Plate 5      Photomicrograph of zoned sphalerite (Type I mineralization) under plane-polarized light.

concentration is consistent with the cathodoluminescence observations as manganese acts as an activator in luminescence (Machel, 1985). Staining of the gangue dolomites shows minor bluish staining indicating local iron enrichment.

While the paragenetic relationships of the sparry dolomite gangue to stratiform ore is unclear from drill core specimens, the high manganese concentration in these dolomites and associated chert, suggests formation from ore-forming fluids. Russell (1974) documented a manganese halo surrounding the Tynagh Pb-Zn deposit in Ireland and manganese is also associated with ore-forming fluids at the Meggan deposit (Gwosdz and Krebs, 1977).

Late calcite veining in stratiform ore, is composed of non-ferroan calcite both as millimetre sized veinlets, which cut gangue dolomite, and as coarse blebs. Calcite commonly displays twinning and exhibits a yellowish-orange luminescence.

As alluded to in Chapter II, Type I ores are associated with a mottled texture in the host dolomite comprised of microcrystalline quartz, dolomite and needle-like sphalerite grains. The needle-like sphalerite grains, which do not appear to be associated with distinct fractures, may represent stalactitic growth in cavities (sample PC-08 295.65m) as described by Russell (1985) in the Irish, Navan deposit. Overgrowths increase in size away from the contact of dolomite and microcrystalline quartz, with pyrite, but the relative timing of this quartz overgrowth is unclear. Stratiform ores are cut by several generations of quartz veining.

### *Type II mineralization*

The mineralogy of the type II ores consists of variable amounts of sphalerite, anhedral pyrite, coarse-grained, saddle dolomite cement, in a coarse-grained dolomitic host rock. Sphalerite is present as coarse-grained colloform and medium-grained reddish-brown varieties. At the Zebra and Zulu showings, pyrite and sphalerite mineralization forms along



rims of white and yellowish-white, coarse-grained saddle dolomitic gangue. The dolomite grains average several millimetres in size. Host rock for this mineralization is a coarse-grained dolomite, averaging one to two millimetres in size. The dolomitic cements have curved cleavage planes and exhibit the distinctive sweeping extinction under cross polars seen in saddle dolomite (Plate 6) (Radke and Mathis, 1980; McQueen and Krebs, 1983). Both dolomites exhibit a dull red luminescence under cathodoluminescence. Minor veinlets of bright red luminescent dolomite cut dull luminescent dolomite, and are suggestive of later dolomitizing fluids.

In contrast to the high manganese values seen in gangue dolomite associated with Type I mineralization, microprobe analyses of the dolomites from Type II mineralization indicate low manganese concentration as well as iron, zinc and strontium. Averages in weight percent for iron, zinc, strontium and manganese in saddle dolomite include iron below detection,  $0.01 \pm 0.02$ ,  $0.02 \pm 0.01$ , and  $0.02 \pm 0.01$  respectively. Averages for Zebra and Zulu host dolomites for iron, zinc, strontium and manganese include  $0.10 \pm 0.05$ ,  $0.01 \pm 0.01$ ,  $<0.01$  and  $0.01 \pm 0.01$  weight percent (Table III-2 and Appendix 1). Bitumen (?) is observed as a pale bluish fluorescence, under fluorescent microscopy, along sphalerite grain margins in Type II ores.

### *Type III mineralization*

Type III, quartz-sulfide vein mineralization is more complex mineralogically than the other types of mineralization. Sphalerite, galena, tetrahedrite and minor pyrargyrite are the principal ore minerals present in vein mineralization, while quartz, pyrite, calcite and dolomite constitute the gangue. Sphalerite forms coarse-grained (up to a cm) tan to yellowish-green colored grains, and often displays deformation features (Plate 7). Sphalerite has fluid inclusions which are often opaque, due to internal reflectance. In the #8 portal, smithsonite veinlets, form in sphalerite in quartz veins indicating late stage



Plate 6      Photomicrograph of saddle dolomite cement illustrating curved cleavage planes and undulose extinction under cross polar light.



Plate 7      Photomicrograph illustrating deformation features in sphalerite, Type III mineralization.

oxidation. Pyrite occurs as anhedral grains and is found as fine to coarse-grained. Sparry dolomite and weakly ferroan calcite are present in fractures in quartz.

The presence of scheelite and stibnite has been reported at Prairie Creek (Financial Post, 1980). While quartz arenites (sample PC-14 314m), of the Whittaker Formation, unit OSw3/1, has detrital scheelite ( $\text{CaWO}_4$ ) and possibly powellite, scheelite has otherwise not been identified in this study.

The mineralized quartz veins cut matrix dolomite and in turn, quartz veins are cut by calcite veining. Locally, quartz overgrowths (up to a mm in size) are observed as a drusy quartz coating over dolomitic rock. In sample 3-D-22 at 194m, quartz overgrowths are seen as euhedral crystals to 5mm in length. In sample PC-28 260m, three generations of quartz are observed; a late veinlet cutting microcrystalline quartz and quartz overgrowths on microcrystalline quartz. Fractures within the late veinlet indicate crack-seal deformation (Ramsey, 1980) as veinlet has opened and filled with dolomite and top of quartz grains are alligned perpendicular to wallrock boundaries.

Gangue dolomite from type III ore was analyzed from sample 3-C-26 and weight percentages for iron, manganese, zinc and strontium include  $1.15 \pm 0.29$ ,  $1.45 \pm 0.18$ ,  $0.13 \pm 0.08$  and  $0.03 \pm 0.01$ . Microprobe analyses on wallrock dolomite from this sample gave the following results for iron, manganese, zinc and strontium concentrations,  $0.09 \pm 0.07$ ,  $0.04 \pm 0.03$ ,  $0.01 \pm 0.01$ , and  $0.01 \pm 0.02$  weight percent.

#### *Other Veining and Brecciation*

Unmineralized vein carbonate is both ferroan (>2.0 weight percent Fe) and non-ferroan. Timing relationships are unclear but ferroan calcite appears to be younger than non-ferroan calcite. While little mineralization is generally associated with calcite veining, pyrite appears in the groundmass with non-ferroan calcite in brecciated structures (sample PC-13 at 282.3m) as crackle breccias. This brecciation is developed within stratiform mineralization and is thought to be related to faulting (based on the presence of fault

gouge). Rounded sphalerite and galena grains within a matrix of calcite suggest brecciation occurred post mineralization.

### 3.2 Sphalerite chemistry

Microprobe analyses of sphalerites from mineralization Types I, II and III are illustrated in the appendix and summarized in Table III-3. Initial microprobe analyses of Types I and II sphalerites indicate very low concentrations of iron, and trace abundances of manganese, gallium, germanium, cadmium and indium. Additional microprobe analyses were performed to include Type II sphalerites and trace elements As, Cd, Sb and Hg were also investigated.

Type I sphalerite typically contains less cadmium (average value  $0.006 \pm 0.02$ ) than both type II and III sphalerites (Table III-3). Type II sphalerites indicate the greatest percentage cadmium with values of  $0.751 \pm 0.25$  from the Zebra showing and  $0.375 \pm 0.13$  from colloform sphalerite. Mercury geochemistry indicates highest values in vein sphalerites from the Rico showing to 0.50 weight percent, while Type II sphalerite mineralization have slightly depleted values in mercury. Iron values are fairly consistent for the three types. Germanium is slightly enriched in stratiform mineralization, ranging from 0.03 to 0.34, averaging  $0.09 \pm 0.10$  weight percent. Germanium values to 0.04 weight percent, were recorded in vein sphalerite. Negligible analytical variation in manganese, gallium, indium, arsenic and antimony were recorded in sphalerites from the two ore types.

Table III-3 Sphalerite Geochemistry from Microprobe Analyses

Sample # Hg	Mn	Fe		As	Cd	Sb
<b>Type I mineralization</b>						
PC-13 290.7m N=22	0.002±0.004	0.508±0.42	0.009±0.02	0.006±0.02	0.006±0.009	0.198 ±0.16
<b>Type II</b>						
Zebra sphalerite N=18	0.009±0.01	0.576±0.43	-	0.751±0.25	0.012±0.02	0.107±0.16
Colloform sph. N=38	0.034±0.03	0.584±0.46	0.006±0.02	0.375±0.13	0.003±0.01	0.033±0.09
<b>Type III mineralization</b>						
PC-37 173.2m N=21	0.003 ±0.004	0.54±0.03	0.01±0.02	0.213 ±0.05	0.012 ±0.02	0.107±0.16
Rico showing N=10	0.006±0.005	0.32±0.11	-	0.26±0.07	0.002±0.004	0.502 ±0.11

## Fluid Inclusion Study - Chapter IV

### 4.1 Introduction

Fluid inclusion studies are commonly used in ore deposits research to determine the chemistry of ore-forming fluids. Such studies are used to determine the composition, temperature, and pressure of the fluids at the time of trapping and thereby assist in defining spatial and temporal relations within a hydrothermal system. Two fundamental assumptions are made when considering the results from fluid inclusion studies: 1) that the fluid within an inclusion represents the bulk composition of the fluid system from which the mineral formed; and 2) that no leakage in or out of the inclusions has occurred.

Roedder (1984) has defined three types of fluid inclusions, primary, pseudo-secondary and secondary. Primary inclusions represent the trapping of fluids from which the grain is growing. Inclusions formed from fluids that were introduced into fractures during crystal growth are termed pseudosecondary inclusions, while fluids introduced into fractures after crystal growth are called secondary. Criteria for recognition of each of the three inclusion types are listed in Roedder (1984).

Aulstead (1987) and Aulstead et al. (1988) obtained fluid inclusion data from Manetoe Facies dolomite, quartz, calcite, barite and fluorite from drill cores from shallow (1000m wells west of Fort Simpson) and deep drilling (4000m wells in the gas-bearing Beaver River area). They found little difference in homogenization and melting temperatures from dolomite cements from different depths, but differences in fluid inclusion results from quartz and calcite cements were noted. Aulstead et al. (1987) and Morrow et al., (1990) concluded that dolomitization was produced by hot (150 - 210°C), hypersaline (18 - 29 eq. wt. % NaCl) brines. They suggested that dolomitization of lower Paleozoic limestone was contemporaneous with formation of white, sparry dolomite cement in the Manetoe Facies. Aulstead et al. (1987) and Morrow et al. (1990) suggested that Pb-Zn mineralization in Manetoe Facies was formed during the Mesozoic and that

fluid inclusion results (broad range in salinities) from quartz and calcite indicated evolution of the fluid regime (from hypersaline brines to meteoric water).

Qing and Mountjoy (1992) examined fluid inclusions from sparry dolomite from the Middle Devonian Presqu'île barrier reef, over a 400 km distance from northeastern B.C. to Pine Point, NWT. Their data from saddle dolomites show an eastward decrease in homogenization temperatures (from 178 to 92°C). Based on stratigraphic reconstructions of the region, they determined that pressure-corrected homogenization temperatures exceeded maximum burial temperatures. They suggested that homogenization temperatures in dolomites, stable isotope and  $^{87}\text{Sr}/^{86}\text{Sr}$  results (and consequently associated Zn-Pb mineralization at Pine Point) may be explained by large scale migration of hydrothermal fluids updip along the Presqu'île barrier related to tectonic events during the Late Jurassic to early Cretaceous and Late Cretaceous to early Tertiary.

On the basis of stable isotopic and fluid inclusion studies of Cambrian carbonate rocks in the southern Canadian Rockies, Nesbitt and Muehlenbachs (1994) suggested that during the Late Devonian to Early Mississippian, a warm brine ( $150 \pm 25$  °C and salinities to 25 eq. wt % NaCl) migrated eastward forming large bodies of coarse sparry dolomite. Such dolomite locally hosts MVT style, Pb-Zn mineralization as seen at the Monarch Mine, near Field, B.C. Nesbitt and Muehlenbachs (1994) speculated that a simultaneous fluid event may have accounted for Pb-Zn mineralization at Pine Point.

As part of this study of the Prairie Creek Zn-Pb-Ag deposit, fluid inclusions in quartz, calcite, dolomite and sphalerite were examined from Type I and vein (Type III) mineralization in Whittaker Formation, minor quartz veins in Arnica Formation (Rico showing) and host and saddle dolomite within Type II sphalerite mineralization in the Root River Formation (Zebra and Zulu showings). These formations are all stratigraphically below the Manetoe Facies (Figure 3).



## Analytical Techniques

A modified Fluid Inc. USGS gas-flow heating-freezing stage with a Doric Trendicator 410A digital thermometric control system attached to a Leitz microscope was used in this study. Calibration of the stage was made using a distilled water bath, pure CO<sub>2</sub> inclusions of Alpine vein quartz, and liquid nitrogen. Errors in microthermometric determinations include  $\pm 0.2$  °C for freezing and  $\pm 2.0$  °C for heating to 250°C (Hardy, 1992).

Doubly polished inclusion 'chips' from vein quartz as well as sections of sphalerite and dolomite gangue from stratiform mineralization were examined from drill core samples, while dolomite and sphalerite from the Zebra showing were taken from outcrop. Two techniques were used in preparing doubly polished thick sections (~100 µm) for fluid inclusion analyses. Quartz samples were polished using aluminium oxide, while sphalerite, calcite and dolomite samples were polished using diamond paste. Initially, the fluid inclusion 'chips' were mounted onto frosted glass slides using a low temperature epoxy, but superglue proved to be more efficient as a glue in mounting chips and eliminated the need of any additional heating process. Once the area of a chip was determined for analysis, the desired section was cut and allowed to sit in an acetone bath overnight, dissolving the superglue and freeing the chip for microscopic study.

*Freezing tests* The procedure used in this study was to first freeze the inclusions (many of which were <5 micrometres in size). Data from freezing studies provide information on composition and salinity of the fluid from which the mineral formed. As the inclusion is allowed to warm up, eutectic temperature ( $T_e$ ) or the temperature of first melt is observed where optics are favourable. The eutectic temperature indicates the proportions of Ca and Mg versus Na chlorides of the fluid within the inclusion. To assist in determining this phase change, the procedure used is based on Shepard et al. (1985, Figure 6.8A). After freezing the inclusion and allowing it to warm until a single ice crystal

remains, the inclusion is allowed to freeze with the last ice crystal growing covering most of the inclusion. The inclusion is frozen to  $-100^{\circ}\text{C}$  and then allowed to warm slowly observing changes. The eutectic temperature change may be observed in the fraction of the inclusion adjacent the newly seeded ice. The temperature of final ice melt ( $T_m$ ) is determined when the last particle of ice melts in the inclusion and is an indication of the total dissolved solids of the aqueous liquid in the inclusion. Determination of this temperature is aided by the technique of 'cycling' (Shepard et al., 1985).

Salinity (as equivalent weight % NaCl) was determined from the  $T_m$  data using the formula of Potter et al. (1979):

$$\text{Eq. wt \% NaCl} = 0.00 + 1.76958 * - 4.2384 \times 10^{-2} *^2 + 5.27 \times 10^{-4} *^3$$

where \* is the depression temperature of final ice melt in  $^{\circ}\text{C}$ .

The presence of gases such as  $\text{CO}_2$  and  $\text{CH}_4$  complicate freezing behavior in inclusions. Upon freezing, in  $\text{H}_2\text{O-NaCl-CO}_2$  inclusions, clathrates form complex molecules with the formula:

$m * 5.75\text{H}_2\text{O}$ , where m may include  $\text{CO}_2$ ,  $\text{CH}_4$ ,  $\text{N}_2$  and/or  $\text{H}_2\text{S}$  (Shepard et al. 1985). The depression of clathrate dissociation below  $+10^{\circ}\text{C}$  (the melting temperature for pure  $\text{CO}_2\text{-H}_2\text{O}$  clathrate at 50 bars pressure) may be used to determine salinities from the equation of Bozzo et al. (1973):

$$\text{Eq. wt \% NaCl} = 15.52023 - 1.02342\theta - 5.286 \times 10^{-2}\theta^2, \text{ where } \theta \text{ is the temperature of clathrate melting in } ^{\circ}\text{C}.$$

Clathrate melting temperatures in excess of  $+10^{\circ}\text{C}$  indicate the presence of gases other than  $\text{CO}_2$ . The presence of methane will inhibit clathrate melting, while salinity increases melting temperatures (Roedder, 1984).

*Heating runs* After completing freezing runs, inclusions were heated to determine their homogenization temperature. As an inclusion is heated, the liquid in the inclusion

expands until the inclusion homogenizes to a single phase. The homogenization temperature ( $T_h$ ), is a minimum trapping temperature, which falls along density isochores leading to true trapping temperatures and pressures (Roedder, 1984). The disappearance of the respective phase (homogenization into the liquid or vapour state), gives an indication of the density of the inclusion fluid (Shepard et al. 1985).

## 4.2 Results of Fluid Inclusion Studies

### Petrographic Observations

Fluid inclusions from the Prairie Creek area were studied in four different minerals: quartz, sphalerite, calcite and dolomite. At room temperature, no daughter salts or three phase assemblages were seen in inclusions. Rarely,  $\text{CO}_2$  rich inclusions were observed in quartz. In vein quartz, many inclusions were less than five micrometre ( $\mu\text{m}$ ) in size. Occasionally large ( $>50\mu\text{m}$ ), two-phase inclusions in quartz were observed, but were avoided as experimental studies (Bodnar and Bethle, 1985) indicate stretching of inclusions is directly proportional to size. Small,  $<10\mu\text{m}$  in size, and isolated inclusions were interpreted as primary. Pseudosecondary and secondary inclusions, (inclusions along growth lines or fractures) were often examined, to compare analytical results with results from primary inclusions. In quartz veins, due to inclusion size, it was often difficult to distinguish primary from secondary inclusions. In Zone #3, vein sphalerite possess pseudosecondary to secondary inclusions (?), many of which are opaque. Necking in inclusions in quartz is indicated by inclusion tails, and variable filling ratios in inclusions.

### Inclusions in quartz

#### Two phase aqueous inclusions

Within stratiform (Type I) mineralization, where quartz forms as a cement in vugs, low salinity fluids are generally observed in (primary ?) inclusions in quartz (Table IV-1 in

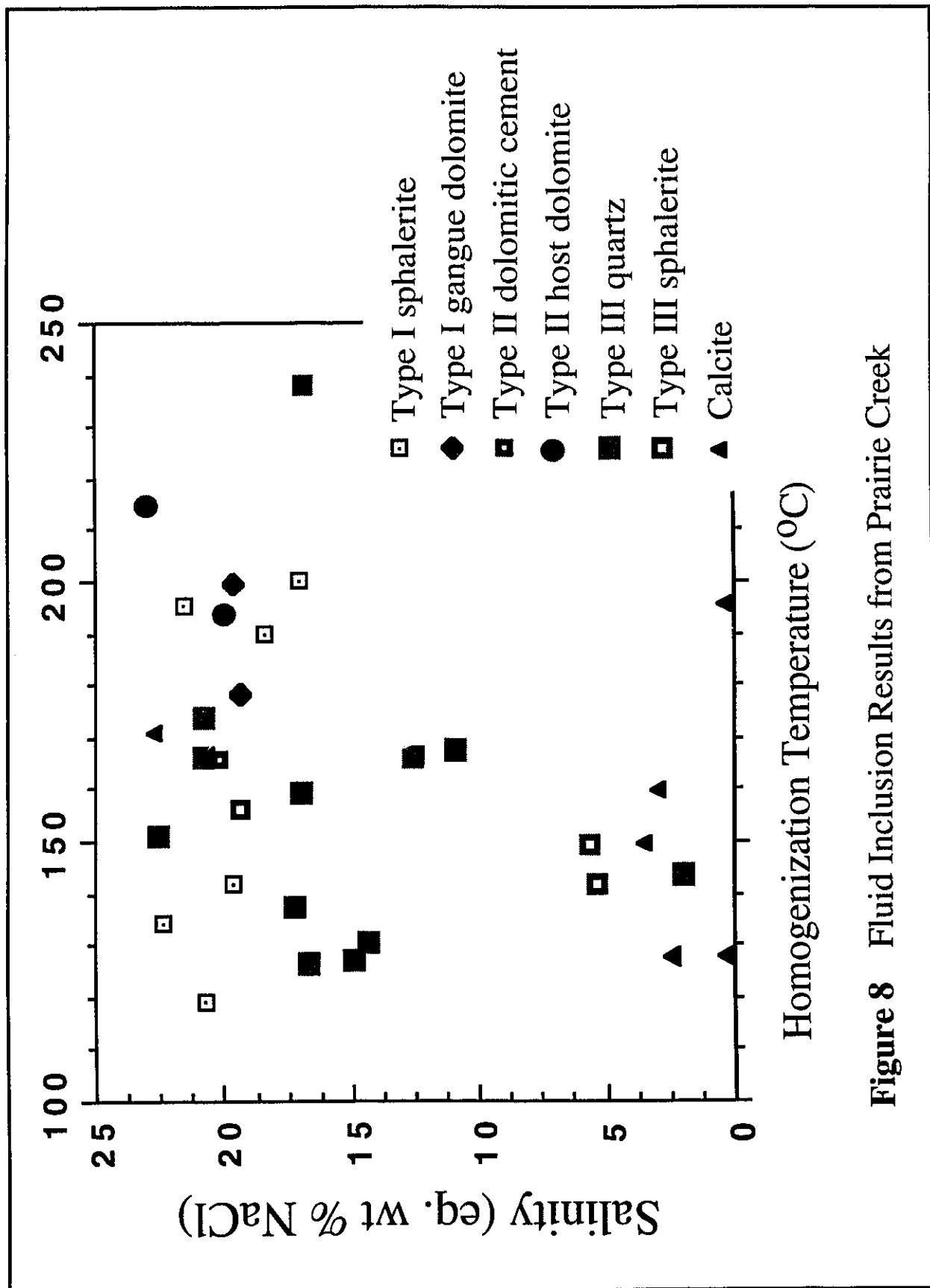


Figure 8 Fluid Inclusion Results from Prairie Creek

Appendix I).  $T_m$  values range from  $-0.6$  to  $-18.1$  °C and average  $-7.1 \pm 4.3$  °C, which corresponds to a salinity of 10.6 eq. wt. % NaCl. Limited eutectic temperatures observed in quartz, range from  $-27$  to  $-35$  °C. Variable homogenization temperatures range from 140 to 264 °C, averaging  $150 \pm 15$  °C for 31 inclusions in quartz. (Table IV-1). No inclusions in quartz were observed in Type II ores.

From Table IV-I and Figure 8, it can be observed that inclusions in vein quartz (Type III ores) have final ice melt temperatures ( $T_m$ ) ranging from  $+1.7$  to  $-20.2$  °C. These temperatures correspond to salinities of 0.5 to 21.1 eq. wt.% NaCl. While low salinity inclusions were observed with quartz overgrowths (sample 3-D-32 198m), the range in higher salinity inclusions in quartz could not be differentiated on the basis of textural relationships from quartz veins. An average  $T_m$  for inclusions in quartz (associated with mineralization) is  $-13.0 \pm 3.7$  °C (based on 113 observations from 9 quartz chips), which corresponds to a salinity of 16.9 eq. wt. % NaCl. Aulstead (1987) observed that inclusions in quartz from the Manetoe Facies had a similar broad range in salinity values and suggested that quartz-forming fluids resulted from mixing of hypersaline fluids and meteoric water.  $T_m$  values from the overgrowths range from  $-0.2$  to  $-2.4$  °C, which corresponds to a salinity of 2.0 eq.wt. % NaCl. Secondary inclusions (Table IV-1), observed along growth zones, have similar low salinities ( $<2.1$  eq. wt % NaCl).

Eutectic temperatures or the temperature of first melt ( $T_e$ ) are inversely proportional to the salinities of the fluids. The higher salinity fluids have lower eutectic temperatures ranging from  $-38$  to  $-42$  °C, while lower salinity fluids have  $T_e$  ranging from  $-25$  to  $-27$  °C. The low eutectic temperatures ( $-38$  to  $-42$  °C) indicate presence of Ca and/or Mg in addition to Na, in the fluids (Shepherd et al., 1985).

All inclusions in quartz from Type III ores were observed to homogenize to the liquid phase. Homogenization temperatures ( $T_h$ ) of low salinity fluids range from 97 to 168 °C (average 142.8 °C), while the range in homogenization temperatures in inclusions in quartz (associated with mineralization) was 110 to 240 °C with an average of  $163 \pm 61$

°C. Temperatures of homogenization for secondary inclusions in quartz, range from 113 to 154 °C, similar to results seen in inclusions from quartz overgrowths.

#### CO<sub>2</sub> inclusions in quartz

While there is little evidence to suggest significant CO<sub>2</sub> contents in aqueous inclusions from vein quartz in this study, two samples (PC-40 301.2m and PC-11 at 281.6m) do possess CO<sub>2</sub>-rich and CO<sub>2</sub>-bearing inclusions. CO<sub>2</sub>-rich inclusions present in this study, are single phase at room temperature, with T<sub>hCO2</sub> to a vapour phase, at temperatures of 3.6 to 16.8 °C. Several CO<sub>2</sub> rich inclusions were observed in a quartz chip near stratiform mineralization, in sample PC-40 at 301.2m. The presence of methane or nitrogen is inferred for these inclusions due to depressed T<sub>mCO2</sub> levels, -59.4 to -61.3 °C, which are below the temperature of melting of pure CO<sub>2</sub> (-56.6 °C).

CO<sub>2</sub>-bearing inclusions in vein quartz (as well as a single CO<sub>2</sub>-rich inclusion) were observed in sample PC-11 at 281m. CO<sub>2</sub>-bearing inclusions are identified mainly from the presence of clathrates, melting at temperatures > 0 °C, as well as CO<sub>2</sub> melting at -56.6 °C. In sample PC-11 at 281m, T<sub>m</sub> range from -13.0 to -14.3 °C, clathrate melting temperatures range from +2.6 to +5.0 and temperature of homogenization for CO<sub>2</sub> range from +16.7 to +19.0 °C.

#### **Inclusions in Sphalerite**

Inclusions in sphalerite were examined in ore types I, II and III. In (Type I) stratiform mineralization, 32 inclusions in sphalerite, from 6 chips were examined. In primary (?) inclusions in zoned sphalerite, T<sub>m</sub> values range from -13 to -22 °C (average -16.2 ± 2.1 °C) and correspond to salinity values of 17 to 25 eq. wt. % NaCl (average 20.0 ± 2.0 eq. wt.% NaCl). The criteria used in this study for determination of primary inclusions in sphalerite were based on observation of random inclusions, without association of any growth zones. Ice was seldom observed directly during freezing runs

and often the inclusion bubble in sphalerite appeared to disappear during freezing. As many of the inclusions in sphalerite are  $<5\mu\text{m}$ , observation of this phenomena was not readily apparent, as the collapsed bubble may have been masked along the inclusion wall.

Complete disappearance of the bubble, upon freezing, suggests that stretching of sphalerite inclusions may have occurred (Roedder, 1984). While Aulstead (1987) did not obtain results from inclusions in sphalerite, her study on stretching of inclusions in fluorite, and data from Bodnar and Bethke (1984) suggest that stretching probably did not occur in the Prairie Creek area.

$T_m$  results from inclusions in sphalerite in stratiform (Type I) ores, were obtained by observation of movement of the vapour bubble during melting. Because many of the sphalerite inclusions are opaque, due to internal optics (Roedder, 1984), eutectic temperatures ( $T_e$ ) were difficult to obtain.  $T_e$  (temperature of first melting) data obtained, vary from  $-29$  to  $-46$  °C and suggest presence of Ca and /or Mg in addition to Na.  $T_h$  values for inclusions from sphalerite in stratiform ores range from  $110$  to  $220$  °C. Based on the histogram plot of inclusions in sphalerite (Figure 9),  $T_h$  of zoned sphalerite is  $130 \pm 20$  °C. More massive sphalerite ranges from  $160$  to  $220$  °C. Pseudosecondary inclusions (?) from unzoned, tan colored sphalerite (as in sample PC-12 at 269m) have  $T_m$  values averaging  $-17.8$  °C with corresponding salinities averaging 21 eq.wt. % NaCl. While these salinities are similar to values in primary (?) inclusions in sphalerite,  $T_h$  values for pseudosecondary inclusions in sphalerite average  $130$  °C. Salinities for inclusions in sphalerite are shown in Figure 10.

Six inclusions in sphalerite were investigated from the Zebra showing (Type II mineralization).  $T_m$  results range from  $-21$  to  $-24$  °C, averaging  $-22$  °C from 4 inclusions, which corresponds to a salinity of 25 eq. wt. % NaCl. Eutectic temperatures were not detected from these inclusions.  $T_h$  values for six inclusions range from  $155$  to  $220$  °C, averaging  $199$  °C. No workable inclusions were identified in colloform sphalerite taken from the Zebra occurrence.

From Type III ores, fluid inclusion results in sphalerite were obtained from two samples. Inclusions from the 3050 Level sphalerite vein (Zone # 2 ?) are interpreted as pseudosecondary (?) based on inclusions forming along growth lines and observable cleavage traces in this coarse-grained sphalerite.  $T_m$  values for these inclusions range from -11.8 to -20, with an average of  $-15.7 \pm 4.2$  °C. This corresponds to a salinity of  $19.4 \pm 6.7$  eq. wt. % NaCl. Eutectic temperatures range from -36 to -40 °C.  $T_h$  values range from 140 to 171°C with an average of  $156 \pm 9.6$ °C. Additional inclusions in sphalerite from quartz veining were examined in PC-11 at 281.6m. Here  $T_m$  values for 5 inclusions range from -2.6 to -4.0 °C averaging  $-3.3 \pm 0.5$ °C, which corresponds to 5.3 eq.wt % NaCl. Eutectic temperature for these inclusions was observed at -55 °C, (possible presence of CO<sub>2</sub> ?).  $T_h$  for these five inclusions range from 142.0 to 142.5 °C, averaging  $142.0 \pm 1.1$  °C.

### **Inclusions in Calcite**

Fluid inclusion results from calcite were obtained from six samples.  $T_m$  data for two phase, aqueous fluid inclusions (primary ?) in unmineralized vein calcite can be divided into two populations on the basis of salinity. Low salinity fluids reflect  $T_m$  ranging from +5.6 to -2.6 °C (the former attributed to metastability), and average  $-1.1 \pm 1.1$  °C, which corresponds to a salinity of  $1.9 \pm 1.9$  eq. wt. % NaCl. Eutectic temperatures for these inclusions (-26 to -28 °C) indicate that NaCl constitutes most of the dissolved salt content in the inclusions.  $T_h$  values for these fluids from calcite range from 127 to 205 °C, averaging  $152.3 \pm 31.2$  °C.

High salinity fluids in (primary ?) inclusions in calcite, were observed in a single unmineralized vein within sample PC-41 at 103.4m. Results are similar to quartz and sphalerite with final ice melting temperatures averaging  $-20.1 \pm 0.9$  °C, for a salinity of  $22.7 \pm 1.7$  eq. wt % NaCl. Eutectic temperatures of -48 to -50°C for these inclusions indicate the presence of Ca and/or Mg chlorides in the fluids.  $T_h$  values average  $171 \pm 9.7$



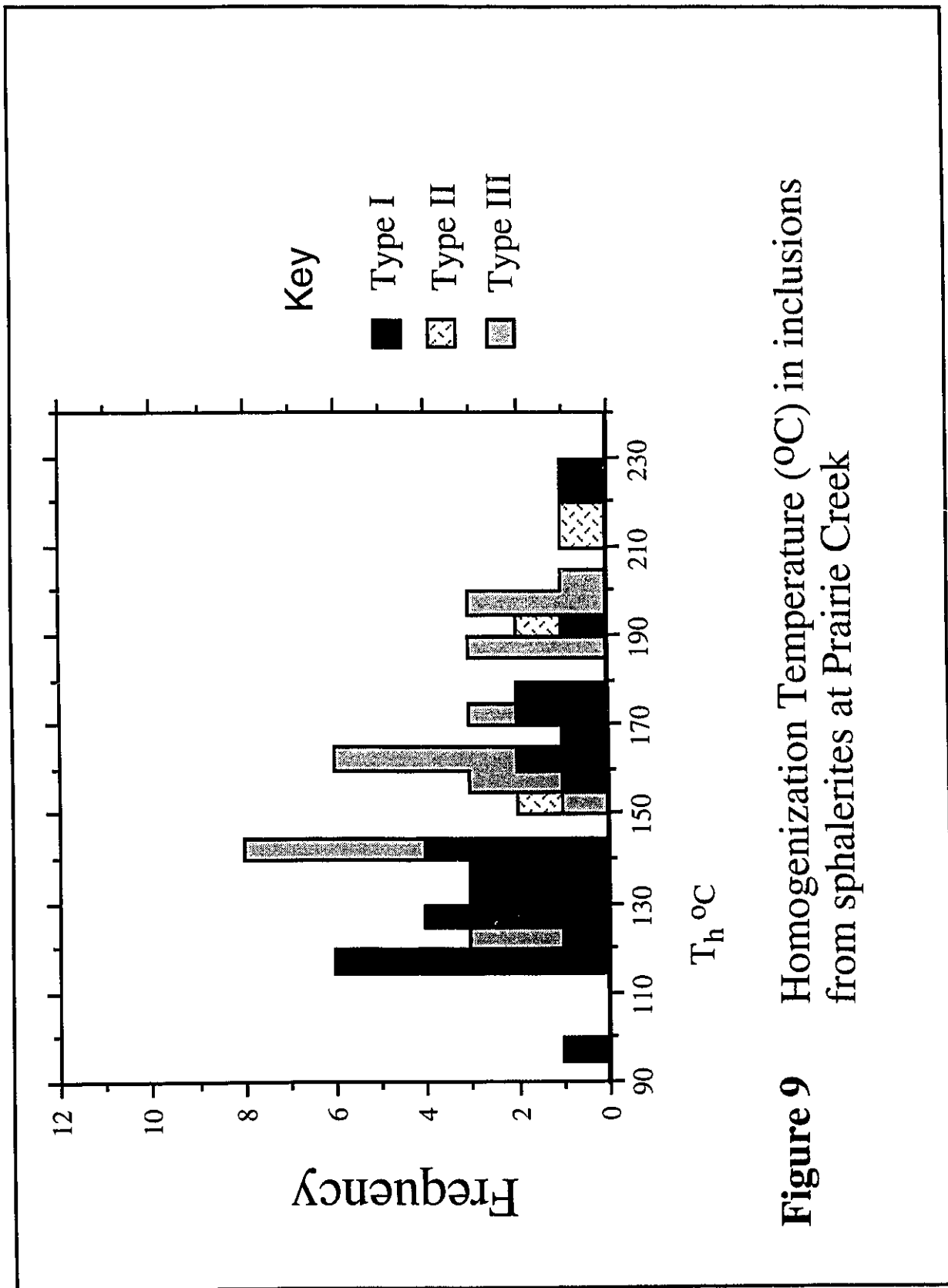


**Figure 9** Homogenization Temperature (°C) in inclusions from sphaalerites at Prairie Creek

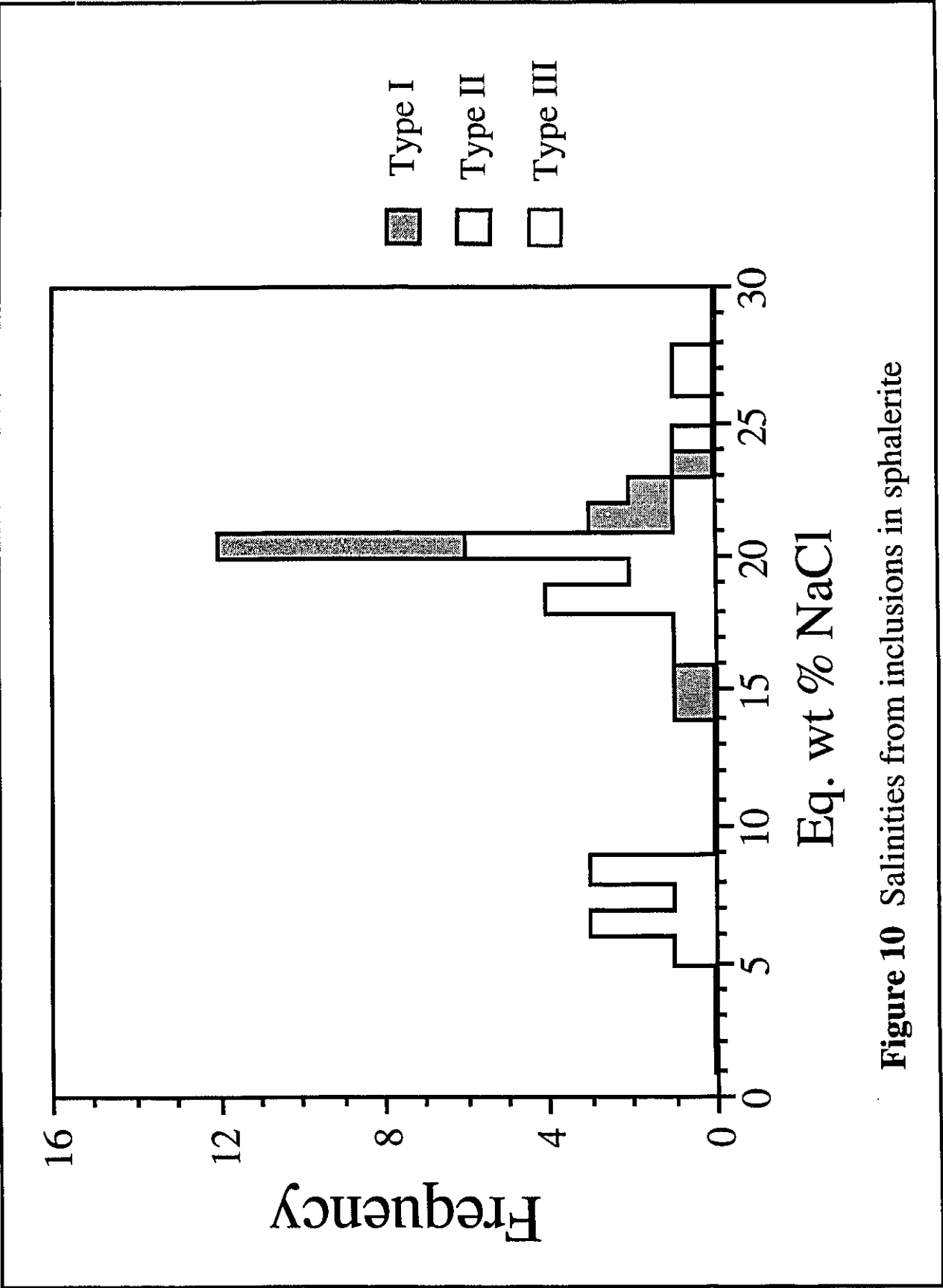


Figure 10 Salinities from inclusions in sphalerite

°C for these inclusions. Pseudosecondary to secondary (?) inclusions in calcite from this sample, having  $T_h$  approaching 200 °C, have similar salinities as primary inclusions. The results in these high salinity inclusions in calcite, show similarities to inclusions in quartz and sphalerite for Type III ores, and suggest the presence of ore stage calcite.

### **Inclusions in Dolomite**

From petrographic observations and cathodoluminescence studies, three types of dolomite have been recognized at Prairie Creek. These dolomites include diagenetic, early matrix dolomite, gangue dolomite associated with Type I ores, and saddle dolomite associated with Type II ores. No fluid inclusion results were obtained from matrix dolomite. In Type I ores, fluid inclusion data from gangue dolomites were obtained from two samples (PC-11 261m and PC-28 269m).  $T_m$  (temperature of final ice melt) data range from -11 to -23 °C with an average of  $-16.2 \pm 3.6$  °C, which corresponds to an average salinity of  $19.6 \pm 5.9$  eq. wt % NaCl. Eutectic temperatures range from -54 to -57 °C indicating the presence of cations other than Na (Ca and Mg).  $T_h$  for inclusions in eight samples of gangue dolomites range from 165 to 221.2 °C, for an average value of  $188 \pm 16.2$  °C.  $T_h$  and salinities for dolomite are illustrated in Figures 11 and 12.

Inclusions in gangue dolomites from the Zebra showing, are up to 50  $\mu\text{m}$  in size.  $T_m$  data from host dolomite range from -11 to -25 °C with an average value of  $-19.1 \pm 4.3$  °C which corresponds to a salinity value of  $21.7 \pm 6.9$  eq.wt. % NaCl. Eutectic temperatures observed for these dolomites were approximately -58 °C. Limited  $T_h$  data recorded for these dolomites range from 166 to 238 °C, with an average value of  $201.6 \pm 36.7$  °C.  $T_m$  and  $T_h$  values for inclusions in the gangue dolomite from the Zebra showing are consistent with  $T_m$  and  $T_h$  values observed in inclusions of sphalerite from this showing.

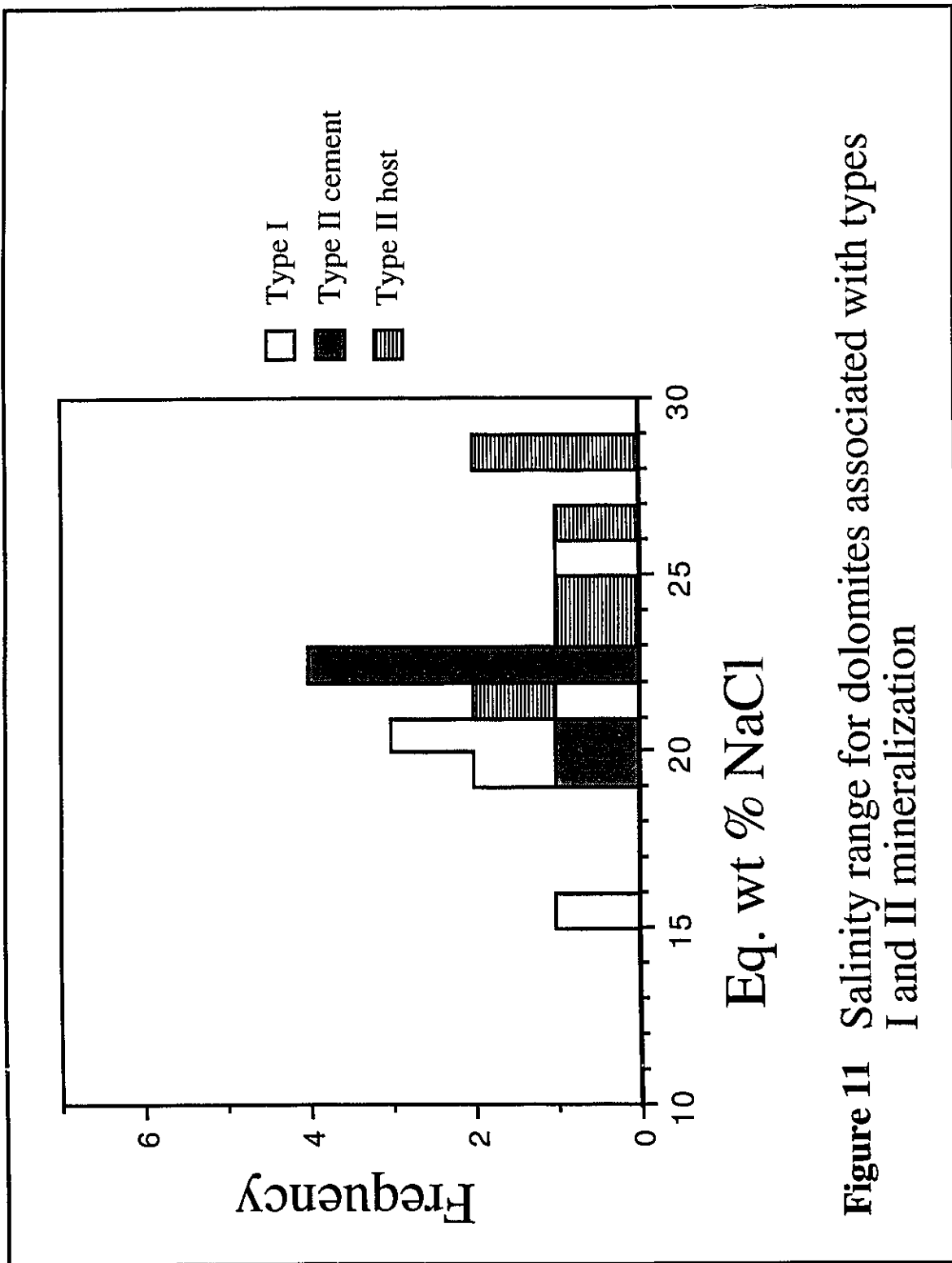


**Figure 11** Salinity range for dolomites associated with types I and II mineralization

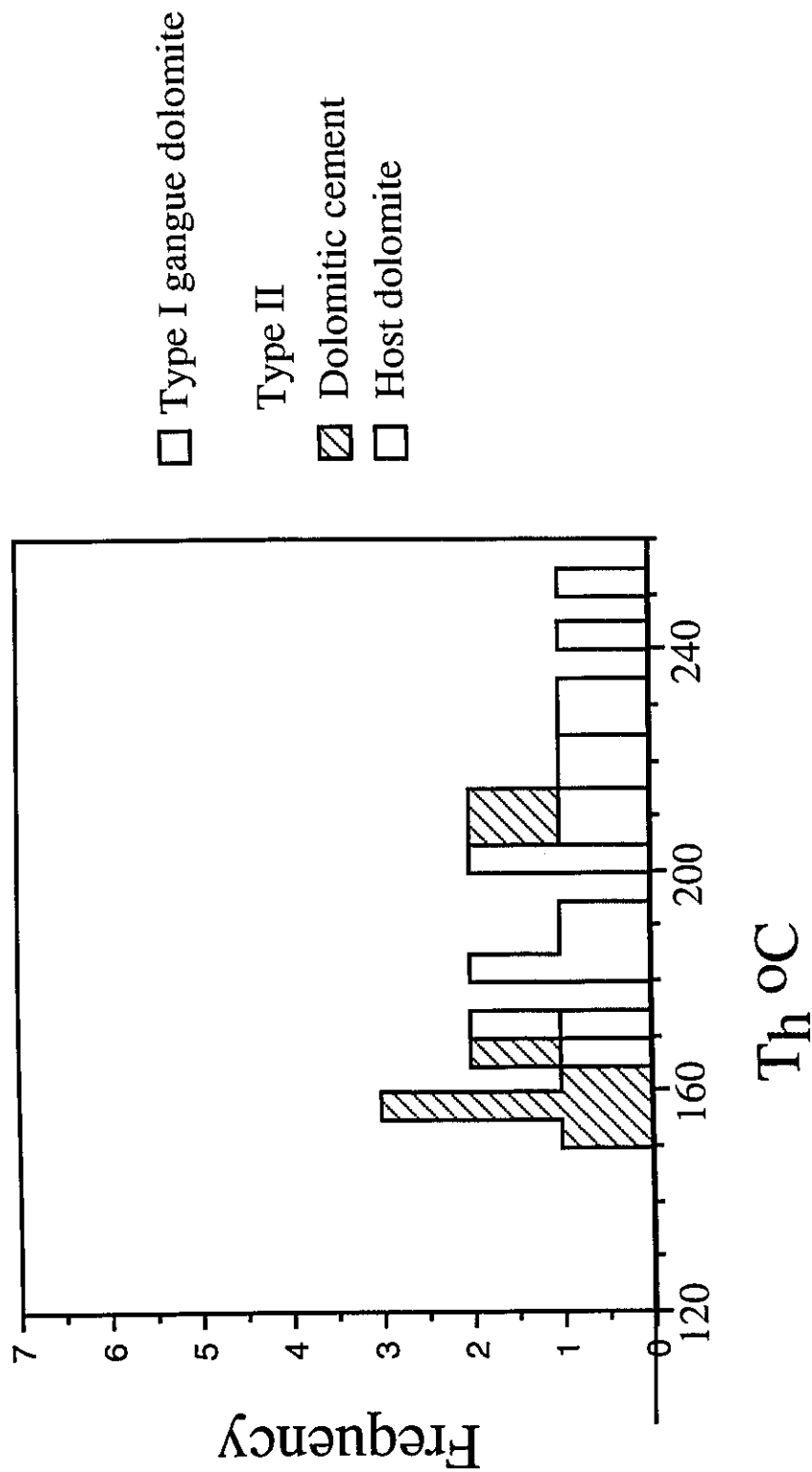


**Figure 12** Homogenization temperatures ( $T_h$ ) °C in inclusions from dolomite associated with types I and II mineralization

### 4.3 Geothermometry and Geobarometry

Roedder (1984) suggests that in order to obtain actual trapping temperatures of original ore forming-fluids, an independent temperature or pressure is needed. From this study, trapping pressures may be estimated for Type III ores, by extrapolating isochores from pure CO<sub>2</sub> inclusions, to isochores of NaCl-H<sub>2</sub>O inclusions, based on coexisting inclusions observed in samples PC-11 at 281.6m and PC-40 at 301m (Figure 13). CO<sub>2</sub>-rich inclusions in quartz have been observed, with CO<sub>2</sub> homogenizing to the vapour phase, at temperatures <16 °C indicating low CO<sub>2</sub> densities (Roedder, 1984; Figure 8-9). In Figure 13, the intersection of the CO<sub>2</sub> inclusion isochores at A, with the NaCl-H<sub>2</sub>O inclusion isochores at B, indicates a trapping temperature of approximately 270 °C at C and a trapping pressure of approximately 150 bars at D. The data support a temperature correction of about 10 °C, which is consistent with the observations of Aulstead (1987) below. Using the results of Morrow et al. (1986) and Major-Drees (1975), Aulstead (1987) observed T<sub>h</sub> values in inclusions of dolomites from the Manetoe Facies, in oil and gas wells, did not change with depth of burial, while noting variation in T<sub>h</sub> values in inclusions in quartz and calcite, varied from 30 to 60 °C. These observations were based on samples from oil well depths of 1500m west of Fort Simpson, to 4000m depths at the Pointed Mountain gas fields, Laird Basin. Assuming a geothermal gradient of 38 °C/km, Aulstead (1987) reasoned that the quartz and calcite cements must have formed under depths of 1 to 2 km, and therefore must have formed during the Mesozoic to Cenozoic. Based on these depths, Aulstead (1987) determined a temperature correction of about 12 °C.

### 4.4 Fluid inclusion data summary

At least three separate fluid events are indicated from the data presented in Table IV-1. The inclusions from sphalerite and gangue dolomite in Type I, stratiform

mineralization indicate that the ore-forming fluids possessed generally high salinities (both average >19 eq. wt.% NaCl) and moderately low eutectic temperatures ranging from -29 to -52 °C indicating the presence of Ca and Mg chlorides, in addition to NaCl. Temperatures of homogenization observed in sphalerite from stratiform mineralization have a broad range, from 112 to 225 °C. From limited data, fluid inclusion results from gangue dolomites show less spread ranging from 165 to 221°C. As the stratiform ore fluids are interpreted as the oldest mineralizing fluids present at Prairie Creek, these fluids have been subjected to the greatest burial diagenesis and therefore the chemistry of these inclusions may have been altered.

Although limited, fluid inclusion data from Type II ores suggest that mineralization formed from higher salinity fluids, as seen in both sphalerites (22.1eq. wt. % NaCl) and gangue dolomites (21.4 eq. wt. % NaCl). Both sphalerite and saddle dolomite have relatively high temperatures of homogenization, for MVT style mineralization, ranging from ~160 to 238 °C (Sangster, 1990), but similar high  $T_h$  have been observed at Gay's River, Nova Scotia (Akende and Zentilli, 1984).

Fluid inclusion results from quartz and calcite from Type III ores are consistent with the observations of Aulstead (1987) suggesting fluids evolved over a larger time span, with increasing input of meteoric water, over formation water, through time. As a result of this evolution in fluid chemistry, inclusions in quartz are characterized by the broad range in salinities, and with late fluids characterized by low salinities (quartz overgrowths with a salinity of 2.0 eq.wt.% NaCl), and calcite cements (salinities averaging  $1.9 \pm 1.5$  eq. wt % NaCl). The higher salinity fluids in quartz appear to be associated with mineralization, whereas later fluids are unmineralized.

Calcite fluid inclusion data generally indicate low salinity fluids with relatively low homogenization temperatures (~110 to 135 °C), while pseudosecondary to secondary inclusions indicate higher temperatures of homogenization. The results from inclusions in calcite in this study, are in contrast with the observations of Aulstead (1987), from

inclusions in calcite from the Manetoe Facies. Aulstead (1987) described mainly high salinity fluids from these inclusions and observed eutectic temperatures to  $-58^{\circ}\text{C}$ . Only one sample of calcite, (sample PC-41 103.4m) in this study, showed similar results to that of Aulstead (1987).

No pressure or temperature correction is warranted for Type I mineralization as it is assumed to have formed close to the seawater/sediment interface. Type II mineralization is also thought to have formed at a shallow depth and therefore no correction is justified. These views are consistent with recent interpretations of fluid inclusion results and stable isotope evidence from the Manetoe Facies (Morrow and Aulstead, 1995) who examined criteria to support dolomitization in either the middle Devonian or Tertiary. They suggest that fluid inclusion evidence from Manetoe Facies dolomites (Aulstead, 1987) support middle Devonian dolomitization.



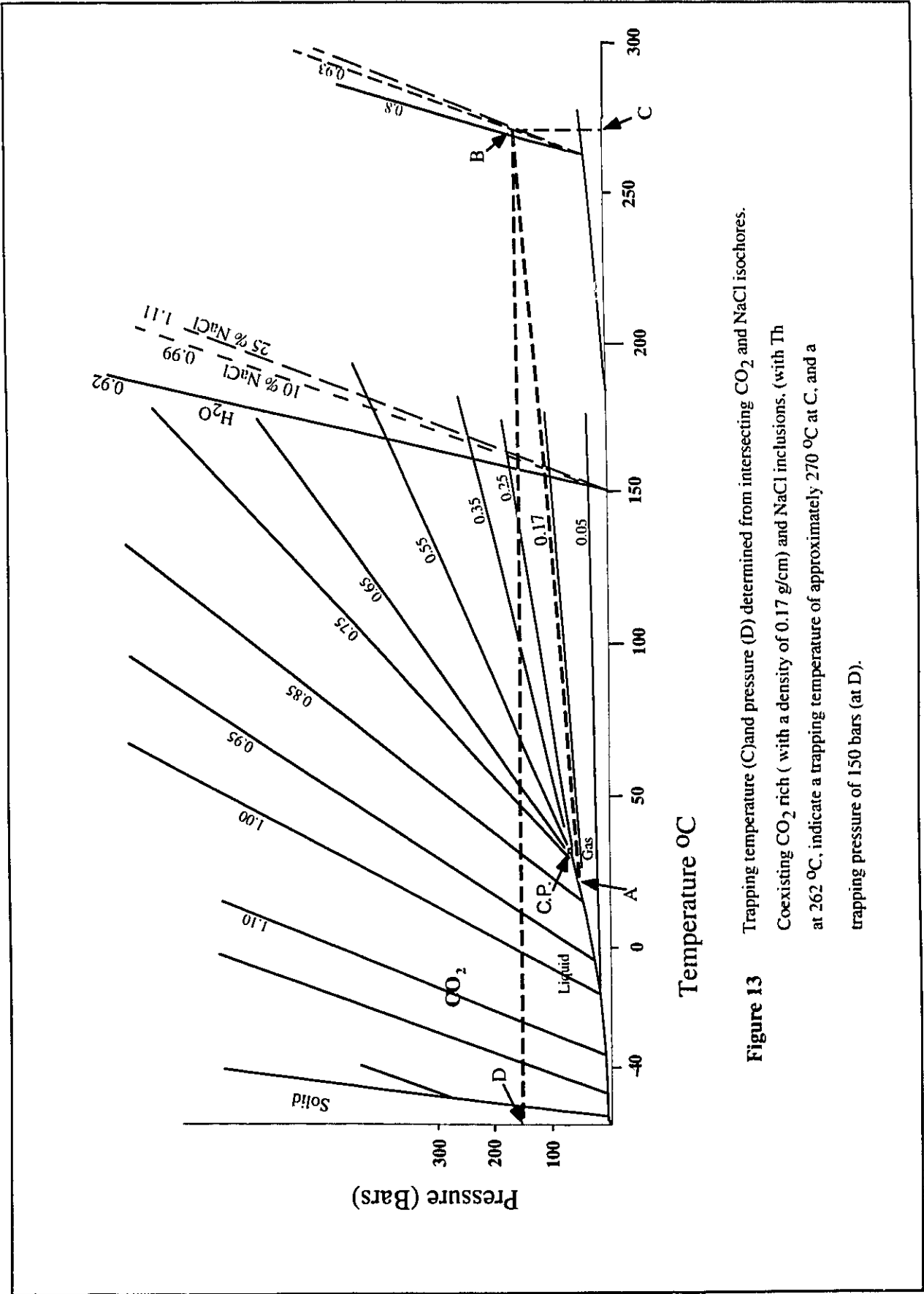


**Figure 13** Trapping temperature (C) and pressure (D) determined from intersecting CO<sub>2</sub> and NaCl isochores. Coexisting CO<sub>2</sub> rich (with a density of 0.17 g/cm<sup>3</sup>) and NaCl inclusions, (with Th at 262 °C, indicate a trapping temperature of approximately 270 °C at C, and a trapping pressure of 150 bars (at D).

## Chapter V- Light Stable Isotope Study

### Introduction

Light stable isotope studies (C, O and H of gangue minerals and S from sulfide minerals) in hydrothermal systems have been useful in outlining geochemistry and determining the origin and evolution of mineralizing fluids in the crust (Field and Fifarek, 1985; Ohmoto, 1986). The most useful application of stable isotopes involves the use of  $\delta D$  and  $\delta^{18}O$  analyses to indicate the origin and history of  $H_2O$  in hydrothermal fluids (Taylor, 1979). Stable isotope geothermometers (Field and Fifarek, 1985) may also be used to determine the temperature of formation of hydrothermal mineral assemblages, but often isotopic disequilibrium precludes the usefulness of such applications (Taylor, 1979).

As a part of the study of the geochemical relationships among stratiform (Type I ores), MVT style (Type II ores) and vein quartz-sulfide (Type III) mineralizations at Prairie Creek, light stable isotope studies were performed. As well as investigating wall rock dolomite from principally the Whittaker Formation, gangue dolomite and cross-cutting calcite veins were examined, while quartz was mainly investigated from type III ores.

Manganese rich, gangue dolomites, associated with stratiform mineralization were analyzed, as well as wall rock dolomites. Wall rock dolomites were sampled adjacent to (<0.2 m distance) and up to several kilometres west of stratiform and vein mineralization. At the Zebra and Zulu showings, host, recrystallized dolomite and coarse-grained, white to yellow, saddle dolomitic cements were analyzed for  $\delta^{13}C$  and  $\delta^{18}O$ . Calcites, as late stage veins, cutting ore types I and III were also analyzed for  $\delta^{13}C$  and  $\delta^{18}O$ . Quartz from mineralized and unmineralized veins, as well as overgrowth crystals, (interpreted as late diagenetic features) were examined isotopically with  $\delta^{18}O$  analysis.  $\delta D$  analyses of inclusion fluids were performed on dolomite, quartz, calcite and sphalerite to investigate the sources of fluids involved in various stages of ore formation. Sulfur isotope analyses were

conducted on sphalerite, galena and pyrite from stratiform ores and sphalerite from vein mineralization.

### **Techniques**

Core samples of host rock dolomite were crushed and x-rayed to determine carbonate mineralogy. Saddle dolomitic cements from the Zebra showing and gangue dolomite from stratiform mineralization were drilled out with a dental drill, to increase purity of sample.

Carbon, oxygen and deuterium isotope analyses of gangue minerals (and sphalerite) were conducted at The University of Alberta. Finely ground dolomite and calcite was reacted in vacuum with  $H_3PO_4$  at 25 °C for seven days and one day respectively (McCrea, 1950). Quartz samples were crushed to approximately 2-3mm size for deuterium analyses and treated by boiling in aqua regia with minor hydrogen peroxide for one to two hours to ensure purity of sample. The quartz samples were washed and hand picked for deuterium analyses.  $\delta D$  of quartz, dolomite and sphalerite were determined by direct extraction of inclusion fluids by bulk thermal decrepitation. The temperature of extraction varied for minerals investigated and the liberated aqueous phase was reduced to hydrogen by reaction with zinc pellets (Coleman et al., 1982).  $\delta^{18}O$  of the quartz veins was analyzed using the  $BrF_5$  technique of Clayton and Mayeda (1963).  $\delta^{18}O$  and  $\delta D$  are quoted in terms of SMOW (Standard Mean Ocean Water), while  $\delta^{13}C$  values are referenced to PDB (Cretaceous PeeDee belemnite) in per mil (‰). Carbonate whole rock samples were analyzed on a VG602 mass spectrometer by the writer, using KMCC standards.

A total of eight sulfide samples (and 1 repeat) were run for sulfur isotope analyses (Table V-2).  $\delta^{34}S$  values were determined courtesy of Dr. R. Krouse at the Stable Isotope Laboratory at the University of Calgary. Sulfide analyses were performed on  $SO_2$  gas extracted by high temperature combustion of the sample with cupric oxide. Mass

spectrometric analyses are referenced to the standard (CDT), which is the sulfur in troilite (FeS) of the iron meteorite in the Canyon Diablo standard (Faure, 1986).

### **Sulfur isotope data**

Sulfur isotope ratios, determined from types I (stratiform) and III (vein) ores, are listed in Table V-1. The  $\delta^{34}\text{S}$  values for stratiform ores range from +21.6 to +23.9 ‰ in pyrite, sphalerite, and galena as shown in Table V-1. While the sphalerite and galena  $\delta^{34}\text{S}$  analyses were extracted from minerals from different samples of Type I ores, assuming isotopic equilibrium existed, temperatures approximating 273 to 314 °C are predicted from sphalerite-galena geothermometry (Ohmoto and Rye, 1979). These temperatures, are reasonable for colour alteration index values observed from conodonts (Morrow et al., 1990). Ohmoto and Rye (1979) stress the importance of clean mineral separates and Type I sphalerite with pyrite, makes the effectiveness of sulfide geothermometry questionable. Ohmoto (1972) has also suggested that mineralization temperatures below 250 °C generally show disequilibrium in sulfur isotopes.

From the  $\delta^{34}\text{S}$  values presented in Table V-1, a distinct variation between stratiform and vein sulfides in  $\delta^{34}\text{S}$  values for sphalerite is apparent. Vein sphalerite (Type III), occurring in host rocks from Ordovician, Whitaker Formation (#3 and #8 veins) to lower Devonian, Arnica Formation (Rico vein) ranges in  $\delta^{34}\text{S}$  from +20.0 to +17.0 averaging  $+18.7 \pm 1.5\text{‰}$ , while sphalerite from stratiform (Type I) ore has a  $\delta^{34}\text{S}$  value of +22.0 ‰. For comparison,  $\delta^{34}\text{S}$  values from the Jason Pb-Zn deposit (Gardner and Hutcheon, 1985) as well as data from Howards Pass (Morganti, 1979) are presented in Table V-1.  $\delta^{34}\text{S}$  values from the End Zone (which contains massive to thickly bedded sulfides and is crosscut by quartz-carbonate veins) more closely resemble Type I sulfur ratios from Prairie Creek.

**Table V-I Prairie Creek  $\delta^{34}\text{S}$  data (‰)**

Hole # and footage	Mineral	$\delta^{34}\text{S}$		
<b>Type I ores</b>				
PC-11 269m	sphalerite	+22.2	contains pyrite to ~3%	
PC-35	galena	+20.0	no contaminants.	
PC-12 274.8m	pyrite	+23.8	contains trace galena	
PC-12 rerun	pyrite	+23.9		
PC-13 274.8m	pyrite	+22.0	contains trace galena	
PC-21 273.5m	pyrite	<u>+21.6</u>	contains trace sphalerite	
average for pyrite		$+22.5 \pm 1.2$ ‰		
<b>Type III ores</b>				
Rico (vein)	sphalerite	+17.0		
3050 level vein	sphalerite	+20.0		
#8 Zone vein near PC fault	sphalerite	<u>+19.1</u>		
average for type III sphalerites		$+18.7 \pm 1.5$ ‰		
<b>Jason Deposit</b>				
Area	pyrite	galena average range	average range	sphalerite range
South Zone		8.5 - 17.0	$13.7 \pm 2.8$ 8.9	12.3
End Zone		17.7 - 20.2	$18.9 \pm 1.2$ 20.0-22.5	$21.2 \pm 1.1$ 20.0
Howards Pass		8.5 - 22.3	$15.2 \pm 3.7$ 15.8-26.2	$19.7 \pm 3.3$ -3.2 - 23.0 $15.7 \pm 9.0$

The heavy  $\delta^{34}\text{S}$  values presented in Table V-1 suggest that seawater sulfate is the source of sulfur for mineralization observed in types I and III. No  $\delta^{34}\text{S}$  values were obtained from Type II mineralization.

### C, O, and H isotope results

The light stable isotope results from wall rock and mineral separates from all three styles of mineralization are given in Tables V-2 and 3. From Table V-2, it can be seen that  $\delta^{18}\text{O}$  values from Whittaker Formation, wall rock dolomite show minor depletions in oxygen (average  $22.0 \pm 1.4$  ‰ SMOW,  $n = 22$ ), compared to typical  $\delta^{18}\text{O}$  variation for Ordovician carbonates which is 23 to 27‰ (Veizer, 1983). From data in Table V-2, the greatest depletion in  $\delta^{18}\text{O}$  values of wall rock samples is seen in contact with stratiform mineralization.  $\delta^{13}\text{C}$  data for wall rock dolomites indicate a range of values of +0.5 to -2.0 ‰, and an average value of  $-0.5 \pm 0.5$  ‰, which is within the range of typical values for marine carbonates (-1 to -3 ‰). Figures 9 and 10 illustrate  $\delta^{18}\text{O}$  and  $\delta^{13}\text{C}$  values from wallrock dolomites seen in drill hole sections 6288N and 6045N.

*Type I ores* Coarse-grained gangue dolomite associated with Type I ores range in  $\delta^{18}\text{O}$  from 22.1 to 23.8 ‰, averaging  $23.0 \pm 0.8$  ‰ ( $n = 5$ ).  $\delta^{13}\text{C}$  values for these dolomites, range from -2.3 to -3.3 ‰, averaging  $-2.8 \pm 0.4$  ‰, which is depleted in  $^{13}\text{C}$  compared to the average value of  $-0.5 \pm 0.5$  ‰ seen in Whittaker Formation host dolomite. A  $\delta^{18}\text{O}$  analysis of 21.0 ‰, obtained from microcrystalline quartz at PC-14 at 297.7m, is interpreted as siliceous precipitate from ore-forming fluids. Typical values for Ordovician marine cherts range from +24 to +26 ‰ (Degens and Epstein, 1962). Deuterium analyses from stratiform sphalerite from sample PC-11 at 261.3m, yielded a value of -98 ‰.

*Type II ores* In Type II ores,  $\delta^{18}\text{O}$  values for the host Silurian, Root River dolomites range from 23.4 to 25.3 ‰, averaging  $24.5 \pm 0.7$  ‰ ( $n = 7$ ). In contrast,  $\delta^{18}\text{O}$  values from dolomitic cements from the Zebra and Zulu showings range from 12.7 to 19.8 ‰, averaging  $16.4 \pm 2.4$  ‰ ( $n = 7$ ).  $\delta^{13}\text{C}$  values for the host dolomites range from 1.2 to -1.4 ‰, averaging  $0.8 \pm 1.0$  ‰.  $\delta^{13}\text{C}$  for the Zebra and Zulu dolomitic cements range from -2.1 to -4.9‰, averaging  $-4.4 \pm 2.2$  ‰.  $\delta\text{D}$  values of dolomitic gangue from PC-94-78 at 242m and 181m include -66 ‰ and -61‰, similar to a value of -64 ‰ obtained from host dolomite in hole PC-95-117 at 46m. Additional  $\delta\text{D}$  values from

dolomitic gangue (-108 ‰) and host rock (-99 and -115 ‰) from outcrops at the Zebra showing, may have erroneous values due to sulfide oxidation. The higher values from drill core are more consistent with  $\delta D$  values (-76 to -42‰) obtained by Yang et al. (1995), who measured the hydrogen isotopic composition of fluid inclusion waters from drill cores from Manetoe Facies dolomites.

*Type III ores* Eleven quartz samples were analyzed for  $\delta^{18}O$  data from Type III ores.  $\delta^{18}O$  results range from 9.1 to 19.7 ‰, averaging  $16.7 \pm 3.5$  ‰. Most of the  $\delta^{18}O$  values of vein quartz cluster between 17.2 and 19.7 per mil. The  $\delta^{18}O$  value of 9.1‰, from low salinity (2.0 eq. wt. % NaCl), quartz overgrowths, is consistent with the observations of Aulstead (1987), who suggested that fluids with low  $\delta^{18}O$  values reflected increasing meteoric water content in the vein-forming fluids.  $\delta D$  analyses, obtained from vein quartz in Type III ores, cluster between -148 and -179 ‰, averaging  $155 \pm 18$  ‰, (n = 17).

*Calcite veining* Three isotopic analyses were obtained from unmineralized, calcite veining (Table V-3). The  $\delta^{18}O$  values in calcite range from 10.2 to 22.0 ‰. Strongest  $^{18}O$  depletion was observed in hole PC-13 at 289m in vein calcite (10.2 ‰), within stratiform ore. From crosscutting relationships, this calcite is interpreted as late veining.  $\delta^{13}C$  range from -15.5 to 2.9 ‰ (Table V-3). A calcite vein at PC-41 at 103.4m has strongest depletion in  $^{13}C$  with a value of -15.5 ‰. This strong depletion in  $^{13}C$ , suggests that oxidation of organic matter occurred. A  $\delta D$  value of -167 ‰ was obtained from a 0.3m thick, calcite vein within the Silurian Cadillac Formation, at the south end of the #8 Portal.

**Table V-2 Prairie Creek stable isotope data (wall rock dolomite)**

Hole # and footage	Mineral	$\delta^{13}\text{C}$ PDB ‰	$\delta^{18}\text{O}$ SMOW ‰
PC-06 207.5m	dolomite	-0.5	21.3
PC-08 239.4m	dolomite	-0.3	23.3
PC-08 269.5m	dolomite	-0.5	21.2
PC-08 282.9m	dolomite	-1.0	21.7
PC-08 298.9m	dolomite	-2.0	20.7
PC-08 308.1m	dolomite	0.5	22.5
PC-11 201.2m	dolomite	0.2	23.4
PC-11 208.4m	dolomite	-0.4	24.0
PC-11 253.5m	dolomite	0.1	24.6
PC-11 260.9m	dolomite	-1.0	22.8
PC-11 260.9m (rerun)	dolomite	-1.0	22.6
PC-11 290.5m	dolomite	-0.0	22.1
PC-13 76.2m	dolomite	-0.4	24.7
PC-13 103m	dolomite	0.1	24.9
PC-13 312.9m	dolomite	-0.2	20.7
PC-14 76.9m	dolomite	-0.6	24.6
PC-14 245.5m	dolomite	-0.7	21.3
PC-28 107.8	brecciated dolomite	-0.3	20.3
PC-28 160.6m	dolomite	-0.04	23.8
PC-28 280.7m	dolomite	-0.5	21.7
PC-40 302.2m	dolomite	-0.5	21.7
PC-R3 o/c w. of Gate Fault	dolomite	-0.5	23.3
		-----	-----
averages		$-0.46 \pm 0.5$	$22.0 \pm 1.4$ ‰

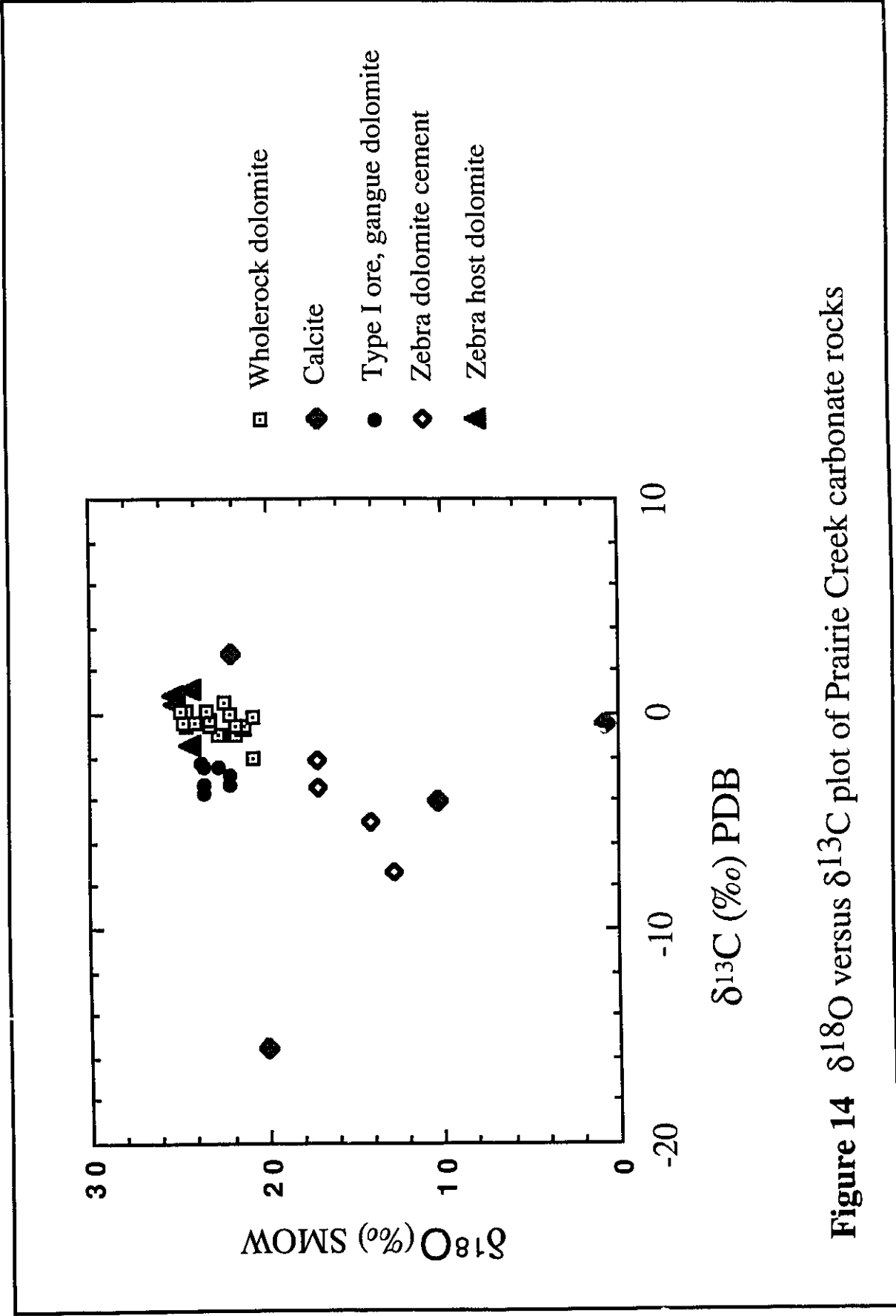


**Table V-3 Prairie Creek stable isotope data (mineral separates)**

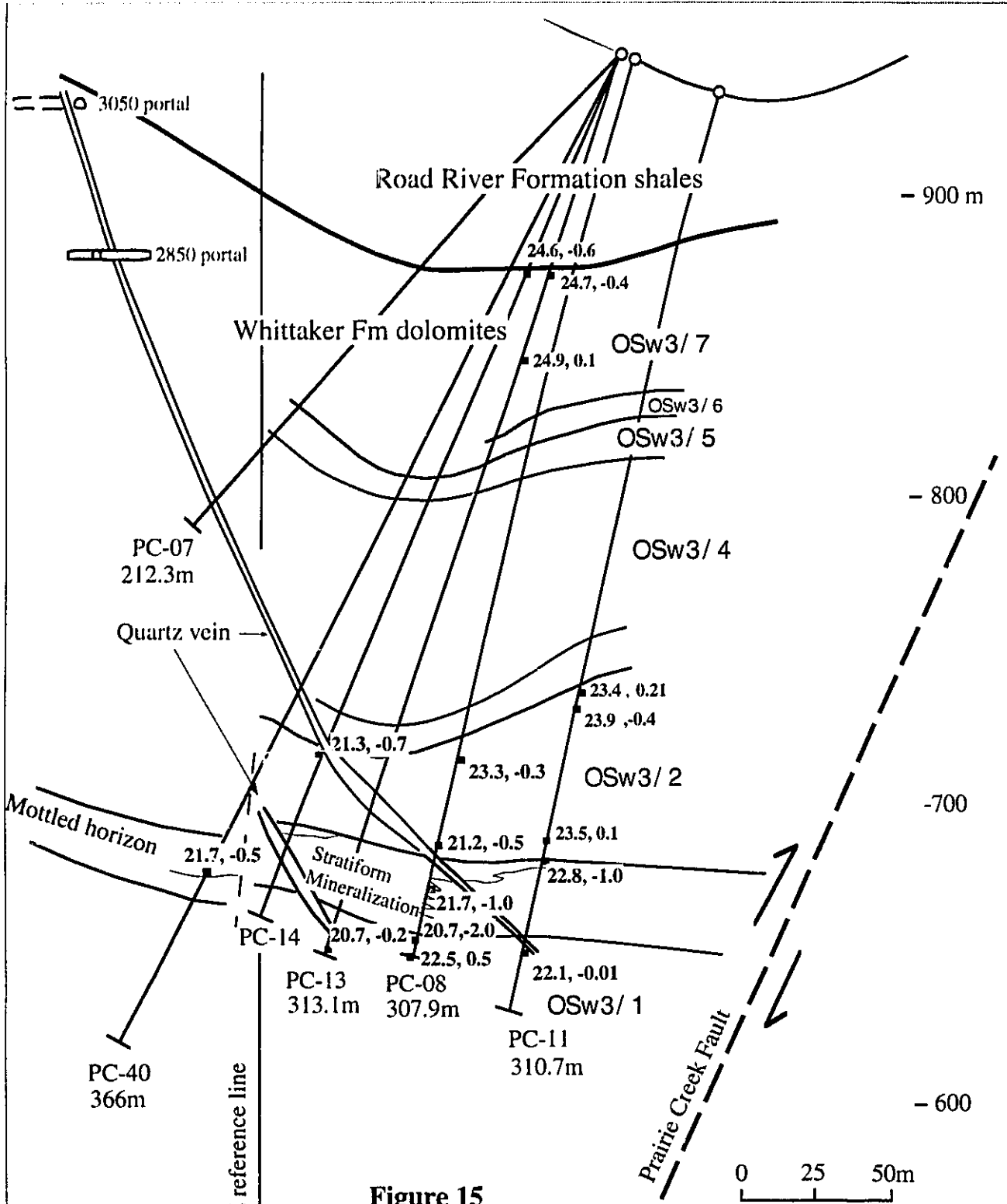
Hole # and footage	Mineral	$\delta^{18}\text{O}$	$\delta\text{D}$	$\delta^{13}\text{C}$
<b>Type I (Stratiform) ores</b>				
PC-08 273.5m	gangue dol.	23.8		-2.3
PC-11 261.3m	gangue dol.	22.1	-126	-2.9
PC-13 290.7	gangue dol.	22.7		-2.5
PC-13 290.7m (rerun)	gangue dol.	23.6		-2.5
PC-14 289.3m	gangue dol.	22.1		-3.3
PC-21 273.5m	gangue dol.	23.6		-3.3
		-----		-----
averages		23.0 $\pm$ 0.8		-2.8 $\pm$ 0.4
PC-14 297.7m	microcrystalline quartz	21.0	-182	
PC-11 261.3m	sphalerite		-98	
<b>Type II (Zebra style) ores</b>				
Zebra showing dol. cem. (1)		16.9	-108	-2.1
Zebra dolomitic cement adjacent colloform sph.		12.7		-7.2
Zebra dol. cement (2)		14.0		-4.9
Zulu dol. cement		16.9		-3.3
PC-94-78 181m dol. cement		17.8	-61	-2.0
208A " "		19.8		-1.0
242m " "		16.8	-66	-1.6
		-----		-----
Averages		16.4 $\pm$ 2.4		-3.1 $\pm$ 2.2
PC-94-78 208B m host dol		25.3		1.5
" " 287m " "		23.8		1.7
PC-95-117 46m " "		23.4	-64	1.0
Zebra HB (heavily bleached dolomite)		25.3	-99	1.0
Zebra host dolomite		25.0	-115	0.6
Zebra host dolomite		24.3		1.2
Zulu host dolomite		24.3		-1.4
		-----		-----
Averages		24.5 $\pm$ 0.7		0.8 $\pm$ 1.0

Table V-3 cont'd  
Hole #  
and footage

	Mineral	$\delta^{18}\text{O}$ SMOW	$\delta\text{D}$ SMOW	$\delta^{13}\text{C}$ PDB
<b>Type III ores</b>				
#9 vein	quartz	13.3	-158	
PC-08 256.6m	quartz	17.7		
PC-08 292.1m	quartz	17.6	-149	
3050 Level	quartz		-161	
PC-40 235.1m	quartz	10.0	-113	
rerun	quartz	15.6		
3-C-21 597'	quartz	17.2	-167	
3-D-32 647'	quartz	9.1	-165	
PC-28 65.2m	quartz	18.3	-148	
Rico showing	quartz	19.7	-171	
rerun		19.7	-135	
8-D-11 391.5'	quartz	19.4	-152	
3-C-26 598'	quartz	19.4	-135	
PC-13 260	quartz	12.1	-175	
PC-13 262	quartz	17.8	-184	
PC-13 290	quartz	17.4	-172	
Cripple Creek	quartz	17.4	-157	
PC-14 192.5	quartz		-166	
PC-08 256.9m	quartz	<u>16.4</u>	<u>-179</u>	
Averages		$16.9 \pm 2.8$	$-158 \pm 18$	
Sphalerite vein 3050 level portal	sphalerite		-118	
<b>Calcite veining</b>				
#8 Zone	calcite	22.0	-167	2.9
PC-13 289m	calcite	10.2		-4.0
PC-41 103.4m	calcite	19.9	-146	-15.5
PC-40 299.7m	calcite		-163	
3-C-21 592	calcite	<u>18.6</u>	_____	<u>-2.3</u>

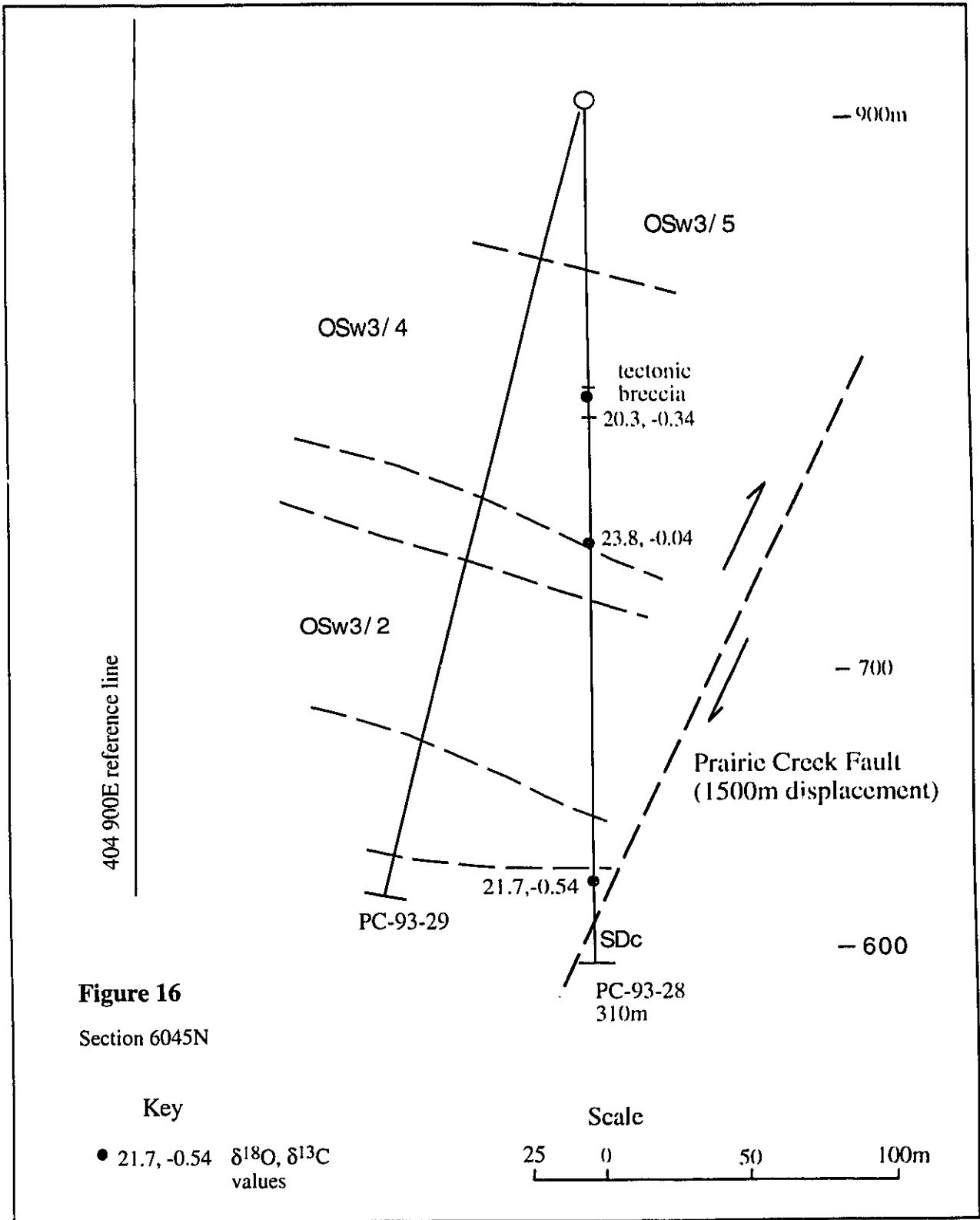


**Figure 14**  $\delta^{18}\text{O}$  versus  $\delta^{13}\text{C}$  plot of Prairie Creek carbonate rocks



**Figure 15**  
**Section 6288N**

$\delta^{18}\text{O}$  and  $\delta^{13}\text{C}$  isotopic values from wallrock dolomites



## Discussion

Taylor (1979) has shown that it is possible to determine the oxygen isotopic composition of a mineralizing fluid from the  $\delta^{18}\text{O}$  of the gangue minerals present, when the following assumptions are satisfied: 1) that the gangue minerals formed contemporaneously and in isotopic equilibrium with the mineralizing fluid and 2) that the temperature of formation is known.

### Type I Fluids

For Type I ore fluids, gangue dolomite has been shown to be associated with stratiform, Zn-Pb mineralization and homogenization temperatures observed in inclusions in sphalerite are similar to those of gangue dolomite. No correction of homogenization temperatures for Type I gangue (range from 165 to 220 °C) has been made for pressure, assuming its formation close to seawater bottom. Because the inclusions in zoned sphalerite are considered primary, and have lower  $T_h$  recorded (average 135 °C), compared to inclusions from other sphalerites (Table IV-1, Appendix I), a temperature of 165 °C (minimum  $T_h$  from gangue dolomite) was chosen for the fractionation formula (below) for this fluid. Due to limited quantities of gangue dolomite available,  $\delta\text{D}_{\text{fluid}}$  values (SMOW) were obtained from only one sample (PC-11 at 261m) which yielded a value -126‰.

For dolomite, the fractionation formula of Mathews and Katz, (1977) was used

$$1000 \ln \alpha_{\text{Dolomite-water}} = 3.06 \times 10^6 T^{-2} - 3.24$$

A plot of  $\delta\text{D}_{\text{fluid}}$  values versus calculated  $\delta^{18}\text{O}_{\text{fluid}}$  values (SMOW) from Table V-4 is presented in Figure 18. A single, calculated  $\delta^{18}\text{O}_{\text{fluid}}$  value from Type I dolomite, plots well to the right of the meteoric water line. The heavy  $\delta^{18}\text{O}$  values suggest modified seawater, with a contaminated  $\delta\text{D}$  signal. The high salinities indicated from fluid inclusion results and heavy  $\delta^{18}\text{O}$  values from dolomitic gangue support an interpretation of buoyant

plumes ponding onto the seafloor. Such a concept would also accommodate pervasive dolomitization observed in Ordovician carbonate rocks within the Prairie Creek Embayment. An alternative interpretation might include highly evolved meteoric water as mineralizing fluid, with mineralization occurring during the Late Paleozoic. Such an interpretation is inconsistent with conodont alteration index values obtained by Morrow et al. (1990).

### Type II fluids

For Type II ore fluids,  $\delta^{18}\text{O}$  values from host dolomites (average 24.5‰) vary significantly from dolomitic gangue (16.4‰). The lower  $\delta^{18}\text{O}$  values in dolomitic gangue suggest a greater component of low  $\delta^{18}\text{O}$  fluids from meteoric waters and/or increasing temperature. Fluid inclusion results obtained from dolomitic cement from drill hole PC-74-78m at 181m (average  $T_h = 160^\circ\text{C}$ ) are similar to the lowest  $T_h$  recorded from inclusions in sphalerite (155 °C). Higher homogenization temperatures recorded from the inclusions in sphalerite may be due to leakage and therefore a temperature of 160 °C is suggested as a fluid temperature in characterizing Type II ores in this study. This temperature is also comparable to temperatures generally reported from fluid inclusions in Mississippi Valley Type deposits (Anderson and MacQueen, 1982).

$\delta\text{D}_{\text{fluid}}$  values from both dolomitic gangue (-61 and -66‰) and host dolomite (-64‰) from drill hole data are plotted in a  $\delta\text{D}$  versus  $\delta^{18}\text{O}$  plot (Figure 17).  $\delta\text{D}$  values (-76 to -42‰) from the Manetoe Dolomite, determined by Yang et al. (1995) are consistent with results from this study. In Figure 17, two possible scenarios are illustrated for resulting  $\delta\text{D}$  values for Type II dolomite cement. These include; 1) dolomitic cements formed from highly evaporated seawater or 2) the cements formed from evolved meteoric fluid. The presence of pseudomorphs of probable evaporites (Plate 8) provides evidence supporting the former interpretation.

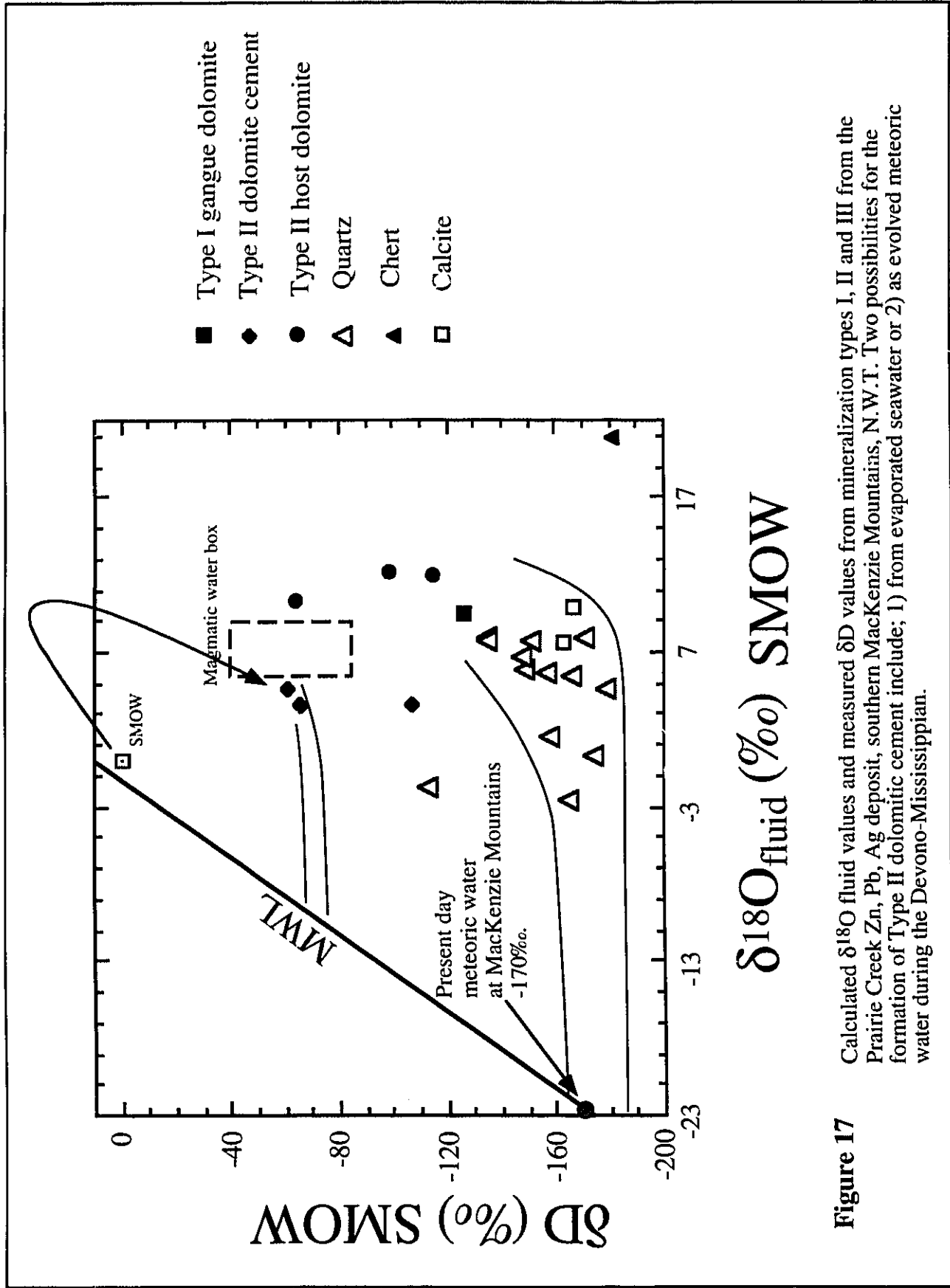


**Figure 17** Calculated  $\delta^{18}\text{O}$  fluid values and measured  $\delta\text{D}$  values from mineralization types I, II and III from the Prairie Creek Zn, Pb, Ag deposit, southern MacKenzie Mountains, N.W.T. Two possibilities for the formation of Type II dolomitic cement include; 1) from evaporated seawater or 2) as evolved meteoric water during the Devonian-Mississippian.



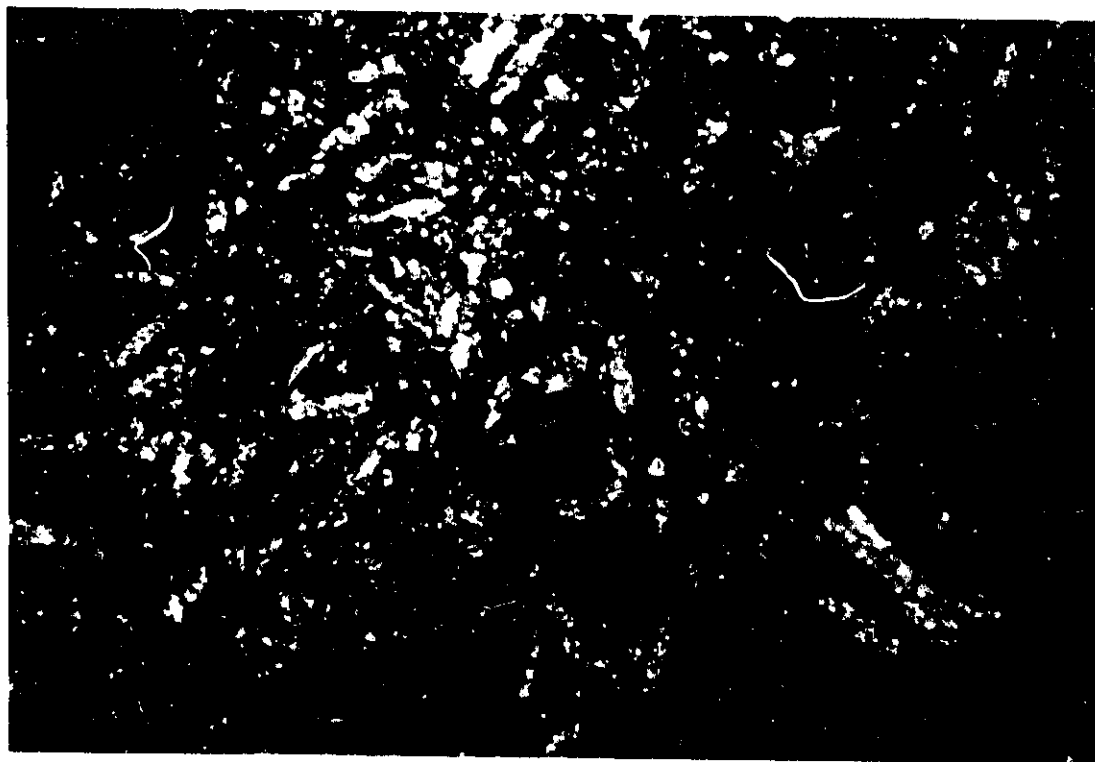


Plate 8      Photomicrograph illustrating evaporite pseudomorphs within siliceous sections of regionally dolomitized Whittaker Formation dolostones.

### Type III fluids

For Type III ores, mineralization appears to be more closely associated with early quartz veining, as (later) quartz overgrowths are barren. Based on the fluid inclusion  $T_h$  results, as well as coexisting  $\text{CO}_2$  and  $\text{NaCl}$  inclusions, temperatures of 200 to 275 °C are suggested for Type III ore fluids.  $\delta^{18}\text{O}_{\text{fluid}}$  values in quartz veins hosting Type III mineralization have become enriched in  $^{18}\text{O}$  mainly due to water-rock interaction, and not solely due to temperature alone. Considering present day meteoric water at -170‰ for the Prairie Creek area, the  $^{18}\text{O}$  shift to the right from the meteoric water line (Figure 17) is consistent with water-rock interaction between meteoric fluids and carbonate rock.

For quartz the fractionation formula of Matsuhisa et al. (1979) was used for the range 250-500°C. A temperature of 200 °C was used in the formula below,

$$1000 \ln \alpha_{\text{Quartz-Water}} = 3.34(10^6 T^{-2}) - 3.31$$

Fluids from vein calcite has been interpreted as low temperature and low salinity based on fluid inclusion results and are also shown on the  $\delta\text{D}$  versus  $\delta^{18}\text{O}$  plot (Figure 17). A single unmineralized, calcite vein gave higher salinity results, but its relationship to mineralization is unclear.

For calcite the fractionation formula of O'Neil et al. (1969) was used

$$1000 \ln \alpha_{\text{Calcite -Water}} = 2.78 (10^6 T^{-2}) - 2.89$$

and a temperature of 150 °C was used for the calculation of  $\delta^{18}\text{O}$  for the fluid in equilibrium with the calcites.

Using  $\delta\text{D}$  values from sparry dolomite from Pine Point and Cambrian dolomites associated with MVT style mineralization in southeastern British Columbia, Nesbitt and Muehlenbachs (1994) determined a correlation between high  $\delta\text{D}$  fluid inclusion values and high salinity inclusions in preorogenic dolomites versus low  $\delta\text{D}$  fluid inclusion values and

low salinity inclusions which are characteristic of syn- to post-orogenic fluids. Plotting salinity versus  $\delta D$ , Nesbitt and Muehlenbachs (1994) interpreted Laramide fluids as low salinity, low  $\delta D$  fluids. In Figure 18, a similar analogy may be drawn from Type III quartz veins as well as vein calcite which are interpreted as Laramide fluids, generally having low  $\delta D$  values and a range in salinities, which are attributed to mixing of meteoric water and dolomitic rocks. In comparison, fluids associated with types I and II mineralization exhibit higher  $\delta D$  and high salinity values. The high salinity values from Type II fluids plot close to values obtained by Nesbitt and Muehlenbachs, (1994) for Alberta basinal brines in a  $\delta D$  versus  $\delta^{18}O$  plot and infer a genetic linkage between the Type II fluids and mineralizing brines at Pine Point.

**Table V-4 Calculated  $\delta^{18}O_{\text{fluid}}$  values**

Hole # and footage	Mineral	$\delta^{18}O_{\text{rock}}$	$\delta D_{\text{fluid}}$	calculated $\delta^{18}O_{\text{fluid}}$ ( $^{\circ}C$ )		
				165	200	250
<b>Type I</b>						
PC-08 273.5m	gangue dol.	23.8		11.1	13.4	16.2
PC-11 261.3m	gangue dol.	22.1	-126	9.4	11.7	14.5
PC-13 290.7	gangue dol.	22.7		10.0	12.3	15.1
PC-13 290.7m rerun	gangue dol.	23.6		10.9	13.2	16.0
PC-14 289.3m	gangue dol.	22.1		9.4	11.7	14.5
PC-21 273.5m	gangue dol.	<u>23.6</u>		<u>10.9</u>	<u>13.2</u>	<u>16.0</u>
averages		23.0 $\pm$ 0.8		10.3 $\pm$ 0.8	12.6 $\pm$ 0.9	
<b>Type II</b>						
				160 $^{\circ}C$	200 $^{\circ}C$	
Zebra showing dol. cem. (1)		16.9	-108	3.8	6.5	
Zebra dolomitic cement adjacent colloform sph.		12.7		-0.4	2.3	
Zebra dol. cement (2)		14.0		0.9	3.6	
Zulu dol. cement		16.9		3.8	6.5	
PC-94-78 181m dol. cement		17.8	-61	4.7	7.4	
208A " "		19.8		6.7	9.4	
242m " "		<u>16.8</u>	-66	<u>3.7</u>	<u>6.4</u>	
dolomitic cement averages				3.3 $\pm$ 2.4	6.0 $\pm$ 2.4	

Table V-4 continued		160 °C	200 °C
PC-94-78 208B m host dolomite	25.3	<b>12.2</b>	14.9
" " 287m " "	23.8	<b>10.7</b>	13.4
PC-95-117 46m " "	23.4	-64 <b>10.3</b>	13.0
Zebra HB (heavily bleached dolomite)	25.3	-99 <b>12.2</b>	14.9
Zebra host dolomite	25.0	-115 <b>11.9</b>	14.6
Zebra host dolomite	24.3	<b>11.2</b>	13.9
Zulu host dolomite	<u>24.3</u>	<u>11.2</u>	<u>13.9</u>
Averages		<b>11.4 ± 0.7</b>	14.1 ± 0.7

sample #	$\delta^{18}\text{O}_{\text{rock}}$	$\delta\text{D}_{\text{fluid}}$	calculated $\delta^{18}\text{O}_{\text{fluid}}$ SMOW		
			150 °C	200 °C	250 °C

### Type III

#9 vein	quartz	13.3	-158	-2.1	<b>1.7</b>	4.5
PC-08 291m	quartz	17.6	-149	2.2	<b>6.0</b>	8.8
PC-40 235.1m	quartz	10.0	-113	-5.4	<b>-1.6</b>	1.2
3-C-21 597'	quartz	17.2	-167	1.8	<b>5.6</b>	8.4
3-D-32 647'	quartz	9.1	-165	-6.3	<b>-2.5</b>	0.3
PC-28 65.2m	quartz	18.3	-148	2.9	<b>6.7</b>	9.5
Rico showing rerun	quartz	19.7	-171	4.3	<b>8.1</b>	10.9
8-D-11 391.5'	quartz	19.4	-152	4.0	<b>7.8</b>	10.6
3-C-26 598'	quartz	19.4	-135	4.0	<b>7.8</b>	10.6
PC-13 260	quartz	12.1	-175	-3.3	<b>0.5</b>	3.3
Cripple Creek	quartz	17.4	-157	2.0	<b>5.8</b>	8.6
PC-08 256.9m	quartz	<u>16.4</u>	<u>-179</u>	<u>1.0</u>	<u>4.8</u>	<u>7.6</u>
Averages				<b>0.4 ± 3.7</b>	<b>4.5 ± 3.7*</b>	7.3 ± 3.7

### Calcite veining

#8 Zone	calcite	22.0	-167	<b>9.8</b>
PC-13 289m	calcite	10.2		-2.0
PC-14 103.4m	calcite	<u>19.9</u>	-163	<u>7.7</u>
averages		17.4 ± 6.3		5.2

\*  $\delta^{18}\text{O}$  values used in Figure 17

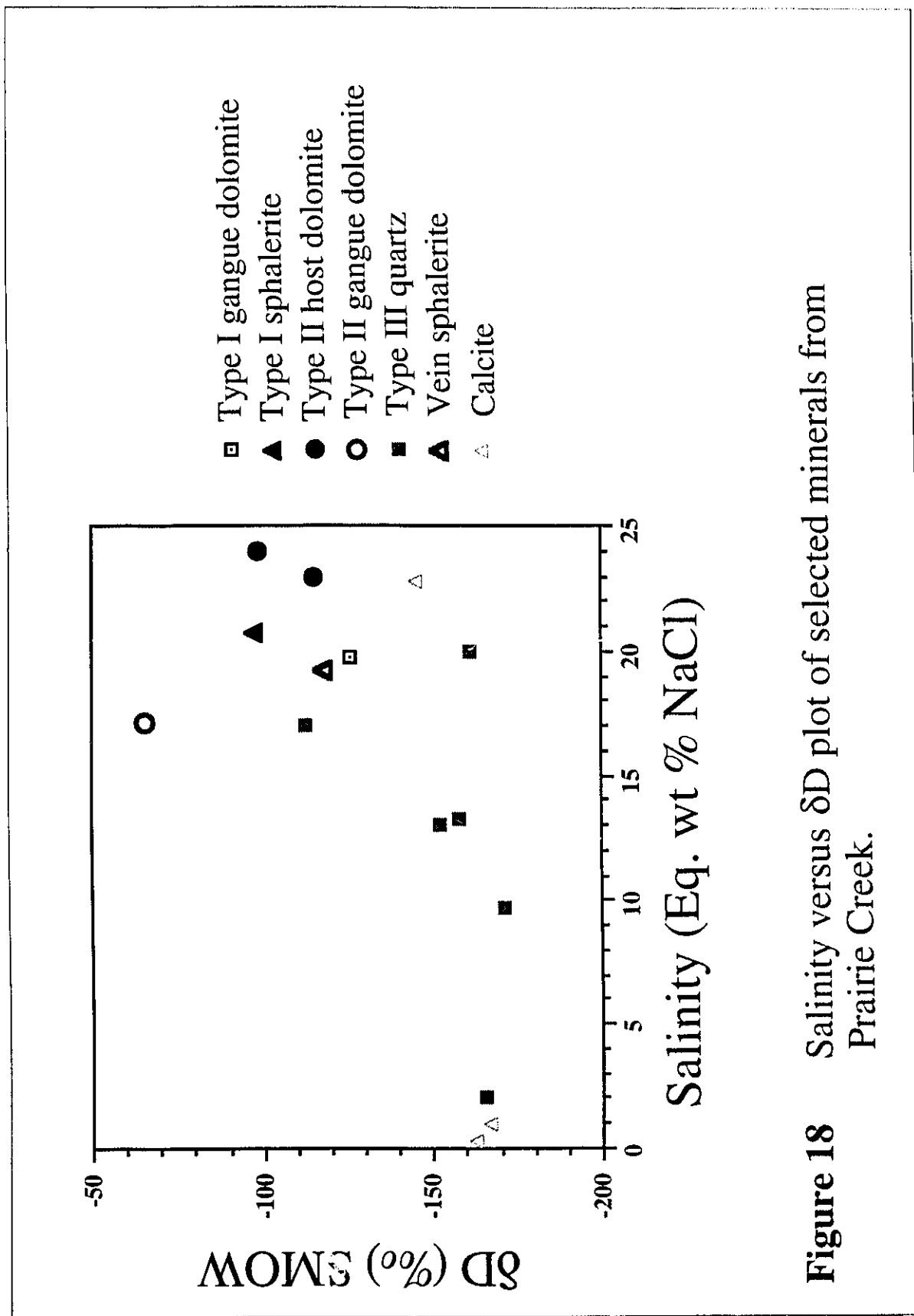


**Figure 18** Salinity versus  $\delta D$  plot of selected minerals from Prairie Creek.

Figure 19, after Land, (1985) illustrates the relative position of gangue dolomite associated with types I and II mineralization and Whittaker Formation wholerock dolomite plotted as a function of homogenization temperature and  $\delta^{18}\text{O}$  rock values (PDB scale). Contours shown are in  $\delta^{18}\text{O}_{\text{fluid}}$  values (SMOW). For comparison, values obtained from Aulstead, (1987) for the Manetoe Facies as well as Pine Point (Qing and Mountjoy, 1992) are also shown.

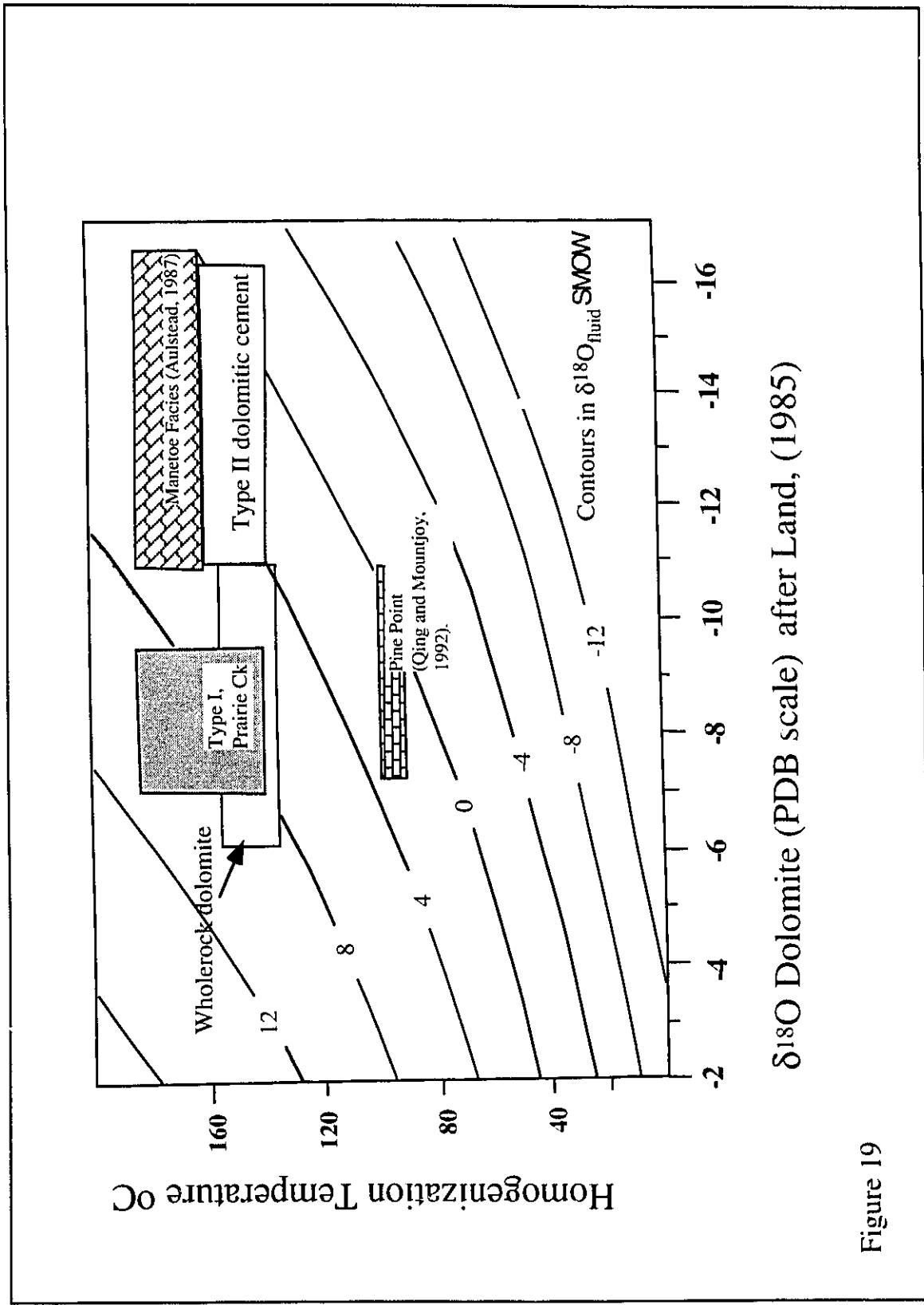


Figure 19

## Chapter VI Radiogenic isotopes

### Introduction

Pb/Pb isotopes have been used in ore deposit research to constrain both source and age of mineralization (Doe and Stacey, 1974; Doe and Zartman, 1979; Gulson, 1986). The use of lead isotope geochemistry relies on two major factors: 1) the isotopic signature of the particular mineralization usually differs from that of other styles of mineralization and barren host rock, and 2) the isotopic composition of lead is unaffected by isotopic fractionation during low temperature processes (Gulson, 1986). More recently,  $^{87}\text{Sr}/^{86}\text{Sr}$  has been used to investigate regional fluid systems and mineralized (carbonate) vein systems (Qing and Mountjoy, 1992; Koffyberg, 1994)

### 6.1 Lead Isotope Systematics

Lead on Earth consists of primeval lead (present when the Earth formed 4.55 Ga ago) plus radiogenic lead derived from radioactive decay of uranium and thorium. The isotopic composition of the Earth's primeval lead is assumed to be identical to the initial non-radiogenic isotope composition in primitive meteorites, and the generally accepted initial lead values are those given by Tatsumoto et al. (1973). These authors measured the isotopic composition of troilite from the Canyon Diablo iron meteorite. The troilite contains lead, but negligible amounts of uranium and thorium so that the Pb isotopic composition has not changed since the time of formation of the meteorite.

The characterization of ore deposits by lead isotope geochemistry is based on variations in the radiogenic lead isotopes. Three isotopes,  $^{206}\text{Pb}$ ,  $^{207}\text{Pb}$ , and  $^{208}\text{Pb}$ , form from the radioactive decay of  $^{238}\text{U}$ ,  $^{235}\text{U}$  and  $^{232}\text{Th}$ , respectively, while a fourth isotope,  $^{204}\text{Pb}$ , has no long-lived parent (Gulson, 1986). Because the parent elements of the lead isotopes  $^{206}\text{Pb}$ ,  $^{207}\text{Pb}$  and  $^{208}\text{Pb}$  have different half-lives, (Faure, 1986) the relative abundance of the radiogenic lead isotopes  $^{206}\text{Pb}$ ,  $^{207}\text{Pb}$  and  $^{208}\text{Pb}$ , to the stable lead isotope  $^{204}\text{Pb}$  varies with time of duration from uranium-bearing materials. The isotopic



values are measured as ratios in a mass spectrometer and plotted as ratios of  $^{207}\text{Pb}/^{204}\text{Pb}$  versus  $^{206}\text{Pb}/^{204}\text{Pb}$  plots and  $^{208}\text{Pb}/^{204}\text{Pb}$  versus  $^{206}\text{Pb}/^{204}\text{Pb}$  plots.

Nier et al. (1941) investigated galenas from different ore deposits and determined that the leads had different isotopic compositions and proposed that the variations in isotopic ratios resulted from different times of addition of radiogenic lead to primeval lead prior to the emplacement of mineralization. Canadian researchers (Russell and Farquhar, 1960) determined that certain variably-aged, lead-rich deposits (Broken Hill, among others) had isotopic values which fell along an average growth curve, and from these values, a single stage model (Faure, 1986) could be used to determine age of mineralization. Such deposits are termed ordinary (Faure, 1986). Single stage lead deposits (as galena) are thought to have been derived in a single mineralizing step from a relatively homogenous portion of the mantle. Common lead is lead whose isotopic composition no longer changes because the Pb mineral contains no U or Th. Other deposits such as the Mississippi-Valley lead-zinc deposits have lead isotopic values which plot above single-stage growth curves on  $^{207}\text{Pb}/^{204}\text{Pb}$  versus  $^{206}\text{Pb}/^{204}\text{Pb}$  plots and are called anomalous leads (Faure, 1986).

Lead isotope studies of ores in carbonate rocks have been used to determine source of ore-forming elements (Godwin et al., 1982), but age determinations have been equivocal (Sangster, 1983). In attempts to determine the age of mineralization in carbonate-hosted Pb-Zn deposits, differences were found in the ages of mineralization in comparison to the geological age of the host rocks (Doe and Zartman, 1979; Sangster, 1986). Certain Pb-Zn mineralization (Mississippi Valley deposits in southeastern U.S.) have model lead ages that are unrealistically young, while others such as Gay's River, Nova Scotia have dates older than the geological age of the host rocks (Akende and Zentilli, 1984). Using multi-stage lead models, Gulson (1986) has suggested that if the source of the lead is known, then an age of mineralization may be determined, and conversely, if the age of the lead mineralization is well constrained, then a source may be determined.

Gulson, (1986) in studying lead-rich carbonate-hosted deposits, observed the following isotopic characteristics for different groups of deposits: 1) deposits that show linear trends on  $^{207}\text{Pb}/^{204}\text{Pb}$  versus  $^{206}\text{Pb}/^{204}\text{Pb}$  plots, with variation within districts, within individual deposits, and occasionally within individual galena crystals (the Mississippi Valley region of the southeastern U.S.); 2) deposits that outline a limited spread in their isotopic compositions and conform to evolution curves, including paleokarsted mineralization as at Nanisivik, NWT, (Olson, 1984); 3) single stage deposits that have homogenous isotopic values and are conformable to growth curves, including Pine Point, NWT (Cumming et al., 1990) and Navan and Silvermines in Ireland (Boast et al., 1981); and 4) deposits that have homogenous isotopic values but data lie significantly above the single stage evolution curve indicating that the lead was derived from an upper crustal source.

Godwin et al. (1982) and Morrow and Cumming (1982) observed that the isotopic compositions of lead from samples from lower Paleozoic, carbonate-hosted, zinc-lead mineralization in the northern Cordillera fall above the Stacey and Kramers (1975) growth curve for common lead. The deposits as a group, plot in a nearly linear array on  $^{207}\text{Pb}/^{204}\text{Pb}$  versus  $^{206}\text{Pb}/^{204}\text{Pb}$  diagrams. On the basis of minor element compositions of sphalerite (McLaren and Godwin, 1979) and lead isotope compositions of galena from shale-hosted deposits in the northern Canadian Cordillera, Godwin et al. (1982) developed shale growth curves to fit the lead data. Their purpose was to explain unrealistically young model ages for galenas from Paleozoic shale-hosted deposits in the Selwyn Basin, based on the Stacey and Kramers (1975) models. In Figure 20, three isochrons represent 1) old (Proterozoic-Cambrian) carbonate-hosted Pb-Zn deposits; 2) young (post Ordovician to Devonian) carbonate-hosted Pb-Zn and shale-hosted Ba-Pb-Zn deposits, and 3) silver-rich, vein-type deposits. Godwin et al. (1982) interpreted the lead isotopic values as falling on secondary isochrons, reflecting a two-stage, lead evolution history (Doe and Zartman, 1979). Godwin et al. (1982) suggested that shale-hosted Ba-Zn-Pb stratiform deposits in

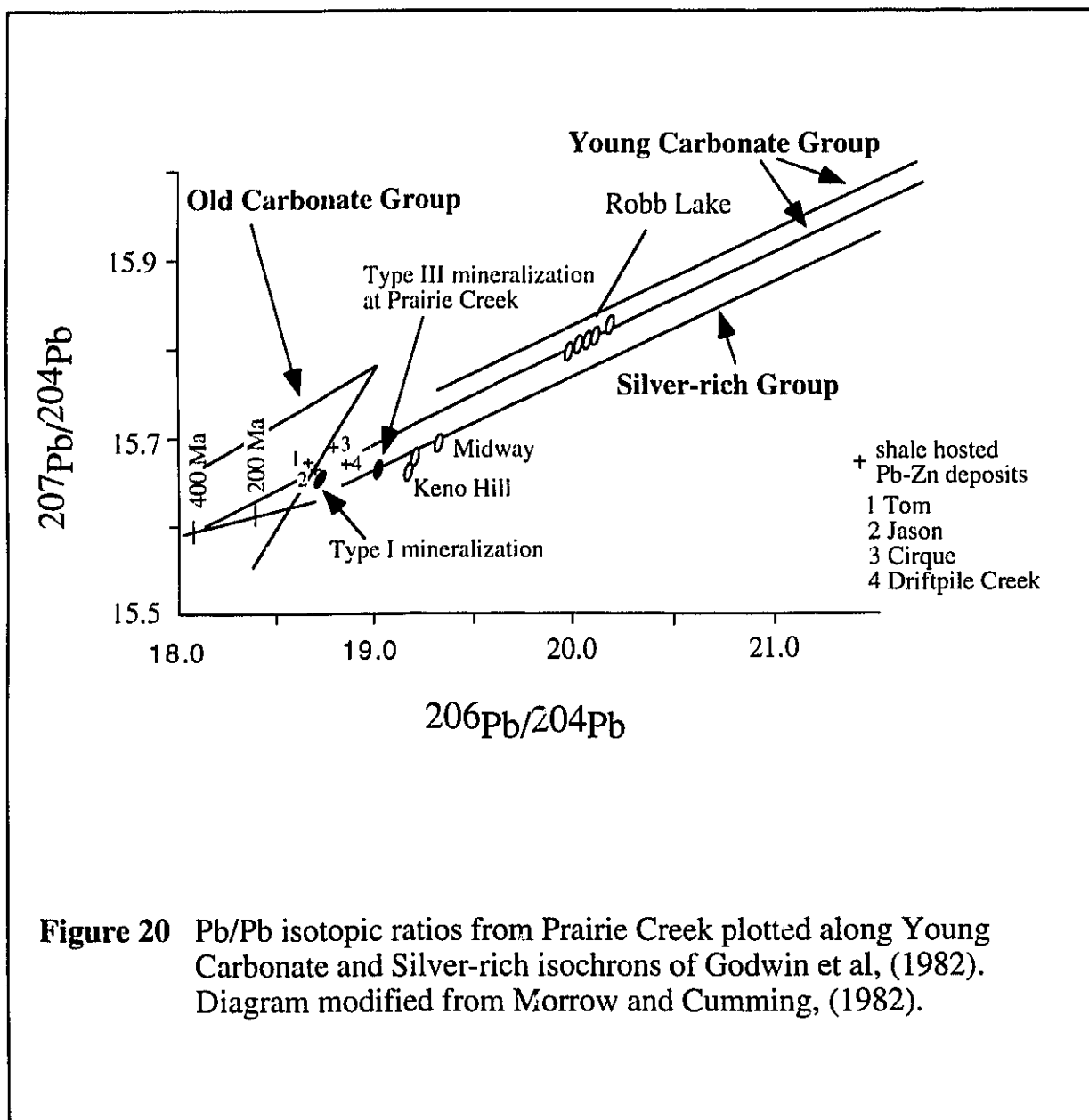


**Figure 20** Pb/Pb isotopic ratios from Prairie Creek plotted along Young Carbonate and Silver-rich isochrons of Godwin et al, (1982). Diagram modified from Morrow and Cumming, (1982).

the Selwyn Basin and epigenetic, young (Silurian to Devonian) carbonate-hosted Zn-Pb deposits in the MacKenzie Platform had similar Proterozoic sources. Godwin et al. (1982) further suggested that fluids, from which syngenetic deposits formed within the Selwyn Basin, are localized by intrabasinal faults and contemporaneous with epigenetic mineralization in adjoining carbonates in the MacKenzie Platform. Morrow and Cumming (1982) criticized the broad generalizations and conclusions of Godwin et al. (1982). In particular, the "Young Carbonate" group of deposits of Godwin et al. (1982) includes two geologically and isotopically distinct types, shale-hosted and carbonate-hosted rocks.

South of the areas examined by Godwin et al. (1982), Morrow and Cumming (1982) investigated several carbonate-hosted, lead-zinc deposits including Robb Lake and the Prairie Creek deposit. At Prairie Creek, Morrow and Cumming (1982) determined the lead isotopic values of galena samples from a 500m strike length along the #3 Zone vein at Prairie Creek. They observed a high degree of homogeneity in lead isotopic values. Based on data from Prairie Creek, and several additional locations, Morrow and Cumming (1982) interpreted carbonate-hosted, lead-zinc mineralization as forming a series of four subparallel linear arrays, reflecting a more complex multi-stage lead evolution pattern and suggested that the (Cadillac) Prairie Creek deposit falls on the "Silver-rich vein" trend of Godwin et al. (1982). Morrow et al. (1990) reinterpreted the data of Morrow and Cumming (1982), and suggested that the source of lead-zinc mineralization within the Manetoe Facies was consistent with the model of Godwin et al. (1982) at approximately 1887 Ma, reflecting a Hudsonian source for mineralization. Morrow et al. (1990) concluded that Pb-Zn mineralization in the southern MacKenzie Mountains area was probably formed soon after shale basin development (Devono-Mississippian), but using a three stage model were unable to determine an exact date of mineralization. They suggested that mineralization associated with the Manetoe Facies occurred in the early Mesozoic, based on the shale-dewatering mechanism proposed by MacQueen and Thompson (1978) for the Robb Lake deposit.

As part of this study, additional galena and sphalerite samples from stratiform (Type I), MVT style (Type II) and vein (Type III) mineralization were analyzed. Four gangue dolomites, associated with stratiform ore, and two dolomites from MVT style mineralization were also analyzed. In addition, one gangue dolomite from vein mineralization was analyzed. The results are presented in Table VI-1, together with data from previous studies (Morrow and Cumming, 1982). For comparison, data are also presented for the stratiform Jason and Tom deposits of MacMillan Pass, and the Howard's Pass deposit, Yukon, (Godwin et al., 1982) and MVT deposits such as Robb Lake, B.C. (Morrow et al., 1990) and Pine Point (Cumming et al., 1990). Lead isotopic data from Keno Hill are also presented (Godwin et al., 1982).

### Techniques

Clean galena grains (~1mm size) were dissolved in pure, warm 2N HCl acid overnight and allowed to gently evaporate to dryness, forming well crystallized  $PbCl_2$  grains. Chloride crystals were purified by washing with 4N HCl and water before final dissolution and mass spectrometric analysis. Predominantly sphalerite samples and dolomite samples were dissolved in 6N HCl and evaporated to dryness. Mixture of 0.7N HBr and a few drops of 2N HCl was added to each residue, and after complete redissolution, lead was separated using anion exchange resin columns in Hydrobromic acid. Samples were loaded on a rhenium filament with silica gel and phosphoric acid. The samples were run on a Micromass MM30 mass spectrometer at an operating temperature of 1250 °C. Overall reproducibility of the measurements was determined from a large number of the NBS SRM 981 Common Lead standard lead measurements. At 1s error level the reproducibility of the measured isotopic ratios is as follows: 0.021%, 0.036% and 0.044% for  $^{206}Pb/^{204}Pb$ ,  $^{207}Pb/^{204}Pb$  and  $^{208}Pb/^{204}Pb$ , respectively. Correlation coefficient of the errors is 0.91. All of the results are normalized to the nominal NRS SRM 981 Common Lead standard values (personal communication, Dragon Krstic).

**Table VI-1 Lead isotope data**

Sample #	Mineral	$^{206}\text{Pb}/^{204}\text{Pb}$	$^{207}\text{Pb}/^{204}\text{Pb}$	$^{208}\text{Pb}/^{204}\text{Pb}$
<b>Stratiform (Type I) ores (from galenas)</b>				
PC-08 273.5		18.664	15.640	38.727
PC-08 281.5		18.698	15.652	38.793
PC-08 281.5B		18.681	15.646	38.748
PC-11 263.3		18.676	15.641	38.745
PC-12 269.2		18.690	15.640	38.769
PC-12 274.7		18.723	15.653	38.778
PC-13 290.7 (1)		18.770	15.656	38.807
PC-13 290.7 (2)		18.692	15.646	38.751
PC-13 290.7 (3)		18.718	15.654	38.775
PC-14 289.3		18.708	15.662	38.806
PC-14 289.6		18.801	15.663	38.861
PC-15 101.7		18.695	15.653	38.782
PC-17 312.4		18.700	15.655	38.763
PC-27 213		18.689	15.655	38.768
PC-27 226.4		18.687	15.650	38.752
PC-35 224		18.773	15.655	38.822
<b>Range of sulfides</b> (16 samples)		<b>18.664-18.773</b>	<b>15.640-15.662</b>	<b>38.727-38.861</b>
<b>Gangue dolomite (type I)</b>				
PC-11 261 gangue dolomite		18.934	15.669	38.981
PC-13 290 gangue dolomite		18.703	15.647	38.778
PC-14 289.3 " "		18.885	15.663	38.934
PC-21 273 gangue dolomite		18.869	15.666	38.935
<b>Range of dolomites</b> (4 samples)		<b>18.703-18.934</b>	<b>15.647-15.669</b>	<b>38.778-38.981</b>
<b>MVT style (Type II) ores</b>				
Samantha MVT ?		18.739	15.647	38.816
Zebra sphalerite		18.581	15.641	38.566
Zulu sphalerite		18.664	15.656	38.552
<b>Range of sulfides</b>		<b>18.581-18.739</b>	<b>15.641-15.656</b>	<b>38.552-38.816</b>
<b>Gangue dolomite from Type II</b>				
Zebra host dolomite		19.288	15.697	38.972
Zebra white dolomitic cement		19.283	15.700	38.844

Table VI-1 continued  
**Mineralization from Quartz veining (Type III ores)**

Sample #	Mineral	$^{206}\text{Pb}/^{204}\text{Pb}$	$^{207}\text{Pb}/^{204}\text{Pb}$	$^{208}\text{Pb}/^{204}\text{Pb}$
Smithsonite #8 Zone	vein	19.018	15.679	39.060
Repeat		19.010	15.676	39.067
Rico galena	vein	19.042	15.675	39.040
Rico sphalerite	vein	19.132	15.685	39.097
PC-11 286.4		19.003	15.667	39.031
additional 23 vein samples analyzed (Morrow and Cumming, 1982)				
1 (#3 drift)		19.020	15.672	39.050
2 (#6 drift)		19.027	15.675	39.066
3 (#9 drift)		19.028	15.675	39.084
4 (#11 drift)		19.037	15.677	39.081
5 (#20 drift)		19.017	15.673	39.062
6 (#31 drift)		19.025	15.674	39.072
7 shear		19.018	15.677	39.066
8 shear		19.027	15.674	39.075
9 #8 showing		19.012	15.675	39.060
45670-1		19.019	15.667	39.035
045669-2		19.025	15.659	39.024
#6 drift		19.036	15.681	39.100
76295		19.009	15.656	39.015
076294-3		19.030	15.669	39.033
076294-2		19.023	15.667	39.045
076294-1		19.019	15.668	39.054
10		19.030	15.674	39.054
11		19.025	15.673	39.060
12		19.030	15.660	38.978
13		19.035	15.672	39.053
14		19.044	15.676	39.069
15		19.036	15.669	39.031
17		19.021	15.674	39.075
<hr/>				
<b>Range of sulfides</b>		<b>19.003-19.132</b>	<b>15.656-15.681</b>	<b>38.978-39.100</b>
(28 analyses)				
3-C-26 598 ft	gangue dol.	19.239	15.695	38.981
<b>Other *</b>				
PC-40 301.9		19.322	15.706	38.906
PC-40 repeat		19.326	15.708	38.929
PC-40 301.9		19.975	15.770	39.190
<hr/>				
<b>Range</b>		<b>19.322-19.975</b>	<b>15.706-15.770</b>	<b>38.906-39.190</b>
* mineralization in veinlets along edge of stratiform ore				

### Comparison with Pb/Pb values from other Pb-Zn deposits

Sample #	Mineral	$^{206}\text{Pb}/^{204}\text{Pb}$	$^{207}\text{Pb}/^{204}\text{Pb}$	$^{208}\text{Pb}/^{204}\text{Pb}$
Jason deposit (Godwin et al., 1982)				
	Range of 5 values	18.661-18.737	15.646-15.693	38.501-38.820
Tom deposit (Godwin et al. 1982)				
	Range of 5	18.633-18.695	15.636-15.727	38.536-38.892
Howard's Pass				
	Range of 3	18.553-18.602	15.621-15.657	38.561-38.592
Robb Lake deposit (Morrow et al. 1990)				
	Range of 5	19.987-20.198	15.801-15.833	40.726-41.068
Pine Point (Cumming et al., 1990)				
	Range of 32 galena samples	18.167-18.186	15.570-15.578	38.155-38.203
Keno Hill (Godwin et al., 1982)				
		19.133-19.206	15.646-15.668	39.157-39.279
Midway Bradford, (1988)				
		19.16-19.35	15.677-15.742	39.832( ave.)

### Results

Lead isotopic analyses of galenas and sphalerites as well as gangue dolomites from ore Types I, II and III and host dolomites from Type II ores are presented in Table VI-1 and Figure 21. For stratiform ores, the results indicate that the lead values are generally homogenous with  $^{206}\text{Pb}/^{204}\text{Pb}$  values ranging from 18.663 and 18.801, with thirteen of sixteen values forming a cluster from 18.664 to 18.723. The data plot above the Stacey-Kramers (1975) evolution curves on a  $^{207}\text{Pb}/^{204}\text{Pb}$  versus  $^{206}\text{Pb}/^{204}\text{Pb}$  plot indicating that the lead was derived from an upper crustal source with higher U/Pb ratio than that of the Stacey-Kramers (1975) second stage value (Gulson, 1986). Gangue dolomites associated with Type I ores have a range in  $^{206}\text{Pb}/^{204}\text{Pb}$  values of 18.703 to 18.934, and align closely to stratiform sulfide values (Godwin et al. 1982) on a  $^{207}\text{Pb}/^{204}\text{Pb}$  versus  $^{206}\text{Pb}/^{204}\text{Pb}$  plot. The gangue dolomite is found in contact with sphalerite and galena mineralization.



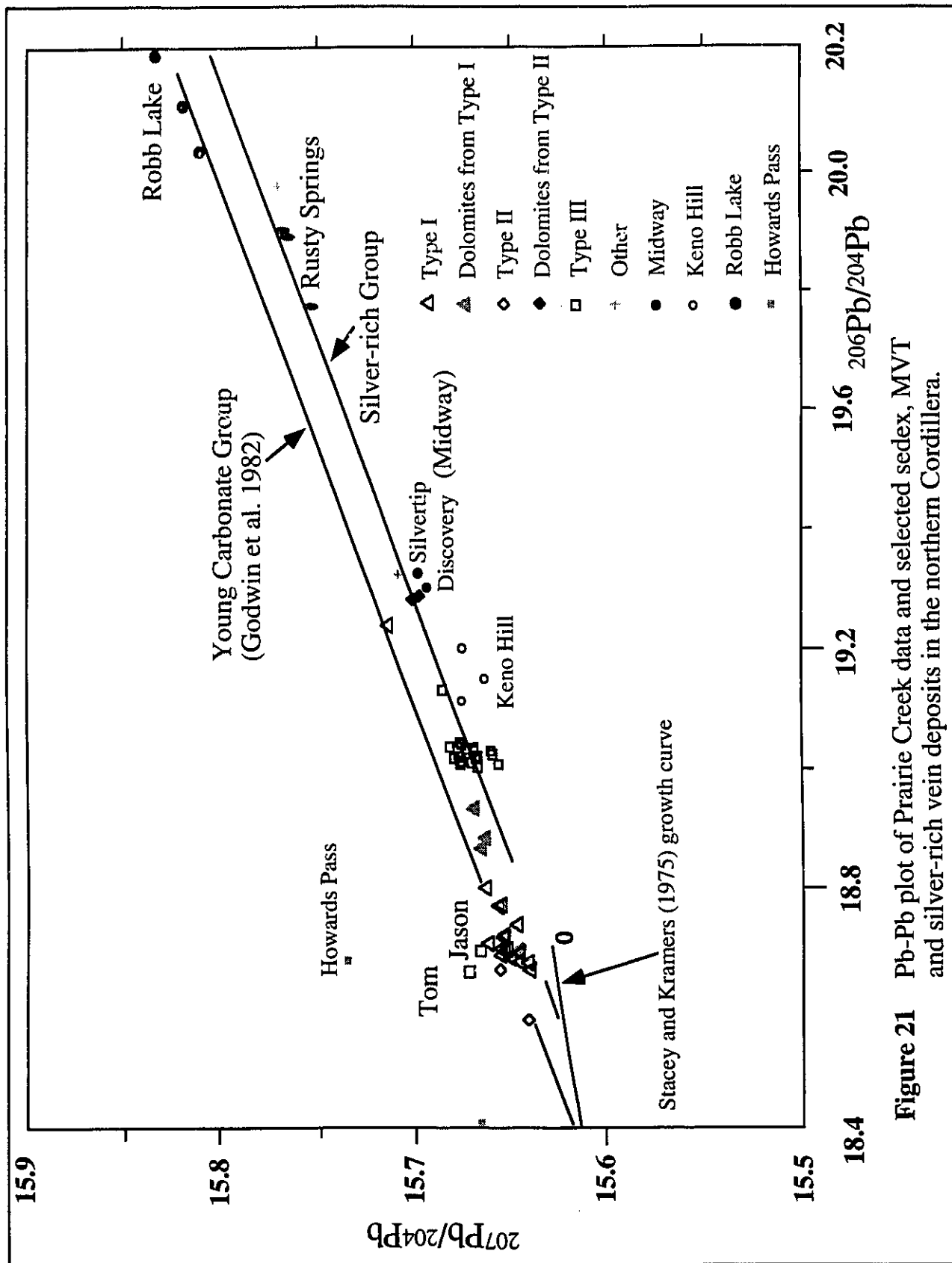


**Figure 21** Pb-Pb plot of Prairie Creek data and selected sedex, MVT and silver-rich vein deposits in the northern Cordillera.

Three lead isotopic analyses were conducted on sphalerite samples from MVT style, (Type II) mineralization as well as adjacent dolomites. The  $^{206}\text{Pb}/^{204}\text{Pb}$  values of the sphalerite samples range from 18.581 to 18.739, in comparison to  $^{206}\text{Pb}/^{204}\text{Pb}$  values of 19.283 and 19.288 from saddle dolomitic cement and host dolomite. The host recrystallized dolomite is within metres of mineralization, while dolomitic cement was taken millimetres away from sphalerite. Lead isotopic results from Type II ores plot above evolution growth curves on  $^{207}\text{Pb}/^{204}\text{Pb}$  versus  $^{206}\text{Pb}/^{204}\text{Pb}$  plots (Figure 19).

Lead isotopic values from Type III ores show the greatest homogeneity of the three ore types. The range in  $^{206}\text{Pb}/^{204}\text{Pb}$  values is 19.003 to 19.132. Excluding the latter value, 19.132 (Rico sphalerite), the spread for 27  $^{206}\text{Pb}/^{204}\text{Pb}$  values is 0.041. The Rico sphalerite is highly fractured and brecciated, and therefore the elevated values may be a result of post crystallization contamination. On a  $^{207}\text{Pb}/^{204}\text{Pb}$  versus  $^{206}\text{Pb}/^{204}\text{Pb}$  plot, Type III ores also plot above growth curves indicating slightly more radiogenic values. A single gangue dolomite analyzed from Type III ores also has a slightly more radiogenic  $^{206}\text{Pb}/^{204}\text{Pb}$  value than most type III ores (Table VI-1).

Additional  $^{206}\text{Pb}/^{204}\text{Pb}$  values (19.322 to 19.975) from hole PC-40 at 301.9m indicate a greater range and represent the greatest radiogenic values. Data (others in Table VI-1) from two separate samples (and a repeat) similarly plot significantly above the growth curve on a  $^{207}\text{Pb}/^{204}\text{Pb}$  plot versus  $^{206}\text{Pb}/^{204}\text{Pb}$  plot. This sample occurs at the edge of stratiform mineralization, within a quartz veinlet.

A plot of  $^{208}\text{Pb}/^{204}\text{Pb}$  versus  $^{206}\text{Pb}/^{204}\text{Pb}$ , shown in Figure 22 indicates that ore types I and III seem to be fall on a single lead line, including gangue dolomites associated with Type I mineralization. In comparison, gangue dolomite from quartz veining and dolomites from the Type II ores exhibit scattered points. During laboratory procedures, the Type I gangue dolomites were noted to be visibly rich in Pb ( $\text{PbCl}_2$ ), in comparison to gangue dolomites associated with Type II mineralization.

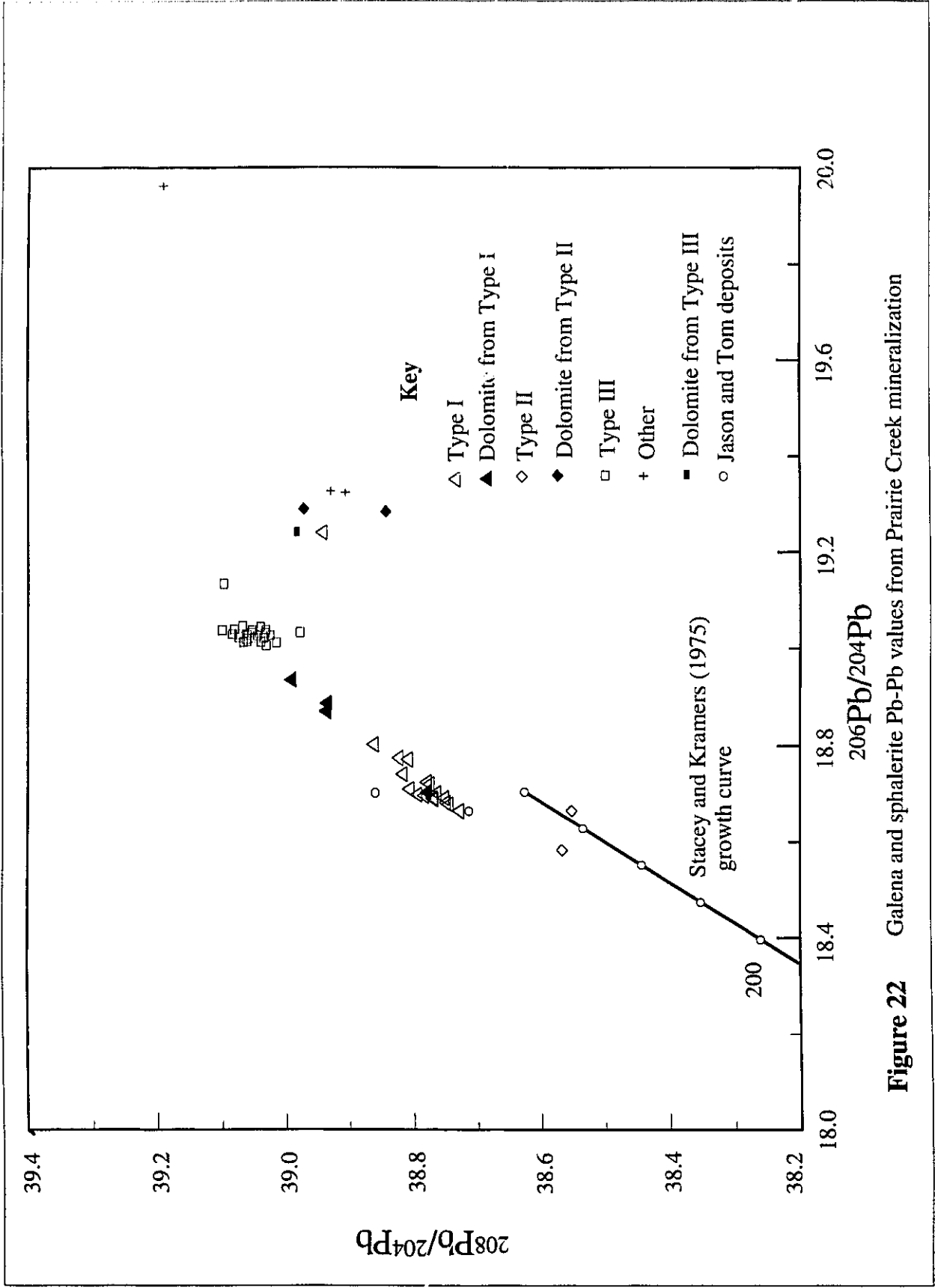
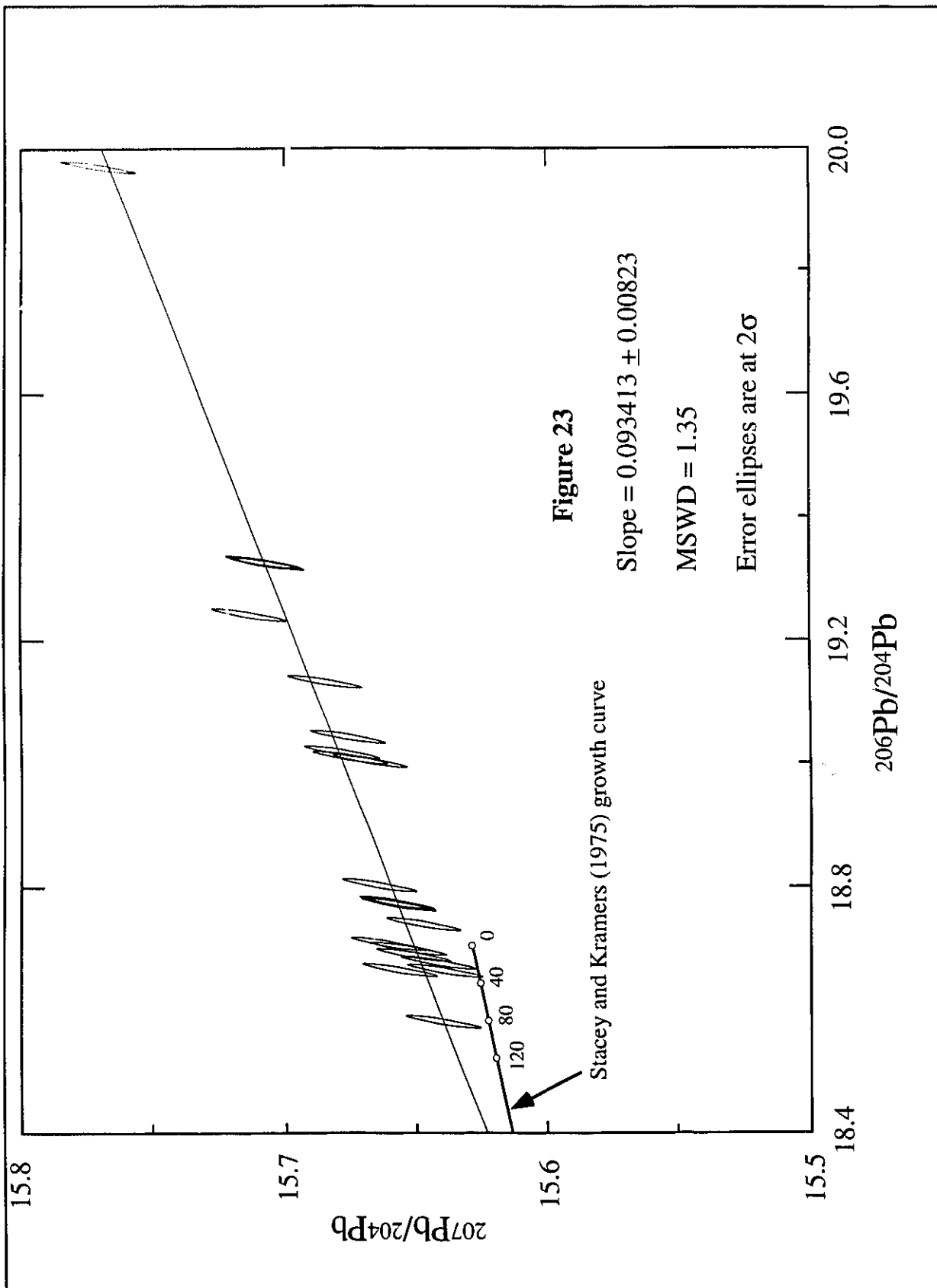


**Figure 22** Galena and sphalerite Pb-Pb values from Prairie Creek mineralization

## Interpretations

From Figure 21, the anomalous nature of Pb isotopes in the three ore types is demonstrated by the plot of the Pb/Pb values above the Stacey and Kramers growth curve. The data indicate a crustal source (Gulson, 1986) and by comparison to model lead compositions (Doe and Zartman, 1979), the upper crust is interpreted as the source of the lead. The narrow ranges of lead compositions for ore types I and III indicate homogenous lead sources. Using a line regression computer output (Yorkfit) (Appendix IV) which provides the slope of the line (Figure 23) and its associated error and MSWD quantity, the intersections of this line along the Stacey and Kramers (1975) growth curve give a best fit of intercepts of 352 and 1249 Ma. The linear regression program also calculates a model isochron age from the slope of the line under the assumption that the radiogenic clock stopped at the time of analyses, and it assumes a mineralizing age of 0 Ma (a simple 2 stage U/Pb evolution history). Using this approach, an estimate of the maximum age of the precursor U/Pb system is calculated to be  $1474 \pm 140$  Ma. The data points form a quasi two stage linear trend and the regression analyses confirms for the given level of analytical error (95% confidence), an almost perfect fit to the line resulting in a MSWD of 1.23. Distribution of isotopic values for vein and stratiform mineralization along the linear trend suggests that the U/Pb systems of the two mineralization styles have a common origin and history, and that the lead values do not represent a case of simple mixing of lead from two different sources. The intersection of the line with the Stacey and Kramers (1975) growth curve at 352 Ma and 1249 Ma ( $\pm 140$  Ma) may indicate closure of the U/Pb system after accumulation of metals in Late Ordovician to early Silurian host rocks.

The ore lead compositions are compared to the data of Godwin et al. (1982) for Pb-Zn-Ag deposits of the northern Cordillera. Plotting Prairie Creek ore types in Figure 23, results for galenas from Type III quartz veins fall closely along the "silver" rich isochron, while Type I, Pb isotopic values for stratiform ores fall more closely along the "young carbonate" isochron. From Table VI-1 and Figure 23, the similarity in lead isotope values



from Type I ores and the Tom, Jason and Howard's Pass shale-hosted deposits is apparent. Data from the Type II ores, fall below the values of Type I ores in Figure 23. These values suggest mixing of fluids may have occurred, consistent with Mississippi Valley Type mineralization, with fluids introduced along a middle Devonian, regional unconformity.

Using the model of Godwin et al. (1982), the ages of mineralization may be speculated upon. As many of the silver-rich deposits (e.g. Keno Hill and Midway, Yukon) studied by (Lynch et al. 1990; Bradford and Godwin, 1987) were associated with Cretaceous plutonism, Godwin et al. (1982) proposed an age of 0.09 Ga for mineralization. Although no Cretaceous plutons are exposed in the Prairie Creek area, from an association with silver-rich mineralization in quartz veins, the model of Godwin et al. (1982) may be used to predict a possible Cretaceous age for Type III vein mineralization. From Table VI-1, the range for  $^{207}\text{Pb}/^{204}\text{Pb}$  and  $^{206}\text{Pb}/^{204}\text{Pb}$  values from Type III mineralization compares closely with the data from Midway (Bradford, 1988) and Keno Hill (Godwin et al. 1982) and Rusty Springs (Kirker, 1982).

Gangue dolomite Pb/Pb analyses from both stratiform and vein ores are presented in Table VI-1. In stratiform ores, gangue dolomite values in both  $^{207}\text{Pb}/^{204}\text{Pb}$  versus  $^{206}\text{Pb}/^{204}\text{Pb}$  and  $^{208}\text{Pb}/^{204}\text{Pb}$  versus  $^{206}\text{Pb}/^{204}\text{Pb}$  plots, plot along isochrons consistent with stratiform mineralization, with one value located within the values for stratiform galenas. In contrast, a single gangue dolomite from Type III ores, plots away from galenas on a  $^{208}\text{Pb}/^{204}\text{Pb}$  versus  $^{206}\text{Pb}/^{204}\text{Pb}$  plot (Figure 22). Lead data from the Type II dolomites also plots separately from sphalerites on a  $^{208}\text{Pb}/^{204}\text{Pb}$  versus  $^{206}\text{Pb}/^{204}\text{Pb}$  plot, suggesting remobilization of metals during some later event.

In Figure 23, Pb/Pb data from Prairie Creek are compared to average Pb/Pb values for galenas from the Tom, Jason and Cirque deposits (Godwin et al., 1982). The close alignment of these deposits in  $^{207}\text{Pb}/^{204}\text{Pb}$  versus  $^{206}\text{Pb}/^{204}\text{Pb}$  plots to the Prairie Creek stratiform ores, further emphasizes their genetic linkage.

Using the above data, the model of Godwin et al. (1982) best characterizes the mineralization styles present at Prairie Creek from Pb values. The two stage model with Pb-Pb values plotted along a single isochron is consistent fully for only a  $^{207}\text{Pb}/^{204}\text{Pb}$  versus  $^{206}\text{Pb}/^{204}\text{Pb}$  plot, not for a  $^{208}\text{Pb}/^{204}\text{Pb}$  versus  $^{206}\text{Pb}/^{204}\text{Pb}$  plot, and scatter in Figure 22 suggests that values may be related to contamination or fractionation during analyses. Excluding the scattered values limits the extrapolation of any slope and consequently the interpretation of an isochron age. The location of Pb-Pb values falling along the two isochrons in Figure 23 support the model of Godwin et al. (1982). By association with other stratiform mineralization at MacMillan Pass and silver-rich vein deposits in the Yukon, types I and III mineralization are consistent with this model.

## 6.2 Rubidium-Strontium Systematics

The  $^{87}\text{Sr}/^{86}\text{Sr}$  ratios of marine carbonate minerals are identical to seawater at the time of deposition, and provided that diagenetic alteration has not occurred, may be measured as such (Faure, 1986). Burke (1982) has shown that the variation of  $^{87}\text{Sr}/^{86}\text{Sr}$  ratios of the oceans during the Phanerozoic follows a distinct path based on analyses of marine carbonate from around the world. Deviations of  $^{87}\text{Sr}/^{86}\text{Sr}$  values away from Burke's (1982) results, suggest that the  $^{87}\text{Sr}/^{86}\text{Sr}$  ratios of carbonate rocks reflect post-depositional interaction of fluids with the host rocks.

Morrow et al. (1990) analyzed fourteen samples of Manetoe Facies dolomite and calcite in the Prairie Creek region. They observed strontium isotope ratios from coarsely-crystalline, Manetoe Facies dolomite range from 0.70906 to 0.71282, while strontium isotope ratios within (middle Devonian) Landry and Nahanni Formation limestones, range from 0.70789 to 0.70802. They determined higher  $^{87}\text{Sr}/^{86}\text{Sr}$  values (up to 0.72389) in late vein calcite. Morrow et al. (1990) suggest that the strontium isotope ratios of the dolomite and vein calcite result from mixing of the original strontium in limestone with more

radiogenic strontium of the dolomitizing and vein-forming fluids. Morrow et al. (1990) envision fluids interacting with shales or with siliciclastic rocks from the continental crust to be possible sources for the more radiogenic strontium enrichment within Manetoe Facies rocks.

Qing and Mountjoy investigated  $^{87}\text{Sr}/^{86}\text{Sr}$  ratios of sparry dolomite cements across northeastern British Columbia to Pine Point, N.W.T. They observed decreasing strontium isotope ratios eastward, ranging from 0.7106 in the subsurface of northeastern B.C. to 0.7081 at Pine Point. They reason that this evidence, as well as west to east decreasing homogenization temperatures, indicates a regional, eastward migration of hot, saline, dolomitizing fluids. These results may be compared with earlier Sr results from Pine Point by Medford et al. (1983), who determined values of 0.7095 to 0.7143 from late stage dolomites and calcites (in contrast to host carbonate rocks of the Presqu'ile Formation which range from 0.7081 to 0.7089) and hypothesized that the ore fluids were derived from sources other than marine carbonates.

Goodfellow and Jonasson (1986) determined  $^{87}\text{Sr}/^{86}\text{Sr}$  ratios of 0.714 to 0.717 in carbonates from the Howards Pass XY deposit. They assumed the source of the strontium to be a Hadrynian arkosic grit unit, underlying Selwyn Basin and suggested that Pb and Sr were released to the fluid phase during the pervasive albitization and sericitization which affected these rocks.

Recently, Koffyberg (1994) investigated regional scale strontium of vein carbonates across the the southern Canadian Cordillera. She determined that vein carbonates display a geographic variation in  $^{87}\text{Sr}/^{86}\text{Sr}$  ratios, decreasing from east to west. She further observed greatest heterogeneity and higher  $^{87}\text{Sr}/^{86}\text{Sr}$  values within Proterozoic sequences (ranging from 0.734 to 0.774 within the Miette Group), in contrast to more homogeneous values in veins hosted by lower Paleozoic carbonate sequences (0.709 to 0.710). Higher values such as 0.710, are associated also with Pb-Zn mineralization at the Monarch Mine near Field, B.C.



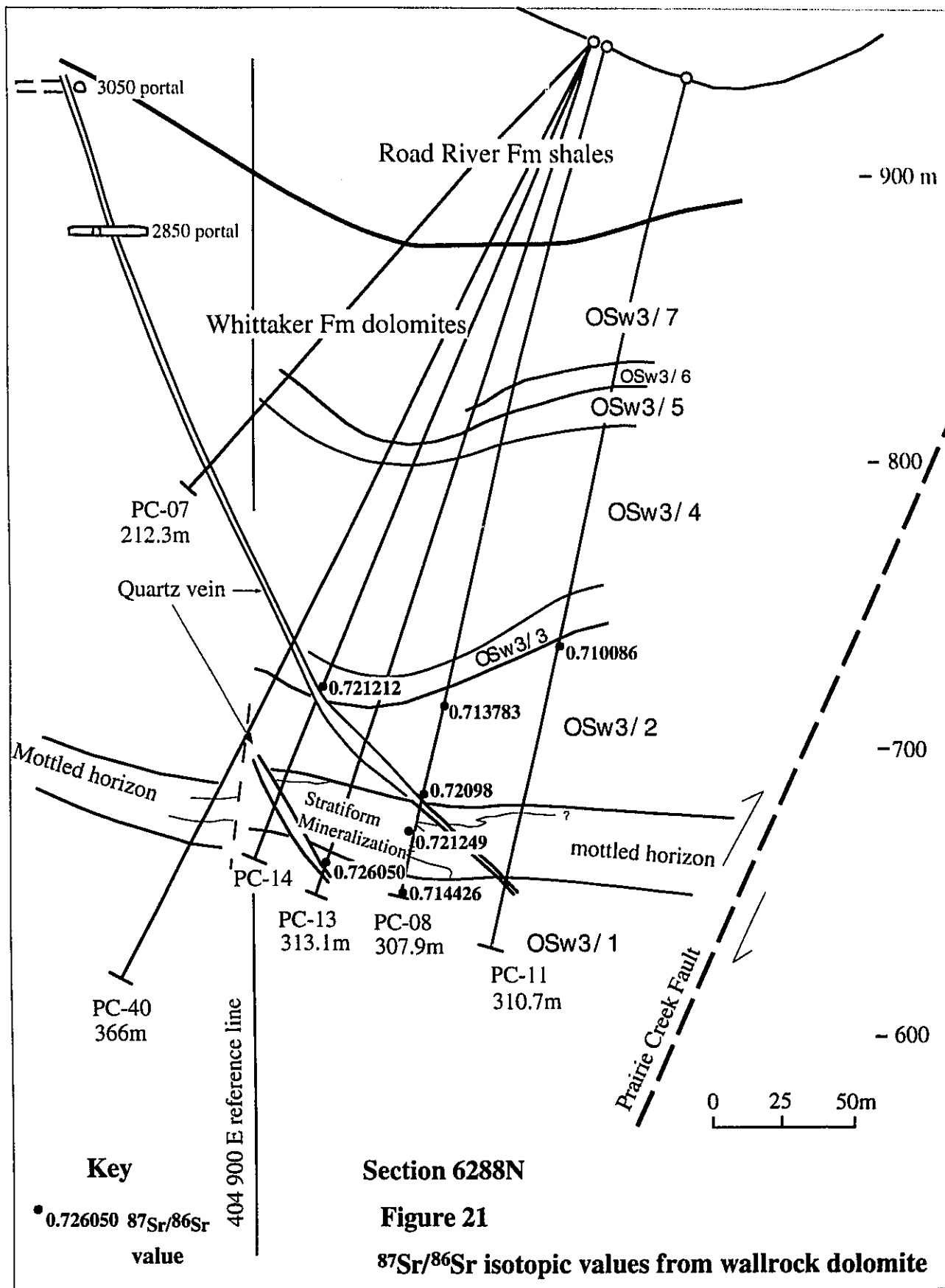
In this study, a total of nine wallrock dolomites from various stratigraphic locations within Whittaker Formation in the Zone #3 area, were analyzed for whole rock  $^{87}\text{Sr}/^{86}\text{Sr}$  values. In addition, two gangue dolomites associated with Type I, stratiform mineralization in the Whittaker Formation, as well as two dolomites associated with Type II, MVT style mineralization in the Root River Formation, were analyzed for strontium ratios (Table VI-2).

#### Analytical Techniques

The dolomitic samples were dissolved in a cold 1N HCl solution to minimize any radiogenic strontium that might have been leached from clay minerals and/or contaminants, by heating or by stronger acid (personal communication, Pat Cavell, 1995). The procedure for purifying strontium for analyses by cation exchange techniques is documented by Koffyberg, (1994).

#### Results

As shown in Table VI-2 and Figure 24,  $^{87}\text{Sr}/^{86}\text{Sr}$  values from whole rock dolomites increase from a value of 0.710 approximately 60 metres above stratiform mineralization to a value of 0.721 adjacent to stratiform ores. From Figure 24, strontium ratios also appear to show enrichment toward quartz veining. The contribution of  $^{87}\text{Sr}$  enrichment from fluids within quartz veins is unclear, as no  $^{87}\text{Sr}/^{86}\text{Sr}$  analyses of dolomite from vein carbonates were determined in this study. However,  $^{87}\text{Sr}/^{86}\text{Sr}$  analyses of gangue dolomite mineral separates, associated with stratiform ores, show highly radiogenic strontium ratios with values up to 0.72387. The gangue dolomites from Type I ores are highly anomalous, in comparison to typical strontium values for upper Ordovician dolomites, 0.708 as determined by Burke et al. (1982) (Figure 25). Whittaker Formation dolomite sampled from outcrop, west of the Gate Fault, approximately 3km west of the mineralized trend,

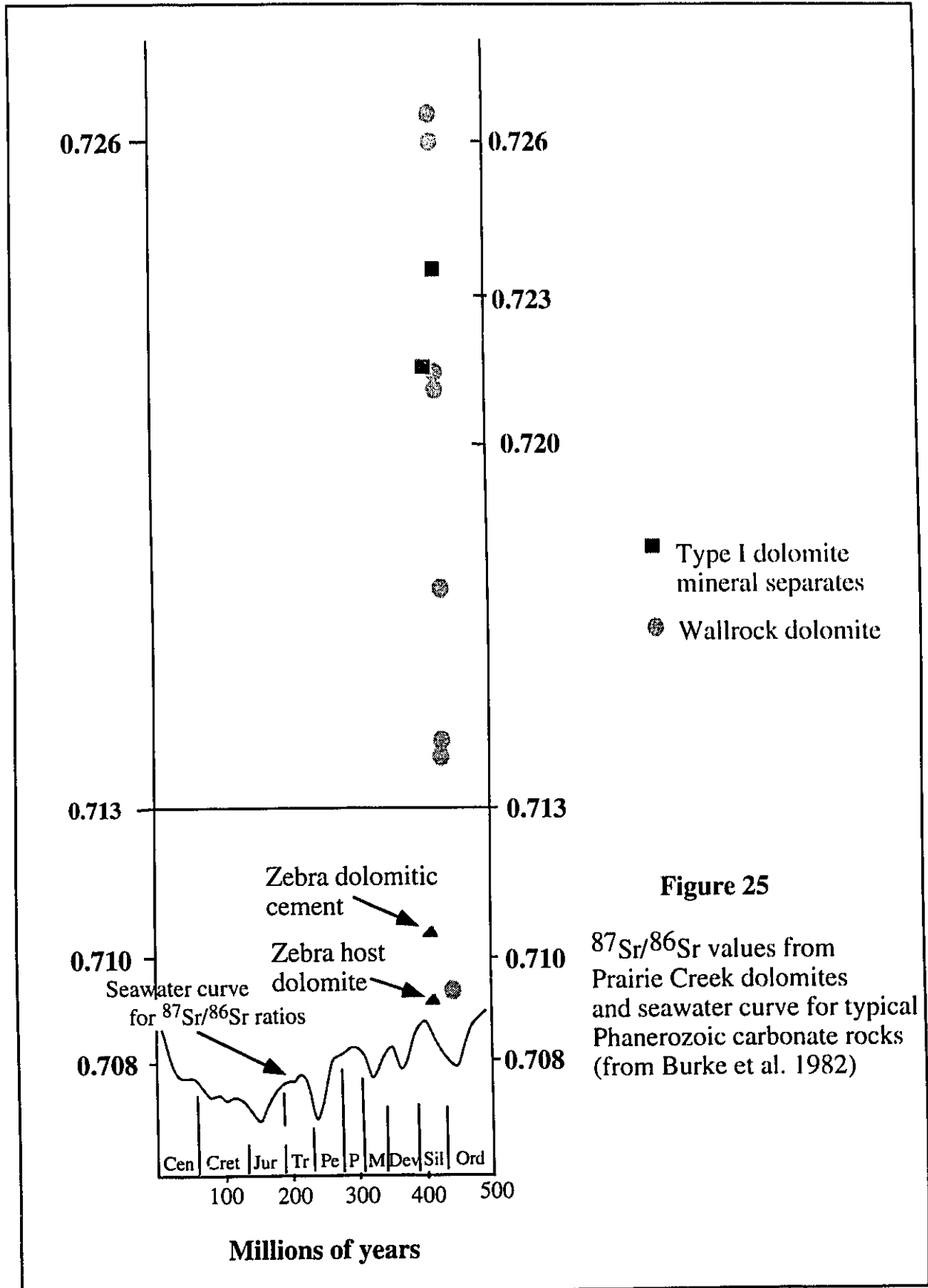


shows only slightly more  $^{87}\text{Sr}$  enrichment (0.70958) relative to upper Ordovician dolomites.

**Table VI-2 Strontium Isotopic Results**

Sample #	rock type	$^{87}\text{Sr}/^{86}\text{Sr}$
<b>Wallrock dolomites</b>		
PC-06 207.5m	dolomite	$0.717865 \pm 0.000046$
PC-08 239m	bioturbated dolomite	$0.713783 \pm 0.000041$
PC-08 272m	mottled dolomite, adj. stratiform ore	$0.720987 \pm 0.000043$
PC-08 283m	mottled dolomite, " " "	$0.721249 \pm 0.000019$
PC-08 308m	dolomite	$0.714426 \pm 0.000024$
PC-13 303.9m	dolomite	$0.726729 \pm 0.000333$
PC-13 303.9m rerun	dolomite	$0.726050 \pm 0.000019$
PC-14 245.5m	dolomite	$0.721212 \pm 0.000042$
PC-R3*	chert nodule dolomite	$0.709576 \pm 0.000021$
*outcrop sampled from Whittaker Fm west of Gate Fault.		
<b>Type I ores</b>		
PC-11 261.3m	gangue dolomite (Whittaker Fm)	$0.72387 \pm 0.00002$
PC-14 289.3m	gangue dolomite " "	$0.72136 \pm 0.00003$
<b>Type II (MVT style) ores</b>		
Zebra showing	host-rock dolomite (Root River Fm)	$0.70934 \pm 0.00003$
Zebra showing	saddle dolomite cement " "	$0.71052 \pm 0.00002$

Dolomitic cement from the Type II ores (Zebra showing) shows only slight enrichment (0.710) in strontium ratios in comparison to host rock dolomites (0.709). The data are similar to values observed by Morrow et al. (1990) for Manetoe Facies dolomites, suggesting that the dolomitizing fluids forming the cements, were enriched in radiogenic strontium in comparison to the host rocks.



## Interpretations

The high strontium isotopic values observed in the Whittaker Formation dolomites (Table VI-2 and Figures 24 and 25) suggest that the fluids interacted with siliciclastics and/or shales to increase  $^{87}\text{Sr}/^{86}\text{Sr}$  values to 0.726.

Fluids forming the gangue dolomites associated with Type I ores may have had a contribution of radiogenic Sr from two sources; 1) due to eastward migration through Selwyn Basin Road River shales, the fluids contacted Rb-rich illite and illite-montmorillonite clays and inherited radiogenic strontium and 2) the fluids may have passed through Proterozoic rocks. While both of these sources may have contributed to increased  $^{87}\text{Sr}/^{86}\text{Sr}$  values, the highly radiogenic values observed in gangue dolomites associated with Type I mineralization most likely have been contributed from a Proterozoic source. From Figure 21,  $^{87}\text{Sr}/^{86}\text{Sr}$  values are also shown to increase toward Type I mineralization and away from the overlying Road River shales, consistent with a Proterozoic source. Chaudhuri and Clauer (1992) have argued that the role of ion exchange by illite and illite-smectite, clay minerals to be minor in elevating the  $^{87}\text{Sr}/^{86}\text{Sr}$  ratios of subsurface waters, and reason that the reaction (albitization) with feldspar favors enrichment of  $^{87}\text{Sr}/^{86}\text{Sr}$  ratios higher than 0.715.

While highly enriched  $^{87}\text{Sr}/^{86}\text{Sr}$  values are associated with Type I mineralization, enriched  $^{87}\text{Sr}/^{86}\text{Sr}$  values are also observed in Type II ores. Host dolomite and dolomitic gangue from Type II ores have  $^{87}\text{Sr}/^{86}\text{Sr}$  values of 0.70954 and 0.71052 respectively. Based on a Ludlovian stage for these Silurian Root River dolomites, (Morrow, pers. comm., 1994) the  $^{87}\text{Sr}/^{86}\text{Sr}$  value for the host carbonates should be 0.7088 (Burke et al. 1981). The two  $^{87}\text{Sr}/^{86}\text{Sr}$  values obtained from saddle dolomite from the Zebra showing indicate Sr isotopic enrichment, consistent with values in saddle dolomite observed by Qing and Mountjoy, (1994) in northeastern British Columbia. The location of the Root River dolostones overlying the Road River Formation shales favours  $^{87}\text{Sr}/^{86}\text{Sr}$  enrichment

as a result of basinal brines migrating eastward through a shale source (Nesbitt and Muehlenbachs, 1994).

### **Conclusions on Radiogenic Isotope Results**

Both the lead and strontium isotopic results from this study point to involvement of mineralizing fluid with Proterozoic rocks. The high strontium isotopic ratios (up to 0.723) from gangue dolomite also suggest a Proterozoic source, consistent with mineralizing fluids in a rifting environment. The lead results appear to indicate two possibilities. 1) The data suggest that all mineralization may be related to an event from Silurian to possibly Jurassic, based on the  $352 \pm 140$  Ma intercept and the age of the host rocks (late Ordovician to early Silurian). This would suggest that Type III mineralization within quartz veins may be feeder systems, as observed at the MacMillan Pass deposits (Goodfellow et al. 1993). 2) An alternative would be to suggest that mineralizing events occurred initially in middle Silurian to late Devonian time, related to rifting events in the Prairie Creek Embayment. Later, mineralization associated with the Laramide orogeny, occurred during Cretaceous time consistent with the model of Godwin et al. (1982). Based on geological and geochemical results presented in this study, the latter interpretation better characterizes mineralization present.

## Chapter VII Discussion

### 7.0 Variation within mineralization Types I, II and III at Prairie Creek

The Prairie Creek Zn-Pb (Ag) deposits comprise three distinct types of mineralization hosted in lower Paleozoic carbonate units. The geological and geochemical characteristics of the three styles of mineralization are shown in Table VII-1. Sangster (1990) in comparing sedex and MVT deposits suggests that geochemical differences between the two deposit types may be minor, while the greatest variation between the two are morphological, in that sedex deposits are stratiform and normally fine-grained, and MVT deposits are stratabound and typically coarse-grained. At Prairie Creek, these characteristics as well as distinct structural variation apply to mineralization types I and II.

#### *Geological Variation*

Type I, stratiform mineralization at Prairie Creek is located within the Prairie Creek Embayment (Morrow and Cook, 1987), which is inferred to be an extensional tectonic structure related to rifting. Stratiform mineralization (discovered from drilling) consists of variably bedded, fine grained subhedral, zoned sphalerite (clear to amber to red) and massive reddish sphalerite, pyrite and lesser amounts of galena within a siliceous matrix. Gangue mineralogy include euhedral, authigenic quartz, as well as microcrystalline quartz, gangue white dolomite up to several millimeters in size and late calcite as fracture fillings and isolated blebs rimmed by pyrite. Host rock lithologies for Type I mineralization within the Upper Ordovician to Lower Silurian Whittaker Formation includes poorly bedded dolomite, locally with chert nodules. Underlying this dolomite unit is a silicified clastic unit, interpreted as quartzite. The quartzite unit is probably gradational with late Ordovician Whittaker Formation unit Ow/2 (Morrow and Cook, 1987).

Type II stratabound mineralization consists of medium-grained, massive yellowish-brown sphalerite, with pyrite and rare galena associated with coarse-grained saddle

**Table VII-I Comparison of Mineralization Types**

Deposit Type	Type I	Type II	Type III
<b>Geological Features</b>			
Host rock	dolomite	dolomite	dolomite
Geologic Setting	stratiform	stratabound	cross-cutting veins
Sulfide occurrence	appears bedded	open space fill	with quartz
sulfide mineralogy	pyrite, sphalerite, minor galena	pyrite, massive and colloform sphalerite, rare galena	galena, sphalerite, pyrite, tetrahedrite, pyrargyrite
Gangue mineralogy	euhedral and microcrystalline quartz, ferroan dolomite, trace fluorite, calcite veinlets	Saddle dolomite, rare quartz	quartz, calcite
<b>Geochemical Features</b>			
Gangue dolomite (Trace elements)	Mn, Sr, Fe, Zn enrichment	Mn and Sr depleted	-----
Sphalerite (Trace elements)	depletions in elements analyzed including Fe (<1 wt %)	enrichment in Cd	enrichments in Cd and Hg
Fluid inclusion results Inclusions in Sphalerite (T <sub>h</sub> )	130 °C from zoned sphalerite (range from 110 200 °C)	range from 155 to 220 °C	bimodal low temp. ~140 high temp. ~ 160 °C
Salinity	19 eq. wt %	23 eq. wt %	~8eq. wt % ~16 eq. wt % NaCl



Table VII-I continued	Type I	Type II	Type III
Lead Values			
Mineral analyzed	galenas n = 16	sphalerites n = 3	galenas n = 26
$^{207}\text{Pb}/^{204}\text{Pb}$			
range	15.640-15.662	15.641-15.656	15.656-15.681
average	$15.651 \pm 0.007$	$15.648 \pm 0.007$	$15.671 \pm 0.006$
$^{206}\text{Pb}/^{204}\text{Pb}$			
range	18.664-18.773	18.581-18.739	19.003-19.044
average	$18.710 \pm 0.039$	$18.661 \pm 0.079$	$19.025 \pm 0.010$
$^{208}\text{Pb}/^{204}\text{Pb}$			
range	38.727-38.861	38.552-38.816	38.978-39.100
average	$38.778 \pm 0.033$	$38.645 \pm 0.148$	$39.053 \pm 0.025$
Gangue dolomite			
$^{87}\text{Sr}/^{86}\text{Sr}$ values	up to 0.723	0.710	
$\delta^{18}\text{O}$ values	$23.0 \pm 0.8$	$16.4 \pm 2.4$	
$\delta^{13}\text{C}$ values	$-2.8 \pm 0.4$	$-3.1 \pm 2.2$	
$\delta\text{D}$ values	-126	-61 to -108 (-78.3)	
Quartz			
$\delta^{18}\text{O}$ values			$16.9 \pm 2.8$
$\delta\text{D}$ values			$-158 \pm 18$
$\delta^{34}\text{S}$ values			
pyrite	$+22.5 \pm 1.2$ (n=3)		
sphalerite	+22.2		$+18.7 \pm 1.5$ (n=3)
galena	+20.0		

dolomitic cement. Saddle dolomite cements also observed at Gayna River (Beales and Hardy, 1980) and Pine Point (Krebs and MacQueen, 1984) and the presence of colloform sphalerite support an interpretation as Mississippi Valley Type (MVT), for Type II mineralization. Host rocks for this mineralization are the Middle Silurian, Root River Formation dolostones, which are located east of the Prairie Creek Embayment, within MacKenzie shelf carbonate rocks.

Type III mineralization, consisting of cross-cutting, westerly dipping quartz-sulfide veins, occurs in twelve discontinuous zones, in a north, northeast trend within the Prairie Creek Embayment. Sulfide mineralization within the steeply-dipping veins consists of variable galena, sphalerite, pyrite, tetrahedrite and pyrargyrite. Gangue mineralogy consists of dolomitic country rock, calcite and rare ankerite.

#### *Geochemical Variations*

Microprobe analyses of gangue dolomites revealed high manganese values (up to 2 wt %) associated with Type I gangue dolomites in comparison to Type II dolomitic cements which include 0.04 weight percent. Similar high manganese values have been reported from the Tynagh ore deposit, Ireland (Russell, 1974).

Type I (stratiform) mineralization as well as Type II MVT-style mineralization are both characterized by high salinity fluids (20 and 23 eq.wt % NaCl respectively). Eutectic temperatures (temperature of first melt) observed in inclusions from both Types I and II mineralizing fluids range from -30 to -45 °C, indicating the presence of Ca and/or Mg chlorides. Homogenization temperatures ( $T_h$ ) from zoned sphalerite from Type I mineralization average  $130 \pm 20$  °C, with more massive sphalerite to 220 °C. Based on observation of primary inclusions in zoned sphalerite, the higher homogenization temperatures from inclusions in sphalerite are thought to be a result of leaked inclusions. Ansdell et al. (1985) reported  $T_h$  for vein ankerites at 258 °C from the shale-hosted Tom deposit, but suggested that post-mineralization deformation probably affected those temperatures, increasing  $T_h$  as a result of leakage. Ansdell et al. (1985) suggested that the range in formation temperatures was probably from 150 to 200 °C based on 1) a lack of variation in the oxygen isotopic composition of the whole rock approaching mineralization and 2) a lack of chalcopyrite mineralization forming in a reducing environment.

Homogenization temperatures from inclusions in sphalerite from Type II mineralization range from 155 to 220 °C, while inclusions from dolomitic gangue (from

drill core) average  $166 \pm 17$  °C. The lower  $T_h$  values from dolomitic cement are consistent with  $T_h$  results generally reported from MVT deposits (Anderson and MacQueen, 1982).  $T_h$  values, up to 220 °C, from inclusions in Type II sphalerite from outcrop, may be due to leaked inclusions.

Type III mineralization, consisting of quartz-sulfide veins, shows a wide variation in fluid chemistry. Fluid inclusion salinities range from 20 eq. wt % from inclusions in quartz veining to 2.0 eq. wt % NaCl from two phase, liquid-vapor inclusions from euhedral quartz overgrowths. The broad spread in salinities from inclusions in quartz suggests that mixing of fluids occurred during prolonged deformation from late Cretaceous to Tertiary. Aulstead (1987) suggested that the broad range in salinities observed in the Manetoe Facies represent mixing of Middle Devonian Elk Point residual brines with meteoric water. Homogenization temperatures from inclusions in quartz from Type III mineralization also show a broad range varying from 110 to 240 °C with an average of  $163 \pm 61$  °C, consistent with values reported by Aulstead (1987).

The  $\delta^{18}\text{O}$  values of the Type I gangue dolomites ( $+23 \pm 0.8\text{‰}$ ) suggest formation from relatively low temperature fluids, consistent with  $T_h$  reported from zoned sphalerite in this study. Wallrock dolomite depletions in  $\delta^{18}\text{O}$  are attributed to proximity of quartz veining, rather than stratiform ore.

Within Type II mineralization, there is a marked lowering of  $\delta^{18}\text{O}$  values from saddle dolomitic cements (average 16.4‰) in comparison to host dolomites (average 24.5‰). The depletion in  $^{18}\text{O}$  values in dolomitic gangue results from a low  $^{18}\text{O}$  fluid, which formed Type II (sphalerite, pyrite) mineralization. The depletion in the  $\delta^{18}\text{O}$  values from host dolomite to dolomitic cement (from drill core), is seen over an interval of less than five centimetres. Alternatively the variation in  $\delta^{18}\text{O}$  values may be a function of higher temperature, related to hydrothermal mineralization based on  $T_h$  observed in sphalerite.

$\delta^{18}\text{O}$  values from quartz from Type III mineralization show a broad range from 9.1 to 19.7‰, averaging  $16.9 \pm 2.8\%$ . The higher  $\delta^{18}\text{O}$  values are from mineralized veins, while lower  $\delta^{18}\text{O}$  values from euhedral quartz overgrowths are associated with low salinity and low temperature meteoric fluids.

$\delta^{13}\text{C}$  values from Types I and II dolomites ( $-2.8 \pm 0.4$  and  $-4.4 \pm 1.2\%$ ) are consistent with average marine carbonate  $\delta^{13}\text{C}$  values, which vary from -4 to +1‰ for late Ordovician dolomites and -3 to +2‰ for late Silurian dolomites (Veizer, 1983). The greater depletion in  $\delta^{13}\text{C}$  values from Type II dolomitic cement is attributed to the oxidation of organic matter.

$\delta\text{D}$  values determined from fluids obtained by thermal decrepitation of fluid inclusion waters were obtained from chert, sphalerite, and gangue dolomite from Type I, saddle dolomite and host dolomite from Type II and quartz from Type III mineralization. Variability between  $\delta\text{D}$  values from Type I fluids from sphalerite and gangue dolomite, presented in Table V-3, suggests a contaminated signal from  $\delta\text{D}$  values in gangue dolomite.  $\delta\text{D}$  values from Type II fluids also shows variation, ranging from -99 to -115‰ from trench samples and -61 to -66‰ from drill core samples. The lower  $\delta\text{D}$  values are thought to be contaminated from more highly oxidized and sulfide-rich trench samples in comparison to drill core samples. The higher  $\delta\text{D}$  values are consistent with values (-42 to -75‰) reported from the Manetoe Facies (Yang et al. 1995).  $\delta\text{D}$  values obtained from quartz from Type III mineralization show a range from -113 to -184 with a average of  $-158 \pm 18.1\%$ . These  $\delta\text{D}_{\text{FI}}$  values are interpreted as syn to post orogenic fluids (Nesbitt and Muehlenbachs, 1994).

$^{87}\text{Sr}/^{86}\text{Sr}$  values from Type I, gangue dolomite (up to 0.723) are highly enriched in  $^{87}\text{Sr}$  as opposed to late Ordovician average carbonates which are 0.7078. These enriched Sr isotopic ratios from Type I mineralization are distinctly different from values obtained from host dolomites (0.709) as well as saddle dolomitic cements (0.710) associated with Type II mineralization. The enriched Sr isotopic values are similar to those reported (0.716)

from Howards Pass (Goodfellow and Jonasson, 1986). The high Sr isotope ratios in Type I fluids suggest a Proterozoic source, accompanied by albitization of feldspars. Pb/Pb results for Type I mineralization also point to a Proterozoic source, but not Hudsonian (Godwin et al. 1982; Morrow et al. 1990), based on the linear regression program (Yorkfit) which suggests a maximum age of  $1474 \pm 140$  Ma. The  $^{87}\text{Sr}/^{86}\text{Sr}$  value from saddle dolomite cement reported here is consistent with values (0.7106) reported by Qing and Mountjoy (1992) from saddle dolomites in northeastern British Columbia.

#### *Age Constraints*

Exact dates on the timing of various mineralization events at Prairie Creek are not available, however Pb/Pb isotopic results can infer relative timing of mineralization. Sixteen  $^{207}\text{Pb}/^{204}\text{Pb}$  and  $^{206}\text{Pb}/^{204}\text{Pb}$  isotopic values for galenas from Type I mineralization fall along the Young Carbonate Group isochron of Godwin et al. (1982) indicating an age of mineralization similar to shale-hosted, Pb-Zn mineralization at the Jason, Tom and Howards Pass deposits, Yukon. While a Devonian-Mississippian age has been inferred for mineralization at the Jason and Tom deposits, a Silurian age has been suggested for mineralization at Howards Pass (Morganti, 1979).

Three lead isotopic values from Type II mineralization have slightly less radiogenic values in comparison to values from Type I, and fall along the Young Carbonate Group isochron of Godwin et al. (1982), inferring a roughly contemporaneous age for mineralization with Type I.

Type III mineralization has very homogenous lead isotopic values (Morrow and Cumming, 1982), which plot along the silver-rich group isochron of Godwin et al. (1982). The Type III values fall along an isochron, which includes the isotopic values from silver-rich mineralization at Midway (Bradford, 1988), Keno Hill (Lynch et al. 1990) and Rusty Springs (Kirker, 1982). As the Keno Hill and Midway deposits are associated with

Cretaceous plutonism (Lynch et al. 1990; Bradford and Godwin, 1988), by association a Cretaceous age is interpreted for Type III mineralization at Prairie Creek.

#### *Structural variation*

While present structural features in the Prairie Creek area, were the result of Laramide compressional tectonics, rapid sediment changes within the Prairie Creek Embayment (Morrow and Cook, 1987) as well as the recognition of volcanics within the Misty Creek Embayment to the north (Cecile, 1982), suggest early Paleozoic rifting, which was accompanied by hydrothermal mineralizing fluids. In the MacMillan Pass area, Abbott et al. (1986) has suggested that lateral facies and thickness variations in the lower Earn group are indicative of synsedimentary faulting during the Middle Devonian and volcanic tuffs have been reported in the MacMillan Pass graben (Carne and Cathro, 1982). While no evidence for a growth fault has been documented at Prairie Creek, synsedimentary faulting attributed to rapid subsidence would allow mineralizing fluids to channel upward from units below.

Sangster (1989) has suggested that MVT mineralization is often associated with brecciation and an overlying unconformity. While brecciation appears absent within Type II mineralization in the Root River Formation, an unconformable relationship has been mapped (Figure 3) by Morrow and Cook (1987), with the Root River Formation overlain by a Sub-Devonian unconformity.

Quartz-sulfide veining hosting Type III mineralization is thought to have formed in response to Laramide folding as linear flexure breaks. Heal (1976) in mapping quartz-sulfide veins at the Wrigley-Lou Pb-Zn showing to the northeast of the Prairie Creek area, observed a similar relationship, with veins forming parallel to axial plane cleavage.

## 7.1 A Heat Source and Conodont Alteration Index (CAI) Values

Morrow et al. (1990) used conodont alteration index (CAI) in the Prairie Creek area to document maturation within sedimentary rocks. Their observations indicate that Devonian and older rocks have CAI values of 5, whereas Mississippian and younger sedimentary rocks have CAI values of 1, indicating normal geothermal gradients. The CAI values suggest a thermal event occurred during the Devonian, consistent with the Antler orogeny (Gordy et al. 1987). Gordey et al. (1987) suggest that the presence of coarse clastic strata as well as chert, and locally alkaline volcanic rocks grade eastward into shelf facies, as a result of rifting within extensional basins.

Based on fluid inclusion results from inclusions in dolomite and sphalerite from Types I and II mineralization in this study, hydrothermal fluids would account for mineralization during Silurian to Devonian time, but are inconsistent with temperatures (300 °C) suggested to account for CAI values observed by Morrow et al. (1990).

## 7.2 Comparison with Other Cordilleran Pb-Zn deposits

### *MacMillan Pass shale-hosted deposits and Type I mineralization*

Goodfellow and Jonasson (1984) suggest that stratabound Zn-Pb sulfide deposits occur at two major stratigraphic positions in the Selwyn basin. The Howards Pass Zn-Pb deposits lie within the Lower Silurian while the Tom and Jason Zn, Pb, Ba deposits occur within the mid-Devonian to Early Mississippian (Carne and Cathro, 1982). Type I, syndiagenetic mineralization at Prairie Creek is consistent with a Lower Silurian age, although conodont alteration index values (Morrow et al. 1990) would tend to support a Devono-Mississippian event. Similar to Howards Pass, no barite is observed in Type I mineralization. Goodfellow et al. (1993) suggest that Zn-Pb mineralization extended over considerable time, based on thicknesses of ore zones (450m) at the Tom deposit in

comparison to relatively narrow stratiform lenses (20 metres) at Prairie Creek. Ankerite-bearing veins are interpreted as feeder veins to stratabound mineralization at the Tom and Jason deposits (Carne and Cathro, 1982; Goodfellow et al. 1993) while such structures have not been observed at Howard Pass or near Type I mineralization at Prairie Creek. Mineralization at the Tom deposit appears as bedded structures while bedded ores as well as replacement mineralization occurs within Type I mineralization, suggesting a prolonged mineralizing event. Gardiner (1983) suggested formation temperatures of 258 °C while Ansdell et al.(1989) argued that temperatures ranging from 150 to 200 °C were more probable, based on presence of later veining related to Laramide tectonics. The lower formation temperatures suggested by Ansdell et al. (1989) are more consistent with  $T_h$  reported from inclusions associated with Type I mineralization in this study. Salinity determined for mineralizing fluids for the Tom and Jason deposits is 9 eq. wt % NaCl compared to 19 eq. wt % from Prairie Creek. Mineralization from the MacMillan Pass deposits, is thought to be structurally controlled along growth faults (Abbott, 1986), in a graben structure. Such a structure is consistent with Type I mineralization, but at present is only conjecture at Prairie Creek.

#### *Robb Lake and Type II mineralization*

The Robb Lake, MVT deposit in northwestern British Columbia occurs within Middle Devonian Stone Formation dolostones close to a major facies change with fine grained clastics. Sulfide mineralization consists mainly of sphalerite, pyrite and galena with gangue including white crystalline dolomite, quartz, pyrobitumen and calcite as cement to dolostone in breccia fragments (Sangster and Carriere, 1991). Type II mineralization is found within a similar geological setting and the presence of saddle dolomite cement at Prairie Creek, further illustrates their similarity. Homogenization temperatures from inclusions in sphalerite reported by Sangster and Carriere (1991) average 119 °C while temperatures from inclusions in quartz reported by Macqueen and



Thompson (1978) range from 210 to 260 °C. Such  $T_h$ , generally high for MVT deposits, possibly may reflect reequilibration due to burial depths estimated at five km during mid-Cretaceous time. Similar high homogenization temperatures have been recorded from inclusions in Type II sphalerite, but are also interpreted as leaked inclusions. Salinities reported from Robb Lake, (16 to greater than 23 equivalent wt. % NaCl) compare closely with values from Type II. Brecciation, which is common with mineralization at Robb Lake, does not appear to be associated with Type II mineralization at Prairie Creek.

#### *Midway and Type III mineralization*

The Rancheria silver deposits at Midway are thought to be related to Cretaceous plutonism and have been described as carbonate-hosted, manto deposits (Bradford and Godwin, 1987) occurring near a major fissure vein. In comparison to mineralizing fluids associated with manto, fissure veins, Type III mineralization at Prairie Creek is far from any igneous source and  $T_h$  from inclusions in sphalerite (110 to 220 °C) are significantly lower than values reported from inclusions in sphalerite (300-340 °C) from Midway (Bradford, 1988). Consistent with high  $T_h$ , wallrock limestones at Midway show extreme lowering of  $\delta^{18}\text{O}$  values to less than 0‰ (SMOW) (Bradford, 1988), in comparison to minor lowering of  $\delta^{18}\text{O}$  values in wallrock dolomites at Prairie Creek. Eutectic temperatures from Midway indicate calcium chloride brines and include the presence of antarcticite (Fraser, unpublished data) in comparison to Mg/Ca chlorides at Prairie Creek. Sulfide mineralogy at Midway is similar to mineralization present at Prairie Creek and mineralizing veins are apparently both structurally controlled.

### **7.3 Conclusions and Implications for Exploration**

The geological and geochemical results from Type I mineralization suggest that Zn-Pb mineralization formed in a basinal environment, close to the seafloor as a result of

protracted hydrothermal activity accompanying continental rifting (Russell et al. 1981) within the Prairie Creek Embayment (Morrow and Cook, 1987). A convected seawater model for Type I mineralization, would account for 1) the pervasive dolomitization of carbonate rocks (Land, 1985) in the Prairie Creek area, and 2) the heavy  $\delta^{34}\text{S}$  values. The high salinities present are probably due to dissolution of evaporites (based on evaporite pseudomorphs observed in thin section). The fluid inclusion results from zoned sphalerite indicate relatively low formation temperatures, suggesting shallow convection, while higher  $T_h$  values may be related to leakage or deeper convected fluids. Gangue dolomite associated with Type I mineralization appears as a replacement of original limestone, and from cathodoluminescence, sphalerite is shown to replace gangue dolomite, similar to observations made at the Lisheen Pb, Zn, Ag deposit, Ireland (Hitzman et al. 1990). The association of rapid facies changes and silicified dolomite/clastic contacts seen in the Prairie Creek Embayment indicates a prospective horizon. Trace metal accumulations of Mn, Zn, and Sr within ferroan gangue dolomite and depleted values of cadmium in sphalerite characterize Type I mineralization.

Type II mineralization is consistent with Mississippi Valley Type mineralization with associated saddle dolomite cement, depletion of  $\delta^{18}\text{O}$  in the cement relative to host dolomite and homogenization temperatures consistent with reported MVT values. Type II mineralization is characterized by non-ferroan, coarse-grained saddle dolomite cement. Salinities for Type II mineralizing fluids are slightly higher than Type I fluids, with similar  $T_h$ . This style of mineralization appears to be related with uniformity contacts, is apparently devoid of brecciation, and occurs outside the Prairie Creek Embayment within shelf carbonate rocks.

Type III mineralization is more structurally-controlled, developed as fissure veins related to the Laramide Orogeny. Thin section observations reveal crack-seal deformation within quartz, and cleavage development in sphalerite. Type III mineralization,

characterized by low salinity and low  $\delta D$  values, represents syn- to post-orogenic fluids, and, by association with other silver-rich deposits, is interpreted as Cretaceous in age.

The results from this thesis indicate two main points. 1) The fluid inclusion data from stratiform Zn-Pb mineralization at Prairie Creek suggest that mineralizing fluids may have significantly lower  $T_h$  than have been previously reported, consistent with the interpretation of Ansdell et al. (1989). 2) The presence of rapid facies changes within an extensional basin, coupled with highly enriched  $^{87}Sr/^{86}Sr$  isotopic values and elevated manganese within gangue dolomite, suggest the presence of stratiform, sedimentary pyrite, zinc and lead mineralization. By implication, additional extensional basins, within shelf carbonate platforms, should be further explored for stratiform Zn-Pb mineralization within the northern Canadian Cordillera. The thesis demonstrates the effectiveness of both radiogenic and stable isotope geochemistry as well as fluid inclusion analyses, in characterizing Zn, Pb, Ag mineralization in the northern Canadian Cordillera.

## References

- Abbott, J.G., Gordey, S.P. and Tempelman-Kluit, D.J., 1986, Setting of sediment-hosted stratiform lead-zinc deposits in Yukon and northeastern British Columbia. *In* : Morin, J.A., ed., Mineral Deposits of Northern Cordillera, Canadian Institute of Mining and Metallurgy, Special Volume 37, p. 1-18.
- Akande, S.O. and Zentilli, M., 1984, Geologic, fluid inclusion and stable isotope studies of the Gays River lead-zinc deposit, Nova Scotia, Canada. *Economic Geology*, vol. 79, p. 1187-1211.
- Anderson, G.M. and MacQueen, R.W., 1982, Ore Deposit models-6. Mississippi Valley-Type lead-zinc deposits. *Geoscience Canada*, vol. 9, p.108-117.
- Ansdell, K.M., 1984, Fluid inclusion and stable isotope study of the Tom Ba-Pb-Zn deposit, Yukon Territory. Unpublished M.Sc. thesis, University of Alberta, Edmonton, 123p.
- Ansdell, K.M., Nesbitt, B.E., and Longstaffe, J., 1989, A fluid inclusion and stable isotope study of the Tom Ba-Pb-Zn deposit , Yukon Territory, Canada. *Economic Geology*, v. 84, p. 841-856.
- Aulstead, K.L., 1987, Origin and diagenesis of the Manetoe Facies, southern Yukon and Northwest Territories, Canada. Unpublished M.Sc. thesis, Department of Geology and Geophysics, University of Calgary, Calgary, 143p.
- Aulstead, K. L. and Spencer, R.J., 1985, Diagenesis of the Keg River Formation, northwestern Alberta-fluid inclusion evidence. *Bulletin of Canadian Petroleum Geology*, vol. 33, p. 167-183.
- Aulstead, K.L., Spencer, R.J., and Krouse, H.R., 1988, Fluid inclusion and isotopic evidence on dolomitization, Devonian of Western Canada. *Geochimica et Cosmochimica Acta*, Vol. 52, p.1027-1035.
- Beales, F. W. and Hardy, J.L., 1980, Criteria for the recognition of diverse dolomite types with an emphasis on studies for Mississippi Valley-Type ore deposits. *In*: Concepts and Models of Dolomitization, D. H. Zenger, J. B. Dunham, and R. L. Ethington, editors, SEPM Special Publication No. 28, p. 197-213.
- Boast, A. M., Swainbank, I.G., Coleman, M.L., and Halls, C., 1981, Lead isotope variation in the Tynagh, Silvermines and Navan base-metal deposits, Ireland. *Econ. Geol.*, v. 76, p. 27-55.
- Bodnar, R.J. and Bethke, P.M., 1984, Systematics of stretching of fluid inclusions I. Fluorite and sphalerite at 1 atmosphere confining pressure. *Econ. Geol.*, v.79, p. 141-161.

- Bodnar, R.J., Reynolds, T.J., and Kuehn, C.A., 1985, Fluid-inclusion systematics in epithermal systems. *In: Geology and geochemistry of epithermal systems*, B.R. Berger and P.M. Bethke, editors, *Reviews in Economic Geology*, v.2, p. 73-97.
- Boucot, A.J., Dunkle, D.H., Potter, A., Savage, N.M., and Rohr, D., 1974, Middle Devonian Orogeny in western North America?: A fish and other fossils. *Journal of Geology*, vol. 82, p.691-708.
- Bozzo, A.T., Chen, H.S., Kass, J.R., and Barduhn, A.J., 1975, The properties of hydrates of chlorine and carbon dioxide. *Desalination*, v. 16, p. 303-320.
- Bradford, J.A., 1988, Geology and genesis of the Midway Silver-Lead-Zinc Deposit, North-Central British Columbia. Unpublished M.Sc. thesis, University of British Columbia.
- Bradford, J.A. and Godwin, C.I., 1987, Midway silver-lead-zinc manto deposit, northern British Columbia. B.C. Ministry of Energy, Mines and Petroleum resources, *Geological Fieldwork, Paper 1988-1*, p. 353-360.
- Brock, J., 1976, Selwyn-MacKenzie Zinc-lead Province Yukon and Northwest Territories. *Western Miner*, p. 9-16.
- Burke, W.H., Denison, R.E., Hetherington, E.A., Koepnick, R.B., Nelson, H.F., and Otto, J.B., 1982, Variation of seawater  $^{87}\text{Sr}/^{86}\text{Sr}$  throughout Phanerozoic time. *Geology*, v.10, p. 516-519.
- Carne, R.C. and Cathro, R.J., 1982, Sedimentary exhalative (sedex) zinc-lead-silver deposits, northern Canadian Cordillera. *CIM Bull.*, v. 75, p. 66-78.
- Cecile, M.P., 1982, The Lower Paleozoic Misty Creek Embayment, Selwyn Basin, Yukon and Northwest Territories. *Geological survey of Canada, Bulletin 335*, 78p.
- Cecile, M.P. and Morrow, D.W., 1978, Galena-sphalerite mineralization near Palmer Lake, Northwest Territories. *In: Current Research, Part A; Geol. Surv. Can., Paper 78-1A*, p. 472-474.
- Chaudhuri, S. and Clauer, N., 1992, Signatures of radiogenic isotopes in deep subsurface waters in continents. *In: Isotopic Signatures and Sedimentary Records, Lecture Notes in Earth Sciences*, vol. 43, Springer-Verlag, Berlin, p. 497-529
- Clayton, R.N. and Mayeda, T.K., 1963, The use of bromine pentafluoride in the extraction of oxygen from oxides and silicates for isotopic analysis. *Geochim. Cosmochim. Acta*, v.27, p. 43-52.
- Clayton, R.N., O'Neil, J.R., and Mayeda, T.K., 1972, Oxygen isotope exchange between quartz and water. *J. Geophys. Res.*, v. 77, p. 3057-3067.

- Coleman, M.L., Shepherd, T.J., Durham, J.J., Rouse, J.E., and Moore, G.R., 1982, Reduction of water with zinc for isotopic analysis. *Analytical Chem.* v.54, p. 993-995.
- Cook, G.C. Two stages of faulting, Virginia Falls map-area, District of Mackenzie. Report of Activities, Part A; *Geol. Surv. Can.*, Paper 77-1A, p. 113-115.
- Cumming, G.L., Kyle, J.R., and Sangster, D.F., 1990, Pine Point: A case history of lead isotope homogeneity in a Mississippi Valley-Type District. *Economic Geology*, vol. 85, p. 133-144.
- Dawson, K.M., 1975, Carbonate-hosted zinc-lead deposits of the Northern Canadian Cordillera. *Geol. Surv. Can.*, Paper 1975-1A, p. 239-241.
- Dawson, K.M., 1979, Regional metallogeny of the northern Cordillera: Recent stratiform base metal discoveries in Yukon Territory and District of MacKenzie; *In: Current Research, Part A, Geol. Surv. Can.*, Paper 79-1A, p. 375-376.
- Dawson, K.M., Panteleyev, A., Sutherland Brown, A., and Woodsworth, G.J., 1991, Regional metallogeny, Chapter 19 *In: Geology of the Cordilleran Orogen in Canada*, H. Gabrielse and C.J. Yorth (ed.); Geological Survey of Canada, *Geology of Canada*, no. 4, p. 707-768.
- de Wit, R., Gronberg, E.C., Richards, W.B., and Richmond, W.O., 1973, Tathlina area, District of MacKenzie, *In: R.G. McCrossum, ed., Future petroleum provinces of Canada. Canadian society of Petroleum geologists Memoir 1*, p. 187-212.
- Degens, E.T. and Epstein, S., 1962, Relationship between O<sup>18</sup>/O<sup>16</sup> ratios in coexisting carbonates, cherts, and diatomites. *AAPG*, v.46, p. 534-542.
- Doe, B.R. and Stacey, J.S., 1974, The application of lead isotopes to the problem of ore genesis and ore prospect evaluation: a review. *Economic Geology*, vol. 69, p.757-776.
- Doe, B.R. and Zartman, R.E., 1979, Plumbotectonics: The Phanerozoic. *In: Geochemistry of hydrothermal ore deposits*, H.L. Barnes (editor), 2nd edition, New York, John Wiley & Sons, p. 22-70.
- Douglas, R.J.W. and Norris, D.K., 1960, Virginia Falls and Sibbeston Lake map-areas, Northwest Territories. *Geological Survey of Canada*, Paper 60-19.
- Eisbacher, G.H., 1983, Devonian-Mississippian sinistral transcurrent faulting along the cratonic margin of western North America. *Geology*, v. 11, p. 7-10.
- Faure, G., 1986, *Principles of Isotope Geology*. New York, John Wiley and Sons, second edition, 589p.
- Feinstein, S., Williams, G.K., Snowdon, L.R., Goodarzi, F., and Gentzis, T. 1991,

- Thermal maturation of organic matter in the Middle Devonian to Tertiary section, Fort Norman area (central Mackenzie Plain). *Can. J. Earth Sci.*, 28, p. 1009-1018.
- Field, C. W. and Fifarek, R.H., 1985 Light stable isotope systematics in the epithermal environment. *In: Geology and Geochemistry of Epithermal Systems*, B.R. Berger and P.M. Bethke (Editors), *Reviews in Economic Geology*, Vol. 2, p. 99-128.
- Fritz, W.H., Cecile, M.P., Norford, B.S., Morrow, D., and Geldsetzer, H.H.J. 1991, Cambrian to Middle Devonian assemblages. *In: Geology of the Cordilleran Orogen in Canada*, H.Gabrielse and C.J. Yorath (ed.); Geological Survey of Canada, *Geology of Canada*, no. 4, p.151-218.
- Gabrielse, H., Blusson, S.L., and Roddick, J.A., 1973, *Geology of Flat River, Glacier Lake, and Wrigley Lake map-areas, District of Mackenzie, and Yukon Territory*. Geological Survey of Canada, Memoir 366.
- Gardner, H.D. and Hutcheon, I., 1985, *Geochemistry, mineralogy and geology of the Jason Pb-Zn deposits, Macmillan Pass, Yukon, Canada*. *Economic Geology*, v. 80, p. 1257-1276.
- Godwin, C.I., Sinclair, A.J., and Ryan, B.D., 1982, Lead isotope models for the genesis of carbonate-hosted Zn-Pb, shale-hosted Ba-Zn-Pb, and silver-rich deposits in the northern Canadian Cordillera. *Economic Geology*, vol. 77, p. 82-94.
- Goldstein, R.H., 1986, Reequilibration of fluid inclusions in low-temperature calcium-carbonate cement. *Geology*, v. 14, p.792-795.
- Goodfellow, W.D. and Jonasson, I.R., 1984, Ocean stagnation and ventilation defined by  $\delta^{34}\text{S}$  secular trends in pyrite and barite, Selwyn Basin, Yukon. *Geology*, v. 12, p. 583-586.
- Goodfellow, W.D. and Jonasson, I.R., 1986, *Geology and geochemistry of the Howards Pass Zn-Pb deposits, Yukon: constraints on metal source, migration and concentration*. *In: The genesis of stratiform sediment-hosted lead and zinc deposits: conference proceedings* R.J.W. Turner and M.T.Einaudi (eds), Stanford University Publications, Vol. XX, p. 22-32.
- Goodfellow, W.D., Lydon, J.W. and Turner, R.J.W., 1993, *Geology and genesis of stratiform sediment-hosted (SEDEX) zinc-lead-silver sulfide deposits*. *In: Kirkham, R.V., Sinclair, W.D., Thorpe, R.I. and Duke, J.M., eds., Mineral Deposit Modelling: Geological Association of Canada, Special Paper 40*, p. 201-251.
- Gordey, S.P., Abbott, J.G., Templeman-Kluit, D.J., and Gabrielse, H. 1987, Antler clastics in the Canadian Cordillera. *Geology*, v. 15, p. 103-107.
- Gulson, B. L. 1986, *Lead isotopes in mineral exploration*. *Development in Economic Geology*, 23 Elsevier, Amsterdam, 245p.

- Gwosdz, W. and Krebs, W., 1977, Manganese halo surrounding Meggan ore deposit, Germany. *Trans. Inst. Min. Metall. (Sect. B: Appl. Earth Sci.)*, p. B73-B77.
- Haas, J.L., Jr. 1976, Physical properties of the coexisting phases and thermochemical properties of the H<sub>2</sub>O component in boiling NaCl solutions. *U.S.G.S. Bull.* 1421 - A, 73p.
- Hardy, R.V., 1992, A light stable isotope and fluid inclusion study of the Sheep Creek Gold Camp, Salmo, British Columbia. unpublished M.Sc. thesis, U. of A.
- Harris, A.G., 1979, Conodont color alteration, an organo-mineral metamorphic index, and its application to Appalachian Basin geology. *In: Aspects of Diagenesis, SEPM special publication no. 26*, p. 3-16.
- Heal, G.E.N., 1976, The Wrigley-Lou and Polaris-Truro Lead Zinc Deposits, N.W.T. Unpublished M.Sc. thesis, University of Alberta, Edmonton, 172p.
- Hedenquist, J.W. and Henley, R.W., 1985, The importance of CO<sub>2</sub> on freezing point measurements of fluid inclusions: Evidence from active geothermal systems and implications for epithermal ore deposition. *Econ. Geol.*, v. 80, p. 1379-1406.
- Hewton, R.S., 1982, Gayna River: A Proterozoic Mississippi Valley-Type Zinc-Lead Deposit. *In: Precambrian Sulfide Deposits*, R.W. Hutchinson, C.D. Spence, and J.M. Franklin (editors) *Geological Assoc. Canada Special Paper 25*, p. 667- 700.
- Hitzman, M.W., O'Connor, P., Shearley, E., Schaffalitzky, C., Beaty, D.W., Allan, J.R., and Thompson, T., 1992, Discovery and geology of the Lisheen Zn-Pb-Ag prospect, Rathdowney Trend, Ireland. *In: The Irish minerals industry 1980-90*, Bowden, A.A. et al. eds (Dublin: Irish Association for Economic Geology), p.227-244.
- Kirker, J., 1982, Geology and geochemistry of the Rusty Springs lead, zinc, silver deposit. Unpublished M.Sc. thesis, University of Calgary.
- Koffyberg, A. M., 1994, Strontium isotopic constraints on the geochemistry and origins of regional vein-forming fluids in the southern Canadian Cordillera. Unpublished M.Sc. thesis, University of Alberta, 102p.
- Krebs, W., and MacQueen, R., 1984, Sequence of diagenetic and mineralization events, Pine Point lead-zinc property, Northwest Territories, Canada. *Bulletin of Canadian Petroleum Geology*, v.32, p. 434-464.
- Kuszniir, N.J., Karner, G.D., and Egan, S. 1987, Geometric, thermal and isostatic consequences of detachments in continental lithosphere extension and basin formation *In: Beaumont, C. and Tankard, A.J. (Eds.), Sedimentary Basins and Basin-Forming Mechanisms. Canadian Society of Petroleum Geologists, Memoir 12*, p. 185-203.
- Land, L. S., 1985, The origin of massive dolomite. *J. Geol. Educ.*, vol. 33, p. 112-125.



- Law, J., 1970, Regional Devonian geology and oil and gas possibilities, Upper MacKenzie River Area. *Bulletin of Canadian Petroleum Geology*, Vol.19, p. 437-486.
- Lynch, J.V.G., Longstaffe, F.J. and Nesbitt, B.E., 1990, Stable isotopic and fluid inclusion indications of large-scale hydrothermal paleoflow, boiling, and fluid mixing in the Keno Hill Ag-Pb-Zn district, Yukon Territory, Canada. *Geochimica et Cosmochimica Acta*, Vol. 54, p. 1045-1059.
- Ludvigsen, R., 1975, Ordovician formations and faunas, Southern MacKenzie Mountains. *Can. J. Earth Sci.*, Vol. 12, p. 663-697.
- Machel, H., 1985, Cathodoluminescence in calcite and dolomite and its chemical interpretation. *Geoscience Canada*, v. 12, p. 139-147.
- MacQueen, R. W. and Thompson, R. I., 1978, Carbonate-hosted lead-zinc occurrences in northeastern British Columbia with emphasis on the Robb Lake deposit. *Can. J. Earth Sci.*, vol. 15, p. 1737-1762.
- Matsuhisa, Y., Goldsmith, J.R., and Clayton, R.N., 1979, Oxygen isotope fractionation in divalent metal carbonates. *J. Chem. Physics.*, v. 51, p. 5547-5558.
- McCrea, J. M., 1950, On the isotopic chemistry of carbonates and a paleotemperature scale. *J. Chem. Phys.*, v. 18, p. 849-857.
- McLarin, G.P. and Godwin, C.I., 1979, Minor elements in sphalerite from carbonate-hosted zinc-lead deposits, Yukon Territory and adjacent district of MacKenzie, Northwest Territories. Yukon Territory, Mineral Industry Report, 1977, Econ. Geol. Survey, 1978-9, p. 5-21.
- Medford, G.A., Maxwell, R.J., and Armstrong, R.L., 1983,  $^{87}\text{Sr}/^{86}\text{Sr}$  ratio measurements on sulfides, carbonates, and fluid inclusions from Pine Point, Northwest Territories, Canada: An  $^{87}\text{Sr}/^{86}\text{Sr}$  ratio increase accompanying the mineralizing process. *Economic geology*, vol. 78, p. 1375-1378.
- Meijer-Drees, N.C., 1975a, Geology of the Lower Paleozoic Formations in the subsurface of the Fort Simpson area, District of MacKenzie, N.W.T., *Geol. Surv. Can.*, Paper 74-40, 65p.
- Meijer-Drees, N.C., 1975b, The Little Doctor Sandstone(new sub-unit) and its relationship to the Franklin Mountain and Mount Kindle Formations in the Nahanni Range and nearby subsurface, District of MacKenzie, *Geol. Surv. Can.*, Paper 75-1C, p. 51-56.
- Morganti, J.M. 1979, The geology and ore deposits of the Howards Pass area, Yukon and Northwest Territories: The origin of basinal sedimentary stratiform sulfides deposits. Unpublished Ph.D. thesis, University of British Columbia, 327p.

- Morrow, D. W. 1984, Sedimentation in Root Basin and Prairie Creek Embayment – Siluro-Devonian, Northwest Territories. *Bull. Can. Pet. Geol.*, v. 32, p. 162-189.
- Morrow, D.W. and Cook, D.G., 1987, The Prairie Creek Embayment and Lower Paleozoic strata of the southern MacKenzie Mountains. Geological Survey of Canada, Memoir 412, 195p.
- Morrow, D.W. and Cumming, G.L., 1982, Interpretation of lead isotope data from lead-zinc mineralization in the northern part of the western Canadian Cordillera. *Can. J. Earth Sci.*, vol. 19, p. 1070-1078.
- Morrow, D.W., Cumming, G.L., and Koepnick, R.B., 1986, Manetoe Facies-A gas bearing, megacrystalline, Devonian dolomite, Yukon and Northwest Territories, Canada. *AAPG.*, v.70, p. 702-720.
- Morrow, D.W., Cumming, G.L., and Aulstead, K.L., 1990, The gas-bearing Devonian Manetoe Facies, Yukon, and Northwest Territories. *GSC, Bull.* 400, 54p.
- Morrow, D.W., Potter, J., Richards, B., and Goodarzi, F., 1993, Paleozoic burial and organic maturation in the Laird Basin Region, northern Canada, *Bulletin of Canadian Petroleum Geology*, Vol. 41, p. 17-31.
- Morrow, D.W. and Aulstead, K.L., 1995, The Manetoe Dolomite - a Cretaceous-Tertiary or a Paleozoic event? Fluid inclusion and isotopic evidence. *Bulletin of Canadian Petroleum Geology*, Vol. 43, p. 267-280.
- Nesbitt, B.E. and Muehlenbachs, K., 1994, Paleohydrogeology of the Canadian Rockies and origins of brines, Pb-Zn deposits and dolomitization in the Western Canada Sedimentary Basin. *Geology*, v. 22, p. 243-246.
- Nier, A.O., Thompson, R.W., and Murphey, B.F., 1941, The isotopic constitution of lead and the measurement of geologic time. III. *Phys. Rev.*, vol. 60, p. 112-116.
- Norford B.S., and MacQueen R.W., 1975, Lower Paleozoic Franklin Mountain and Mount Kindle Formations, District of MacKenzie: Their sections and regional development. *Geol. Surv. Can.*, Paper 74-34, 37p.
- Northrop, D.A., and Clayton, R.N., 1966, Oxygen-isotope fractionations in systems containing dolomite. *Journal of Geology*, v. 74, p. 174-196.
- Nowlan, G.S. and Barnes, C.R. 1987, Thermal maturation of Paleozoic strata in eastern Canada from Conodont colour alteration index (CAI) data with implications for burial history, tectonic evolution, hotspot tracks and mineral and hydrocarbon exploration. *Geol. Surv. Can.*, Bull. 367, 47p.
- Ohmoto, H., Kaiser, C.J. and Geer, K.A., 1990, Systematics of sulfur isotopes in recent marine sediments and ancient sediment-hosted basemetal deposits. *In: Proceedings of the conference on stable isotopes and fluid processes in mineralization, The*

University of Western Australia, Publication No. 23, H. K. Herbet and S. E. Ho, editors, p. 70-120.

- Ohmoto, H. and Rye, R.O., 1979, Isotopes of sulfur and carbon. *In* : H.L. Barnes, ed., *Geochemistry of hydrothermal ore deposits*, second edition, J. Wiley and Sons, New York, p. 509-567.
- Olson, R.A., 1984, Genesis of paleokarst and strata-bound zinc-lead sulfide deposits in a Proterozoic dolostone, Northern Baffin Island, Canada. *Econ. Geol.*, v. 79, p. 1056-1103.
- Potter, R.W. II, and Brown, D.L. 1977, The volumetric properties of aqueous sodium chloride solutions from 0° to 500°C at pressures up to 2000 bars based on a regression of available data in the literature. *U.S.G.S. Bull.* 1421 - C, 36p.
- Potter, R.W. II, Clynne, M.A., and Brown, D.L., 1978, Freezing point depression of aqueous sodium chloride solutions. *Econ. Geol.* v. 73, p. 284-285.
- Powell, T.G. and MacQueen, R.W., 1984, Precipitation of sulfide ores and organic matter: sulfate reactions at Pine Point, Canada. *Science*, v. 222, p. 63-66.
- Qing, H. and Mountjoy, E., 1992, Large-scale fluid flow in the Middle Devonian Presqu'ile barrier, Western Canadian Sedimentary Basin. *Geology*, v.20, p. 903-906.
- Radke, B.M., and Mathis, R.L., 1980, On the formation and occurrence of saddle dolomite. *Journal of Sedimentary Petrology*, v. 50, p. 1149-1168.
- Roedder, E., 1968, Temperature, salinity and origin of the ore-forming fluids at Pine Point, Northwest Territories, Canada, from fluid inclusion studies. *Econ. Geol.*, v. 63, p. 439-450.
- Roedder, E., 1984, *Fluid Inclusions*. Mineralogical Society of America, *Reviews in Mineralogy*, v. 12, 644p.
- Russell, M.J. 1974, Manganese halo surrounding the Tynagh ore deposit, Ireland: a preliminary note. *Trans. Instn. Min. Metall. (Sect.B: Appl. Earth Sci.)* 83, B65-B66.
- Russell, M.J., Solomon, M., and Walshe, J.L., 1981, The genesis of sediment-hosted, exhalitive zinc + lead deposits. *Mineral Deposita*, v. 16, p. 113-127.
- Russell, R.D., and Farquhar, R.M., 1960, *Lead Isotopes in Geology*. Wiley Interscience, New York, 243p.
- Sangster, D.F., 1989, Breccia-hosted lead-zinc deposits in carbonate rocks, N.P.James and P.W. Choquette, eds., *In: Paleokarst*, Springer-Verlag, New York, p.102-116.

- Sangster, D.F., 1990, Mississippi Valley-type and sedex lead-zinc deposits: a comparative examination. *Trans. Instn. Min. Metall. (sect. B: Appl. earth sci.)*, 99, p. B21-B42.
- Sangster, D. F. and Carriere, J.J., 1991, Preliminary studies of fluid inclusions in sphalerite from Robb Lake Mississippi Valley-type deposit, British Columbia. *In: Current Research, Part E, Geological Survey of Canada, Paper 91-1E*, p. 25-32.
- Sangster D.F. and Lancaster, R.D., 1976, Geology of Canadian lead and zinc deposits. *Geol. Surv. Can.*, Paper 76-1A, p. 301-310.
- Sangster, D.F., Nowlan, G.S., and McCracken, A.D., 1994, Thermal comparison of Mississippi Valley-Type lead zinc deposits and their host rocks using fluid inclusion and conodont color alteration index data. *Economic Geology*, v. 89, p. 493-514.
- Shepherd, T.J., Rankin, A.H., and Alderton, D.H.M., 1985, A practical guide to fluid inclusion studies. Glasgow, Blackie and Son Limited, 293p.
- Skall, H., 1977, The geology of the Pine Point Barrier Reef Complex, *In: I.A. McIlreath and R.D. Harrison, eds., The geology of selected carbonate oil, gas and lead-zinc reservoirs in western Canada . Canadian Society of Petroleum Geologists, 5th Core Conference*, p. 19-38.
- Smith, M.T., Dickinson, W. R., and Gehrels, G. E., 1993, Contractional nature of Devonian-Mississippian Antler tectonism along the North American continental margin. *Geology*, vol. 21, p. 21-24.
- Stacey, J.S. and Kramers, J.D., 1975, Approximation of terrestrial lead isotope evolution by a two-stage model. *Earth Plan. Sci. Lett.*, v. 26, p. 207-221.
- Tatsumoto, M., Knight, R.J. and Allegre, C.J., 1973, Time differences in the formation of meteorites as determined from the ratio of lead-207 to lead-206. *Science*, v. 180, p. 1279-1283.
- Taylor, H.P. Jr., 1979, Oxygen and hydrogen isotope relationships in hydrothermal mineral deposits. *In: Geochemistry of hydrothermal ore deposits, second edition, H.L. Barnes, editor, J. Wiley and Sons, New York*, p. 236-277.
- Thorpe, R.I., 1972, Mineral exploration and mining activities, mainland Northwest Territories, 1966 to 1968. *GSC Paper 70-70*, 139p.
- Utting, J., Goodarzi, F., Dougherty, B.J., and Henderson, C.M., 1989, Thermal maturity of Carboniferous and Permian rocks of the Sverdrup Basin, Canadian Arctic Archipelago. *Geol. Surv. Can.*, Paper 89-19, 20p.
- Veizer, J., 1983, Trace elements and isotopes in sedimentary carbonates. *Reviews in Mineralogy*, v. 11, p. 265-300.

Yang, W., Spencer, R.J., and Krouse, H.R., 1995, Stable isotope and major element compositions of fluid inclusions in Devonian and Cambrian dolomite cements, western Canada. *Geochimica et Cosmochimica Acta*, Vol. 59, p. 3159-3172.

**Appendix I Fluid Inclusion Data - Table IV-1**

Sample	Mineral Phase <sup>1</sup>	Inclusion Type & no.	Vol. % H <sub>2</sub> O	<sup>2</sup> T <sub>f</sub>	<sup>3</sup> T <sub>m</sub> CO <sub>2</sub>	<sup>4</sup> T <sub>H</sub> CO <sub>2</sub>	<sup>5</sup> T <sub>e</sub>	<sup>6</sup> T <sub>m</sub> clath	<sup>7</sup> T <sub>m</sub> Ice	<sup>8</sup> T <sub>h</sub>	Eq. Wt % NaCl
<b>Type I (Stratiform) ores</b>											
PC-08	sphalerite	I/v P	4	85 to 90	-68	ND	ND	ND	-15.7 to -16.4 -16.1 ± 0.3	135 to 145 142 ± 3	19.7
"	quartz	I/v P	3	85	-31	ND	ND	ND	-3.1 to -3.6 -3.3 ± 0.3	138 to 149 145 ± 6 @3	5.4
PC-11	sphalerite	I/v P-Ps	6	85	-70	ND	ND	ND	-16 to -19.5 -17.5@5	112 to 130 119 @6	20.8
261m											
"	quartz	I/v P?	7	80	-33_-37	ND	ND	ND	-3.3 to -16.5 10.8 ± 5.9	106 to 144 131 @6 14.8	
	gangue dolomite	I/v P?	7	80	-56 to -80	ND	ND	ND	-11 to -23 -16.2 ± 3.6	165 to 221 199 ± 19	19.6
PC-11	sphalerite	I/v P	3	70 to 80	-65 to -74	ND	ND	ND	-16 to -20 -18.4 ± 1.6	172 to 225 194.6 ± 27	21.5
263.3											
PC-12	sphalerite	I/v P?	8		-54_-64	ND	ND	ND	-13.2 to -17.4 -14.6 ± 5.7	170 to 205 190 ± 11	18.4
269m											
PC-13	sphalerite	I/v P-Ps	10	80	-59 to -71	ND	ND	ND	-17 to -22 -17.6 ± 3.2	121 to 140 134 ± 14	22.4
290m											
PC-28	quartz	I/v P?	9	80	-32 to -50	ND	ND	ND	-3.4 to -18.1 -10.8 ± 5.1	145 to 185 163 ± 13	14.5
269.7m											
	sparry dolomite	I/v P?	3	80	-62	ND	ND	ND	-15 to -17 -15.6 ± 0.6	175 to 180 178 ± 2	19.3

Sample	Mineral Phase <sup>1</sup>	Inclusion Type & no.	Vol. % H <sub>2</sub> O	2Tf	3TmCO <sub>2</sub>	4THCO <sub>2</sub>	5Te	6Tmclath	7TmIce	8Th	Eq. Wt % NaCl
<b>Type I ores continued</b>											
PC-40 301.9	quartz	I/v P 12		-30_-41	ND	ND	-27	ND	-0.6 to -9.2 -3.5 ±3.2	143 to 192 161 ±11	5.7
"	sphalerite	I/v Ps? 4		-57	ND	ND	-31	ND	-10 to -18 -13 ±3.0	180 to 210 200 ±11	17.0
<b>Type II ores</b>											
Zebra	sphalerite	I/v P? 4	80	-52 to -70	ND	ND	ND	ND	-21 to -24 -19.6 ± 5.8	155 to 220 191 ± 31 @6	22.1
Zebra	host dol.	I/v P? 9	80	-43 to -88	ND	ND	-31_-40	ND	-11.4_-24 -16.3 ± 6.2@4	166 to 238 194 ± 63@9	19.9
Zebra HB host dolomite		I/v P 6	80	-58 to -82	ND	ND	-58	ND	-18 to -25 -21 ± 2.4@6	203 to 226 215 ± 10@4	23.0
PC-94-78 dolomite cement		I/v P 9	80	-51 to -67	ND	ND	-45 to -50	ND	-15.1 to -19 -17.1 ±1.5@5	153 to 203 166 ± 17	20.2
<b>Type III ores (Quartz veining)</b>											
3-C-21 637.5m	quartz	I/v Ps? 8	60-80	-39 to -48	ND	ND	-23	ND	-6.4 to -8.1 -7.4 ±0.6	155 to 175 167 ± 8	11.0
"	"	I/v S? 5		--29	ND	ND	ND	ND	-0.8 to -1.4 -1.2 ±0.2	139 to 154 147 ± 6	2.1
PC-37 173.2m	quartz	I/v P? 19	80	-50 to -60	ND	ND	-31 to -49	ND	-15.5 to -21 -17.9 ±1.9	127 to 223 166 ±26	20.9

Sample	Mineral Phase <sup>1</sup>	Inclusion Type & no.	Vol. % H <sub>2</sub> O	<sup>2</sup> Tf	<sup>3</sup> TmCO <sub>2</sub>	<sup>4</sup> T <sub>HCO<sub>2</sub></sub>	<sup>5</sup> Te	<sup>6</sup> Tmclath	<sup>7</sup> TmIce	<sup>8</sup> T <sub>h</sub>	Eq. Wt % NaCl
PC-11 281.6m	quartz	I/v P? 5	70 to 80	-46_-55	-56.8 to -57.5	+16.7 to +19	--55		-13 to -14.4 +2.6 to +5.0	187 to 265 238 ± 44	16.9
"	sphalerite	I/v Ps? 5	85	--46	ND	ND	--30	ND	-2.6 to -4.0 -3.3 ± 0.5	142 to 142.5 142 ± 0.3	5.3
PC-28 258.2m not mineralized	quartz	I/v P? 10	85_90	-45_-55	ND	ND	-38_-42 -40@5	ND	-15 to -20 -17.6 ± 1.7	169 to 241 173.3 ± 22	20.9
PC-40 235.1m	quartz	I/v P? 9		-48	ND	ND	-27 to -31	ND	-3.2 to -16 -8.8 ± 5.3	145 to 207 166 ± 22	12.6
#9 Zone mineralized	quartz	I/v ? 14			ND	ND	-30 to -42	ND	-5.4 to -15.6 -11.7 ± 3.7	106 to 195 130 ± 24	14.4
"	"	I/v Ps-S 2		--31			ND		+1.7 to -1.7 --0.7	122 to 127 125.0	1.2
#9 Zone non-mineralized	quartz	I/v P? 13		-45 to -56	ND	ND	--41	ND	-13.6 to -20.2 -15.8 ± 2.2	120 to 205 137 ± 23	17.3
"	"	I/v Ps? 4		-31 to -37			--27		+1.7 to -7.8 --3.1 @4	113 to 140 124 ± 10	5.1
PC-40 299.3m	quartz	I/v ? 9	80	-38_-51	ND	ND	-41	ND	-10.5 to -16.5 -13.3 ± 2.3	118 to 182 159 ± 25	17.1
PC-40 301.2m	quartz	liq P 7	0	-95.2 to -98.3	-59.4_-61.3	+3.6 to 16.8					
Rico showing quartz	quartz	I/v Ps-S? 3		-49_-51	ND	ND	--38	ND	-8 to -12 -11@3	110 to 13 127@3	15.0



Sample	Mineral Phase <sup>1</sup>	Inclusion Type & no.	Vol. % H <sub>2</sub> O	<sup>2</sup> Tf	<sup>3</sup> TmCO <sub>2</sub>	<sup>4</sup> T <sub>HCO<sub>2</sub></sub>	<sup>5</sup> Te	<sup>6</sup> Tmclath	<sup>7</sup> TmIce	<sup>8</sup> Th	Eq. Wt % NaCl
<b>Type III cont'd</b>											
Vein 3050 portal -	Sphalerite	I/v P?	16	-34_-66	ND	ND	-39	ND	-11.8 to -20.2 -15.7 ±2.0	140 to 171 156 ±9.6	19.4
PC-13 260m	quartz	I/v P?	4	~35	ND	ND	~41	+2.6	-3.0 to -4.0 -3.4 ± 0.3	131 to 165 149 ± 16	5.6
	sphalerite	I/v P	4	-46	ND	ND	ND		-5.0 to -5.3 -5.1 ± 0.1	120 to 144 127 ± 11	8.0
3050 level vein quartz	I/v	P?	7	-49 to -53	ND	ND	~43	ND	-15.9 to -19 -17.3 ± 1.2	120 to 275 175 ± 68	20.4
<b>Calcite Veining</b>											
PC-08 256.9m	calcite*	I/v P?	6	-25_-41	ND	ND	-27	ND	-0.6 to +5.6* -1.7 ± 1.6@4	<90 to 266 160 ±70	2.9
PC-11 282.3m	calcite	I/v P?	9	-38_-45	ND	ND	ND	ND	-0.1 to -2.6 -1.4 ± 1.1	112 to 135 128 ± 8	2.4
PC-13 282.3m	bx calcite	I/v P?	14	-39_-44	ND	ND	ND	ND	-0.1 to -2.8 -2.1 ± 1.0	126 to 194 150 ± 30	3.5
PC-13 304.6	calcite	I/v ?	7	-38_-39	ND	ND	ND	ND	0 to -0.4 -0.15 ± 0.1	161 to 234 196 ±33	0.3
"	quartz	I/v P?	4	-45_-47	ND	ND	ND	ND	-12 to -14.2 -12.7@3	116 to 137 126@2	16.7
PC-40 299.3	calcite*	I/v ?	6	-39 to -60	ND	ND	ND	ND	+2.9 to -0.7 -0.3 ± 0.1	110 to 142 128 ± 14.6	0.3
PC-41 103.4	calcite	I/v P?	8	-52_-63	ND	ND	-49	ND	-18.6_-22 -20.1 ± 0.9	160 to >190 171 ± 10	22.7
Unmineralized quartz 637.5ft	quartz	I/v P?	9	-31	ND	ND	-32	ND	-0.2 to -2.4 -1.3 ± 0.7	97 to 168 143 ± 23	2.0

Sample	Mineral	Phase <sup>1</sup>	Inclusion Type & no.	Vol. % H <sub>2</sub> O	<sup>2</sup> T <sub>f</sub>	<sup>3</sup> T <sub>mCO<sub>2</sub></sub>	<sup>4</sup> T <sub>HCO<sub>2</sub></sub>	<sup>5</sup> T <sub>e</sub>	<sup>6</sup> T <sub>mclath</sub>	<sup>7</sup> T <sub>mIce</sub>	<sup>8</sup> T <sub>h</sub>	Eq. Wt % NaCl
PC-28 108m	quartz	I/v	P? 5		--50			--45	ND	-18 to -22 20.5 ± 1.7	130 to 162.5 150.7 ± 13.7	22.7

**Legend**

- \* exhibits metastability
- ND not detected
- phase<sup>1</sup> phase assemblage at room temperature
- <sup>2</sup>T<sub>f</sub> Temperature of freezing
- <sup>3</sup>T<sub>mCO<sub>2</sub></sub><sup>3</sup> Temperature of melt of CO<sub>2</sub>
- <sup>4</sup>T<sub>HCO<sub>2</sub></sub> Temperature of Homogenization of CO<sub>2</sub>
- <sup>5</sup>T<sub>e</sub> Temperature of first melt
- <sup>6</sup>T<sub>mclath</sub> Temperature of clathrate melting
- <sup>7</sup>T<sub>mIce</sub> Temperature of final ice melt
- <sup>8</sup>T<sub>H</sub> Temperature of Homogenization
- P Primary inclusion/inclusions
- P<sub>s</sub> Pseudosecondary inclusion
- S Secondary inclusion

**Appendix 2 Microprobe data on dolomites**

**I - Sparry dolomite from stratiform ore**

Weight percent		sample: <b>PC-11 261m</b>							
Runs	1	2	3	4	5	Minimum	Maximum	Average	Sigma
Ca	31.270	30.780	29.380	31.080	30.990	29.380	31.270	30.700	0.759
Mg	22.060	21.950	21.890	22.630	22.190	21.890	22.630	22.144	0.295
Fe	0.034	0.395	0.356	0.020	0.351	0.020	0.395	0.231	0.295
Mn	0.422	0.770	0.814	0.511	0.818	0.422	0.818	0.667	0.187
Zn	0.008	0.025	0.053	0.041	0.044	0.008	0.067	0.034	0.018
Sr	0.067	0.042	0.030	0.055	0.046	0.030	0.067	0.048	0.014
<b>totals</b>	<b>53.861</b>	<b>53.962</b>	<b>52.523</b>	<b>54.337</b>	<b>54.439</b>	<b>52.523</b>	<b>54.439</b>	<b>53.824</b>	

**Weight percent**

Weight percent		Sample: <b>PC- 13 290.7m</b>						
Runs	1	2	3	4	5	6	7	
Ca	30.310	30.800	30.100	29.980	29.620	30.130	29.450	
Mg	21.290	21.340	21.490	20.790	20.840	21.270	21.290	
Fe	0.230	0.191	0.070	0.058	0.008	0.014	0.059	
Mn	2.070	2.040	1.400	2.190	2.370	2.380	2.160	
Zn	0.060	0.016	-	0.015	-	0.035	0.016	
Sr	0.032	0.043	0.036	0.043	0.022	0.034	0.029	
<b>totals</b>	<b>53.992</b>	<b>54.430</b>	<b>53.096</b>	<b>53.075</b>	<b>52.860</b>	<b>53.864</b>	<b>53.003</b>	

PC-13 290.7m continued

	8	9	10	Minimum	Maximum	Average	Sigma
Ca	30.650	29.770	30.610	29.450	30.800	30.142	0.454
Mg	21.300	20.360	21.180	20.360	21.490	21.115	0.344
Fe	0.030	0.389	0.413	0.008	0.413	0.136	0.153
Mn	1.700	2.200	2.370	1.400	2.380	2.088	0.020
Zn	-	-	-	-	0.060	0.014	0.020
Sr	0.037	0.048	0.030	0.022	0.048	0.035	0.008
<b>totals</b>	<b>53.717</b>	<b>52.767</b>	<b>54.603</b>	<b>52.767</b>	<b>54.603</b>	<b>53.541</b>	

Weight percent

Sample: PC-08 273m

	1	2	3	4	5	6
Ca	30.360	30.080	30.100	29.620	30.880	30.880
Mg	20.960	22.660	21.540	21.900	21.380	21.380
Fe	1.570	0.132	0.032	0.035	0.211	-
Mn	1.059	0.557	2.000	1.760	1.440	1.740
Zn	0.346	0.930	0.045	0.057	0.025	0.028
Sr	0.020	0.045	0.008	0.015	0.028	0.014
<b>totals</b>	<b>54.315</b>	<b>54.405</b>	<b>53.725</b>	<b>53.387</b>	<b>53.965</b>	<b>53.172</b>
Ca	30.350	30.470	30.420	30.320	30.400	30.270
Mg	21.570	20.970	21.360	21.480	21.270	21.660
Fe	0.057	0.129	0.206	0.081	0.283	0.052
Mn	1.610	2.010	1.890	1.690	1.510	1.650
Zn	0.048	-	0.030	-	-	0.016
Sr	0.027	0.015	0.0017	0.020	0.011	0.018
<b>totals</b>	<b>53.661</b>	<b>53.594</b>	<b>53.922</b>	<b>53.590</b>	<b>54.474</b>	<b>53.666</b>

PC-08 cont'd	Minimum	Maximum	Average	Sigma
Ca	29.620	30.880	30.279	0.300
Mg	20.960	22.660	21.505	0.451
Fe	-	1.570	0.232	0.430
Mn	0.557	2.010	1.576	0.413
Zn	-	0.930	0.127	0.270
Sr	0.008	0.045	0.020	0.010
<hr/>				
totals	53.172	54.405	53.740	

Weight percent

sample: PC-21 273.4m

Element	1	2	3	4	5	6	7	8
Ca	30.270	30.840	30.460	30.540	29.180	30.560	29.790	30.700
Mg	21.680	21.880	21.500	21.750	21.520	21.910	21.100	21.680
Fe	0.322	0.307	0.422	0.174	0.244	0.339	0.199	0.479
Mn	1.420	0.956	1.440	1.181	1.239	0.758	1.410	1.209
Zn	-	0.020	-	0.318	-	0.022	0.030	-
Sr	0.033	0.026	0.042	0.035	0.020	0.027	0.033	0.023
<hr/>								
totals	53.725	54.030	53.864	53.998	52.202	53.616	52.562	54.090

	9	10	Minimum	Maximum	Average	Sigma
Ca	30.350	30.600	29.180	30.840	30.329	0.495
Mg	20.710	21.640	20.710	21.910	21.537	0.370
Fe	0.324	0.353	0.174	0.479	0.316	0.094
Mn	1.190	1.790	0.758	1.790	1.259	0.283
Zn	0.011	0.045	-	0.318	0.045	0.097
Sr	0.035	0.022	0.020	0.042	0.030	0.007
<hr/>						
totals	52.620	54.451	52.202	54.451	53.516	

II - Saddle dolomite and dolomitic cement associated with MVT style mineralization

Weight percent Element 1 Sigma	Sample: Zulu, dolomitic cement							
	2	3	4	5	Minimum	Maximum	Average	
Ca	31.490	31.560	31.860	31.660	31.490	31.860	31.626	0.144
Mg	22.320	22.610	22.320	22.570	22.322	22.660	22.496	0.164
Fe	-	-	-	-	-	-	-	-
Mn	0.007	0.007	-	-	-	0.022	0.007	0.009
Zn	-	-	-	-	-	-	-	-
Sr	0.024	0.022	0.014	0.034	0.014	0.034	0.025	0.008
totals	53.841	54.206	54.194	54.264	53.841	54.264	54.154	

Weight percent Element 1	Sample: Zebra saddle dolomite							
	2	3	4	5	6	7	8	
Ca	31.580	31.570	31.420	30.950	31.510	31.110	31.05	
Mg	22.600	22.440	23.120	22.480	22.620	22.400	22.450	
Fe	0.304	0.103	0.089	0.183	0.026	0.181	-	
Mn	0.021	0.023	0.007	0.021	0.016	0.025	0.025	
Zn	0.036	-	0.032	-	-	0.019	-	
Sr	-	0.011	0.019	0.018	0.017	-	0.01	
totals	54.286	54.146	54.688	53.652	54.189	53.735	53.535	

Zebra saddle dolomite continued

Element	9	10	Minimum	Maximum	Average	Sigma
Ca	31.280	31.000	30.950	31.580	31.248	0.253
Mg	22.580	22.710	21.610	23.120	22.501	0.375
Fe	0.081	0.152	-	0.304	0.013	0.083
Mn	0.029	0.016	-	0.029	0.018	0.006
Zn	-	-	-	0.043	0.013	0.010
Sr	0.018	-	-	0.019	0.009	0.004
totals	53.988	53.878	52.555	55.095	53.802	

Weight percent

Sample: Zebra dolomitic cement

Element	1	2	3	4	5	6	7	8
Ca	31.820	32.160	31.790	31.650	31.470	31.380	31.380	31.190
Mg	22.770	23.020	22.840	22.860	22.620	22.950	22.950	22.420
Fe	-	-	-	-	-	-	-	-
Mn	0.029	0.040	0.021	0.007	0.049	0.021	-	0.023
Zn	0.040	-	-	-	-	-	-	-
Sr	0.019	0.015	0.007	0.008	0.012	0.019	-	0.014
totals	54.678	55.236	54.658	54.525	54.151	54.370	54.330	53.647

Zebra dolomitic cement continued

	9	10	Minimum	Maximum	Average	Sigma
Ca	31.360	31.860	31.190	32.160	31.606	0.299
Mg	22.970	22.930	22.420	23.020	22.833	0.186
Fe	-	-	-	-	-	-
Mn	0.036	0.037	0.007	0.049	0.026	0.015
Zn	-	0.043	-	0.043	0.008	0.017
Sr	0.016	0.019	0.007	0.019	0.013	0.006
<b>totals</b>	<b>54.381</b>	<b>54.888</b>	<b>53.664</b>	<b>55.291</b>	<b>54.486</b>	

Weight percent Sample: Zebra host rock

Element	1	2	3	4	Minimum	Maximum	Average	Sigma
Ca	31.450	31.500	31.320	30.830	30.830	31.500	31.275	0.306
Mg	22.730	22.640	22.700	22.510	22.510	22.730	22.645	0.097
Fe	0.084	0.077	0.091	0.069	0.069	0.091	0.080	0.009
Mn	-	0.009	-	0.013	-	0.013	0.005	0.006
Zn	-	-	-	-	-	-	-	-
Sr	-	0.008	0.008	-	-	0.008	0.004	-
<b>totals</b>	<b>54.264</b>	<b>54.233</b>	<b>54.119</b>	<b>53.422</b>	<b>53.418</b>	<b>54.342</b>	<b>54.009</b>	



Weight percent Sample: 3-C-26 598 feet, probe analyses on dolomite  
hosted within quartz vein.

Element	1	2	3	4	5
Ca	30.210	30.350	30.730	30.120	30.880
Mg	21.050	20.800	20.690	20.780	21.000
Fe	1.310	1.320	0.856	1.330	1.400
Mn	1.440	1.680	0.856	1.330	1.400
Zn	0.101	0.101	0.078	0.097	0.107
Sr	0.031	0.041	0.025	0.031	0.030

-----  
 totals 54.142 54.292 53.858 53.807 54.907

Element	6	7	8	9	10
Ca	30.840	30.780	30.460	30.400	30.000
Mg	20.400	20.810	20.690	21.600	20.310
Fe	1.267	1.350	1.330	0.559	0.817
Mg	1.510	1.540	1.520	0.989	1.400
Zn	0.155	0.111	0.322	0.145	0.041
Sr	0.052	0.027	0.028	0.034	0.029

-----  
 totals 54.223 54.618 54.350 53.727 52.836

Weight percent Element	Minimum	Maximum	Average	Sigma
Ca	30.000	30.880	30.477	0.316
Mg	20.310	21.600	20.813	0.360
Fe	0.559	1.400	1.154	0.295
Mn	0.989	1.680	1.450	0.179
Zn	0.041	0.322	0.126	0.076
Sr	0.025	0.052	0.033	0.008
totals	51.924	55.934	54.053	

3-C-26 ; probe analyses on matrix (wallrock) dolomite

Element	1	2	3	4	5	Minimum	Maximum	Average	Sigma
Ca	31.620	29.680	30.650	31.320	31.190	29.680	31.620	31.063	0.606
Mg	22.060	22.320	22.040	21.910	22.470	21.900	22.670	22.248	0.281
Fe	0.047	0.148	0.069	0.101	0.235	0.016	0.235	0.088	0.066
Mn	0.044	0.094	0.040	0.051	0.073	-	0.094	0.038	0.030
Zn	0.019	0.037	0.023	-	-	-	0.037	0.014	0.010
Sr	0.047	0.007	0.029	0.010	0.036	-	0.047	0.014	0.017
totals	53.836	52.287	52.852	53.391	54.004	51.596	54.703	53.465	
Element	6	7	8	9	Minimum	Maximum	Average	Sigma	
Ca	31.510	31.340	30.830	31.430	29.680	31.620	31.063	0.606	
Mg	22.330	21.900	22.530	22.670	21.900	22.670	22.248	0.281	
Fe	0.052	0.067	0.062	0.016	0.016	0.235	0.088	0.066	
Mn	0.009	-	0.024	0.007	-	0.094	0.038	0.030	
Zn	-	0.025	0.007	0.017	-	0.037	0.014	0.010	
Sr	-	-	-	-	-	0.047	0.014	0.017	
totals	53.901	53.332	53.453	54.140	51.596	54.703	53.465		

### Appendix III - Sphalerite Geochemistry

#### Sample PC-13 290.7m Type I mineralization, zoned sphalerite

Run #	1	2	3	4	5	6	7	8	9	10	11	12	13	14	15
Elements															
Zn	65.73	65.10	66.18	65.93	66.01	65.22	65.45	65.44	65.80	65.84	65.86	65.08	66.40	66.59	66.10
S	33.09	33.19	32.18	32.75	33.01	32.94	32.88	32.90	33.64	33.09	33.0	34.18	33.16	33.51	33.38
Mn	0.009	-	-	-	-	-	-	-	-	-	-	-	-	-	-
Fe	0.167	0.437	0.188	0.122	0.184	0.212	0.241	0.20	0.916	0.326	0.614	0.096	0.265	0.245	0.419
As	0.03	0.013	-	-	-	-	-	-	-	-	-	-	0.015	-	-
Cd	0.111	-	-	-	-	-	-	-	-	0.028	-	-	0.008	-	-
Sb	0.014	-	-	0.005	-	-	-	-	-	0.028	-	0.005	0.007	-	-
Hg	-	-	0.204	0.272	0.437	0.32	0.485	0.223	0.243	0.34	0.272	0.428	0.136	0.349	0.33
averages	99.15	98.74	99.38	99.08	99.64	98.69	99.06	98.76	100.60	99.62	99.74	99.79	99.99	100.69	100.13

Element	16	17	18	19	20	21	22	Minimum	Maximum	Mean	Sigma
Zn	66.05	65.28	65.05	65.46	64.83	65.35	66.04	64.83	66.59	65.67	0.47
S	33.31	34.07	33.41	33.2	33.10	33.09	33.65	32.75	34.18	33.23	0.37
Mn	-	-	-	-	0.012	-	0.014	-	0.014	0.002	0.004
Fe	0.676	1.34	1.0	1.55	1.04	0.713	0.225	0.122	1.55	0.508	0.42
As	0.081	-	-	-	0.049	-	-	-	0.081	0.009	0.02
Cd	-	-	-	-	0.02	-	-	-	0.111	0.006	0.02
Sb	-	-	-	0.034	0.006	-	-	-	0.034	0.006	0.009
Hg	0.175	0.155	0.078	-	-	-	-	-	0.485	0.198	0.16
average	100.29	100.84	99.54	100.24	99.05	99.16	99.93	97.70	103.04	99.63	

Zebra sphalerite - Type II mineralization

Element	1	2	3	4	5	6	7	8	9	10	11	12	13	14
Zn	64.54	65.49	65.18	65.36	64.69	65.18	66.02	65.32	64.63	65.82	64.33	65.55	64.99	64.73
S	33.39	33.38	33.52	33.52	33.10	33.25	33.70	33.42	33.37	33.10	32.73	32.64	33.02	32.76
Mn	0.008	0.022	0.019	0.012	0.016	0.013	-	-	0.008	-	-	0.008	0.010	0.017
Fe	0.477	0.275	0.164	0.423	0.525	0.066	0.399	0.417	0.350	0.416	0.552	0.439	1.09	0.966
As	-	-	-	-	-	-	-	-	-	-	-	-	-	-
Cd	0.874	0.733	0.579	0.770	1.29	0.725	0.775	1.18	0.797	0.830	0.794	0.627	0.856	0.838
Sb	0.007	-	-	-	0.033	-	-	0.007	-	0.008	0.015	-	-	-
Hg	-	-	-	-	-	-	-	-	-	-	-	-	-	-
averages	99.30	99.90	99.46	100.09	99.65	99.23	100.89	100.34	99.15	100.17	98.42	99.26	99.97	99.31

Element	15	16	17	18	Minimum	Maximum	Mean	Sigma
Zn	65.41	64.69	65.3	65.95	64.33	66.02	65.18	0.50
S	32.94	33.08	32.97	33.1	32.64	33.7	33.17	0.30
Mn	0.015	-	-	0.008	-	0.022	0.009	0.01
Fe	0.501	1.69	1.37	0.249	0.066	1.69	0.576	0.43
As	-	-	-	-	-	-	-	-
Cd	0.691	0.225	0.679	0.255	0.225	1.29	0.751	0.25
Sb	-	-	0.019	-	-	0.033	0.012	0.02
Hg	-	0.193	-	-	-	0.193	0.107	0.16
averages	99.56	99.88	100.34	99.56	97.26	102.95	99.80	-

Colloform sphalerite-Type II mineralization (traverses across growth lines)

Run #	1	2	3	4	5	6	7	8	9	10	11	12	13	14	15
<b>Elements</b>															
Zn	64.74	64.07	64.01	63.07	63.94	64.63	64.73	64.06	63.37	65.24	64.72	63.57	64.53	64.30	64.51
S	33.35	33.17	33.38	33.26	32.65	34.06	33.10	32.99	32.96	33.42	33.2	33.48	33.41	33.08	33.25
Mn	0.012	0.022	-	-	0.052	-	0.029	0.04	0.007	-	0.084	0.056	0.014	0.046	0.024
Fe	0.593	0.157	1.13	1.15	0.017	1.14	0.943	0.185	1.81	0.571	0.116	1.50	0.622	0.106	0.466
As	-	-	-	-	-	-	0.013	-	-	0.015	0.015	0.008	-	-	-
Cd	0.38	0.449	0.562	0.565	0.504	0.407	0.589	0.371	0.427	0.138	0.432	0.391	0.189	0.550	0.474
Sb	-	-	-	-	-	-	-	-	-	-	-	0.014	-	-	-
Hg	0.059	-	0.02	0.235	-	0.107	0.049	-	-	-	-	-	-	-	-
average	99.13	97.87	99.10	98.28	97.16	100.34	99.45	97.64	98.57	99.38	98.57	99.02	98.77	98.14	98.74
<hr/>															
	16	17	18	19	20	21	22	23	24	25	26	27	28	29	30
Zn	64.45	66.47	65.85	66.79	65.79	65.34	64.87	63.88	65.08	64.05	64.79	64.83	65.53	64.69	64.26
S	33.79	33.14	33.55	33.15	33.55	32.52	33.50	31.23	32.46	32.67	32.38	32.10	32.44	32.16	32.08
Mn	0.024	0.021	0.025	0.021	0.040	0.025	0.038	0.028	0.055	-	0.044	0.010	0.030	0.136	0.024
Fe	1.33	0.225	0.098	0.095	0.173	0.025	0.531	1.22	0.282	1.18	0.231	0.196	0.153	0.480	0.695
As	-	-	-	-	-	-	-	0.117	-	-	-	-	-	-	-
Cd	0.164	0.417	0.299	0.118	0.089	0.403	0.417	0.303	0.266	0.244	0.604	0.510	0.311	0.338	0.228
Sb	-	-	-	-	-	-	-	-	-	-	-	-	-	-	-
Hg	-	-	-	-	-	-	-	0.348	-	-	-	-	-	-	-
average	99.76	100.27	99.82	100.17	99.52	98.31	99.36	97.12	98.17	98.14	98.05	98.01	98.46	97.80	97.29
<hr/>															
	31	32	33	34	35	36	37	38		Minimum	Maximum	Mean	Sigma		
Zn	64.46	66.44	65.11	64.83	64.59	64.23	65.11	64.15		63.07	66.79	64.71	0.81		
S	31.98	32.72	33.29	33.08	34.14	33.29	33.24	32.88		31.23	34.14	32.96	0.61		
Mn	-	0.026	-	-	0.038	0.048	0.025	0.150		-	0.15	0.034	0.03		
Fe	0.713	0.160	0.843	0.958	0.437	0.482	0.789	0.388		0.017	1.81	0.584	0.46		
As	-	-	-	0.015	-	-	-	-		-	0.117	0.006	0.02		
Cd	0.301	0.242	0.364	0.380	0.449	0.502	0.421	0.464		0.089	0.604	0.375	0.13		
Sb	-	-	-	-	0.057	-	-	0.005		-	0.057	0.003	0.01		
Hg	-	-	-	-	-	-	-	-		-	0.367	0.033	0.09		
average	97.45	99.59	99.61	99.26	99.71	98.55	99.58	98.04		94.41	104.03	98.70			

Sample PC-37-173.2m Type III mineralization

Element	1	2	3	4	5	6	7	8	9	10	11	12	13	14
Zn	66.79	65.86	66.22	66.15	68.27	66.06	67.01	67.07	66.24	66.71	66.40	66.45	66.90	66.87
S	31.24	33.17	32.99	33.24	31.26	33.25	33.25	33.23	33.36	33.26	32.91	33.22	33.06	33.29
Mn	-	-	-	-	-	-	-	-	-	-	0.012	-	0.007	0.01
Fe	0.065	0.022	0.061	0.086	0.05	0.084	0.035	0.112	0.109	0.106	0.074	0.035	0.04	0.005
As	0.047	0.023	-	-	0.024	-	0.04	-	0.053	-	-	-	-	-
Cd	0.256	0.262	0.118	0.227	0.199	0.198	0.174	0.213	0.134	0.179	0.20	0.182	0.256	0.307
Sb	0.039	0.021	0.036	-	0.009	-	-	-	-	-	-	-	-	-
Hg	0.557	0.404	0.327	-	-	-	0.048	-	-	0.144	-	-	0.317	-
averages	98.99	99.76	99.75	99.70	99.81	99.59	100.56	100.63	99.84	100.45	99.60	99.89	100.58	100.48

Element	15	16	17	18	19	20	21	Minimum	Maximum	Mean	Sigma
Zn	66.48	67.41	66.53	66.58	66.69	66.25	67.0	65.86	67.41	66.66	0.53
S	33.14	33.13	33.64	33.43	33.18	32.84	33.56	31.24	33.64	33.03	0.62
Mn	-	-	0.01	-	-	-	0.005	0.012	0.003	0.004	-
Fe	0.029	0.03	0.029	0.033	0.03	0.019	0.085	0.019	0.112	0.054	0.03
As	-	-	-	-	-	-	-	-	0.053	-	-
Cd	0.232	0.219	0.283	0.216	0.181	0.189	0.189	0.118	0.307	0.213	0.05
Sb	0.052	-	-	-	0.031	0.018	0.018	0.039	0.012	0.02	-
Hg	-	0.134	-	0.201	0.115	-	-	-	0.557	0.107	0.16
average	99.93	100.92	100.49	100.46	100.23	99.41	100.86	97.29	102.14	100.06	

Rico Showing sphalerite Type III mineralization

Run #	1	2	3	4	5	6	7	8	9	10	Minimum	Maximum	Mean	Sigma
Zn	66.69	65.89	66.23	66.75	65.97	65.33	66.70	66.18	66.67	66.31	65.33	66.75	66.27	0.46
S	32.77	32.97	33.01	32.85	32.95	32.87	32.79	32.57	32.66	32.55	32.55	33.01	32.80	0.16
Mn	0.014	0.008	0.007	-	0.007	-	0.011	-	0.007	-	-	0.014	0.006	0.005
Fe	0.288	0.185	0.327	0.162	0.363	0.538	0.280	0.425	0.295	0.369	0.162	0.538	0.32	0.11
As	-	-	-	-	-	-	-	-	-	-	-	-	-	-
Cd	0.279	0.378	0.215	0.260	0.290	0.201	0.327	0.290	0.145	0.233	0.145	0.378	0.26	0.07
Sb	-	-	-	-	-	0.014	-	-	-	-	-	0.014	0.002	0.004
Hg	0.674	0.559	0.376	0.637	0.425	0.444	0.511	0.444	0.579	0.367	0.367	0.674	0.502	0.11
average	100.71	99.99	100.16	100.16	100.66	100.00	99.40	100.62	99.91	100.36	99.83	98.55	100.16	101.38

PC-13 290.7 sphalerite

Element	1	2	3	4	5	6	7	Minimum	Maximum	Average	Sigma
Zn	66.02	65.85	65.88	65.47	65.80	65.66	66.36	65.47	66.36	66.86	0.28
Fe	0.08	0.17	0.12	0.14	0.15	0.09	0.11	0.08	0.17	0.12	0.03
Mn	0.02	-	-	0.01	0.01	-	-	-	0.02	0.01	-
S	32.40	32.52	32.45	32.47	32.71	32.62	32.66	32.40	32.71	32.55	0.12
Cd	0.21	0.23	0.17	0.21	0.16	0.18	0.17	0.16	0.23	0.19	0.03
In	-	-	-	-	-	-	-	-	-	-	-
Ga	0.14	0.18	0.21	0.18	0.13	0.15	0.09	0.09	0.21	0.15	0.04
Ge	-	0.12	0.02	0.34	0.04	0.08	0.08	-	0.34	0.10	0.12
totals	98.88	99.08	98.85	98.82	98.99	98.77	99.49	98.20	100.06	98.98	

#8 Zone -Sphalerite from #8 vein

Element	1	2	3	4	7	8	Minimum	Maximum	Average	Sigma
Zn	66.54	65.26	65.77	65.46			65.26	66.54	65.76	0.56
Fe	0.01	0.01	0.03	0.28			0.01	0.28	0.08	0.13
Mn	-	0.01	0.01	0.02			-	0.02	0.01	-
S	32.46	32.55	32.23	32.54			32.23	32.55	32.44	0.15
Cd	0.43	0.48	0.43	0.36			0.36	0.48	0.42	0.05
In	0.06	-	-	-			-	0.06	0.01	-
Ga	0.10	0.22	0.15	-			-	0.22	0.12	0.01
Ge	-	-	-	-			-	-	-	-
totals	99.60	98.52	98.62	98.78			97.86	100.15	98.84	

3050 Level, sphalerite vein

Element	1	2	3	4	5	6	7	8	Minimum	Maximum	Average	Sigma
Zn	66.42	66.39	66.24	66.22	66.33	65.80	66.05	65.79	65.79	66.42	66.15	0.25
Fe	0.16	0.17	0.10	0.12	0.07	0.15	0.08	0.13	0.07	0.17	0.12	0.04
Mn	0.01	-	0.01	0.03	-	-	-	0.02	-	0.03	0.01	-
S	32.79	32.76	32.84	32.76	32.68	32.48	32.59	32.42	32.42	32.84	32.66	0.15
Cd	0.43	0.38	0.44	0.45	0.42	0.48	0.49	0.52	0.38	0.52	0.45	0.04
In	0.05	-	-	-	-	0.01	-	-	-	0.05	0.01	-
Ga	0.18	0.13	-	0.02	0.28	0.25	0.05	0.24	-	0.28	0.14	0.10
Ge	-	-	-	-	0.03	0.04	-	0.01	-	0.04	0.01	-
totals	100.05	99.83	99.62	99.60	98.81	99.21	99.26	99.13	98.66	100.35	99.54	



### Appendix IV - Linear Regression Program (Yorkfit)

Errors are in  $2\sigma$ , in percent

Set #	$^{206}\text{Pb}/^{204}\text{Pb}$	%error	$^{207}\text{Pb}/^{204}\text{Pb}$	% error	Error Correlation
1	18.698	.042	15.652	.072	0.91
2	18.681	.042	15.646	.072	0.91
3	18.676	.042	15.641	.072	0.91
4	19.003	.042	15.667	.072	0.91
5	18.723	.042	15.653	.072	0.91
6	19.240	.042	15.713	.072	0.91
7	18.770	.042	15.656	.072	0.91
8	18.692	.042	15.646	.072	0.91
9	18.718	.042	15.654	.072	0.91
10	18.708	.042	15.662	.072	0.91
11	18.801	.042	15.663	.072	0.91
12	19.018	.042	15.679	.072	0.91
13	19.010	.042	15.676	.072	0.91
14	19.326	.042	15.708	.072	0.91
15	19.975	.042	15.770	.072	0.91
16	18.664	.042	15.640	.072	0.91
17	18.690	.042	15.652	.072	0.91
18	18.695	.042	15.653	.072	0.91
19	18.700	.042	15.655	.072	0.91
20	18.689	.042	15.655	.072	0.91
21	18.689	.042	15.650	.072	0.91
22	18.773	.042	15.655	.072	0.91
23	19.042	.042	15.575	.072	0.91
24	18.739	.042	15.647	.072	0.91
25	19.011	.042	15.670	.072	0.91
26	19.132	.042	15.685	.072	0.91

Model 1 Solution - Assumes all scatter is due to analytical error

	Slope	Y-intercept	X-intercept
Best Fit	0.0923196	13.9233	-150.817
-----			
Error ( $1\sigma$ , A Priori)	.003596	0.0679	
Error (1s, from scatter)	.003992	0.07537	
Error (95% confidence limits)	.007048	0.1331	13
Coordinates of Centroid: X = 18.8788		Y = 15.6662	

Analytical errors alone will cause the observed amount of scatter or more 20% of the time, as indicated by the M.S.W.D of 1.23

**Growth curve intercepts are at 352 and 1249 Ma**

**Model 1 Isochron Age =  $1474 \pm 140$  (95% confidence) Ma**